UNIVERSITÉ DE SHERBROOKE
Faculté de Génie
Département de Génie Chimique et de Génie Biotechnologique
Centre de Recherche en Énergie, Plasmas et Électrochimie (CREPE)

ÉTUDE DE LA FABRICATION DE PILES À COMBUSTIBLE NANOSTRUCTURÉES SOFC PAR L'INJECTION DE SUSPENSIONS ET DE SOLUTIONS DANS UN PLASMA INDUCTIF

NANO-STRUCTURED SOFCS FABRICATION USING SOLUTION/SUSPENSION INDUCTION PLASMA SPRAY TECHNOLOGY

Thèse de doctorat ès sciences appliquées
Spécialité : génie chimique

Lu JIA

Jury : François Gitzhofer, ing. PhD (Directeur)
Jerzy Jurewicz, ing. PhD
Hugues Ménard, PhD
Christian Moreau, PhD

Sherbrooke (Québec), Canada Mai, 2010

Your file Votre référence
ISBN: 978-0-494-70625-1
Our file Notre référence
ISBN: 978-0-494-70625-1

RÉSUMÉ

Dans ce travail, les anodes et électrolytes des piles à combustible à oxyde solide (SOFC) ont été produits à l'aide de la technologie des plasmas inductifs utilisés avec l'injection de suspension ou de solution. La technologie de projection par plasma inductif utilisant la technologie d'atomisation des suspensions (SPS) a été utilisée pour produire des électrolytes de SOFCs nanostructurés, minces et étanches aux gaz. Cette étude vise aussi à apporter une réponse à la problématique des coûts de production des SOFCs qui sont prohibitifs pour l'instant pour leur introduction dans le marché.

Pour préparer la suspension utilisée dans la technologie SPS, des nanopoudres d'oxyde de cérium (CeO_2) et d'oxyde de gadolinium (Gd_2O_3) ont été dispersées dans un liquide. Elles ont ensuite été injectées séparément pour synthétiser des revêtements composites pour produire un électrolyte d'oxyde de cérium dopé au gadolinium (GDC). Ces nanopoudres ont été préparées par la technologie GNP (Glycine Nitrate Process) qui utilise des nitrates et de la glycine qui réagissent violemment pour produire les nanopoudres désirées.

Un système de masque dynamique a été développé pour atténuer les effets de surchauffe présents dans le procédé de synthèse des dépôts par plasma inductif. Les résultats des expériences de production des électrolytes nanostructurés en GDC en utilisant le procédé de projection de suspension dans les plasmas inductifs ont été comparés avec l'utilisation du masque et sans le masque. Le potentiel et les bénéfices de l'utilisation de cette

technique de masque pour produire des électrolytes denses et uniformes ont été démontrés.

Les anodes des SOFCs nécessitent une grande longueur de jonction des phases triples (TPB) et aussi une diffusion de gaz suffisante pour le transport rapide du carburant vers l'électrolyte et des gaz d'échappement qui cheminent en sens inverse. Ceci représente un compromis avec une réponse proposée dans cette thèse qui peut apporter en même temps un allongement de la jonction des phases triples et une meilleure diffusion des gaz. C'est l'utilisation d'anodes gradées en composition et en porosité qui peut apporter le meilleur compromis possible.

En utilisant des conditions de déposition par injection de solution dans un plasma inductif (SolPS) optimisées, il a été possible de réaliser des nanostructures NiO-GDC pour des anodes. Les analyses élémentaires faites sur ces anodes ont permis de démontrer l'existence de cette gradation en composition qui varie de 35 à 9 % suivant l'épaisseur de l'anode.

La réussite de la synthèse et déposition d'électrolytes denses et d'anodes nanostructurées fait partie des jalons indispensables qui vont mener le Centre de Recherche en Énergie, Plasma et Électrochimie (CREPE) à réussir à fabriquer des piles SOFCs à haute performance.

Mots clefs : Déposition par plasma de suspensions (SPS), déposition par plasma de solutions (SolPS), piles à combustible à oxyde solide (SOFC), électrolyte nanostructuré, anode nanostructurée, anode avec une gradation de composition, revêtement mince

ABSTRACT

In this work, the nano-structured components of solid oxide fuel cells have been produced, using radio frequency (RF) solution or suspension plasma spraying processes.

The emerging technology of suspension plasma spraying was explored to produce thin and gas tight nano-structured solid oxide fuel cells electrolytes, which in an effort to develop a cost-effective and scalable fabrication technique for high performance solid oxide fuel cells (SOFCs). Glycine-nitrate process (GNP) produced cerium oxide (CeO_2) and gadolinium oxide (Gd_2O_3) nano-powders were used to prepare suspensions and then separately injected to form composite GDC electrolyte coatings. A dynamic mask system has been developed to control the heating effects of a high-temperature plasma deposition process. The experimental results of the nano-structured SOFCs GDC electrolytes production by means of a RF suspension plasma spraying process using the newly proposed mask were compared to the ones without mask. The potential of this deposition technique to improve the electrolyte coating uniformity and to reduce the coating porosity was demonstrated.

SOFCs anodes require long triple phase boundary (TPB) and appropriate gas diffusion pass for the fast transport of both fuel and exhaust gases, but the area where gas diffusion passes are especially required would be different from the area suitable for electrochemical reaction in the anodes. Functionally graded anodes in both composition and porosity have been proposed to fulfill the anodic functions in adequate anodic areas. On the basis of the optimized spraying conditions and the laboratory-

developed solution feeding system, NiO-GDC functionally graded nanostructure anodes were prepared using solution plasma spraying (SolPS) process. Then the microstructure and material composition of the anodes were analyzed. A graded distribution in contents of both nickel and GDC was confirmed in the coating. Field emission scanning electron microscopy (FESEM) observation exhibited a continuous variation in porosity from 35% to 9% along the direction across the coating thickness. The functionally graded anodes deposited by SolPS process may minimize the thermal expansion mismatch between SOFC components and increase the length of triple phase boundary, which should lead to the improvement of the anodic performances.

The successful fabrication of the functionally graded nano-structural electrodes as well as dense electrolyte coatings represents an opportunity for the Centre de Recherche en Énergie, Plasma et Électrochimie (CREPE) to fabricate the fully integrated nano-structured SOFC using solution and suspension plasma spraying processes.

Keywords: Suspension plasma spray (SPS), solution plasma spray (SolPS), solid oxide fuel cells (SOFCs), nano-structured electrolyte, nano-stuctured anode, functionally graded anode, thin film

ACKNOWLEDGEMENT

I had never dreamed to be a Ph.D before I met my advisor Prof. Francois Gitzhofer. I immigrated to Canada to explore my new life in 2001. I barely spoke English at that time. So I went to Bishop's University to study English. After I got my bonus bachelor degree in Computer Science in 2003, I realized that I am not computer genius. One day, I visited the personal website of Prof. Gitzhofer. Hey, maybe I am a genius of plasma technology. Through six years master and Ph. D study, I know I am not plasma genius as well.

Foremost, I would like to express my sincere gratitude to Prof. Gitzhofer for the continuous support of my master and Ph.D study and research, for his patience, motivation, enthusiasm, and immense knowledge. Moreover, his guidance helped me in all the time of solving problems in my daily life. He is more than a professor for me.

Besides my advisor, I would like to thank the rest of my thesis committee: Prof. Jerzy Jurewicz, Hugues Ménard, and Christian Moreau, for their encouragement, insightful comments, and hard questions.

The help of Mr. Stéphane Gutierrez for coating characterization and analysis is gratefully acknowledged.

Furthermore, I am deeply indebted to my friend Dr. Dong-il Shin. He is a gift from God to help me and support me to chase best life.

No one, however, helped more directly and continuously in my study than my wife Xiao Yan Jiang. She shared the burdens, anxieties and pleasures of my life. She also worked

hard (of course under my supervision) to support me financially so that I could complete this study according to schedule. Without the love of Xiao Yan and my son Yi Zhen, this degree could not have been gained. To Xiao Yan and Yi Zhen I own an immeasurable debt and deep affection.

TABLE OF CONTENTS

LIST OF FIGURES

LIST OF TABLE

LIST OF ABBREVIATIONS

APS	Atmospheric Plasma Spray
CTE	Coefficient of Thermal Expansion
CI-LPPS	Center Injection-Low Pressure Plasma Spray
CREPE	Energy, Plasma and Electrochemistry Research Centre
DC	Direct Current
GDC	Gadolinium-Doped Ceria
HVOF	High Velocity Oxy-Fuel
HVSFS	High Velocity Suspension Flame Spraying
HYPS	Hybrid Plasma Spray
IT-SOFCs	Intermediate Temperature Solid Oxide Fuel Cells
LPPS	Low Pressure Plasma Spray
LPPS-TF	Low Pressure Plasma Spray-Thin Film
LSGM	Strontium-Magnesium-Doped $LaGaO_3$ Perovskite Oxide
LSCF	Lanthanum-Strontium-Cobalt-Iron Perovskite Oxide
MIECs	Mixed Ionic and Electronic Conductors
MCFC	Molten Carbonate Fuel Cell
PAFC	Phosphoric Acid Fuel Cell
RF	Radio Frequency
RF-IPS	Radio Frequency Induction Plasma Spraying
RFPS	Radio Frequency Plasma Spray
SDC	Samarium Doped Ceria
SOFCs	Solid Oxide Fuel Cells
SolPS	Solution Plasma Spraying
SPS	Suspension Plasma Spraying
TPBs	Triple-phase boundaries
TPBL	Triple Phase Boundary Length
TTPR	Triple Torch Plasma Reactor
VPS	Vacuum Plasma Spray
YSZ	Yttria-Stabilized Zirconia

1. INTRODUCTION

The successful introduction of solid oxide fuel cells (SOFCs) as an environmentally friendly energy converter into the highly competitive market for electric power and heat will strongly depend on the imperative achievement of a drastic reduction in production costs. SOFCs developers aim to reach this goal by further optimizing the standard cells under system-specific conditions, by using lower-cost materials, developing new materials for lower operating temperature and by developing more economical fabrication processes.

The use of thermal plasma spraying process for the manufacture of SOFCs presents many advantages over the more traditional wet ceramic process techniques, with regards to both performance and cost. Atmospheric plasma spray (APS), vacuum plasma spray (VPS), radio frequency plasma spray (RFPS), and high velocity oxy-fuel (HVOF) spray have demonstrated their capacity to produce dense electrolyte layers and as well as porous functionally graded electrode layers.

Since the nano-structured SOFCs components offer superior mechanical and physical improvement, for example, higher ionic conductivity, higher surface area, lower electrode/electrolyte interfacial polarization resistances, better coherency and longer triple phase boundary length, there is an increasing interest in developing thermal plasma spraying techniques in which coatings with nano-structural features are deposited. However, in order to effectively inject small feedstock particles (< 1μm) into a direct current (DC) or radio frequency (RF) plasma jet, the required carrier gas

flow-rate has to be increased to levels that match the momentum of the plasma jet. This condition translates into an important perturbation of the jet flow and compromises the efficiency of the process.

As a promising extension of conventional thermal plasma spraying, the use of a liquid precursor permits feeding and spraying of either precursor solutions or a suspension of nano or submicron-sized particles to form thin coatings with more refined microstructure and grain size. The former is known as solution plasma spraying (SolPS) while the latter is known as suspension plasma spraying (SPS). In the SolPS process, solution feedstock of desired materials is injected into the plasma jet either by atomization or by a liquid stream. Rapid heating up and evaporation of the solution droplets results in the formation of the solid particles, which are heated up and accelerated to the substrate to generate coatings. The as-deposited coatings have desired porosity, fine grain and pore size. Its microstructure has nano and sub-micrometric features.

Alternatively, suspension precursor can replace the solutions. In this process, a suspension of micron or nano-powders is fed to RF or DC plasma torch and axially or radially injected into the plasma flame. The solid particles enclosed in each droplet are accelerated, evaporated, melted, and then flattened onto a prepared substrate rapidly forming thin (5-10 μm) coatings with a more refined microstructure.

During the last decades, many novel types of electrolyte and electrode materials have been developed. The most common solid electrolyte material used in high temperature

solid oxide fuel cells is yttria-stabilized zirconia (YSZ). At present the two most promising alternative electrolytes to YSZ, which have been intensively studied in recent years, are ceria based and lanthanum gallate based electrolytes. Both these electrolytes offer the possibility of lower temperature operation of SOFCs between 500 °C and 700 °C. The cathode materials consist in most cases of mixed conducting oxides of perovskite type, e.g., strontium-doped lanthanum manganite (LSM) in YSZ-based SOFCs. In contrast, $La_{1-x}Sr_xCo_yFe_{1-y}O_{3-d}$ does not react with doped ceria, and hence it is a promising material for IT-SOFCs based on this electrolyte. The anodes are mostly built as cermets, for example, mixtures of ceramics and metal, are consisting of about one-third of electrolyte material to adapt the thermal expansion of the anode to that of the electrolyte and also to extend the reaction domain of oxygen-ions and the fuel. The most-common SOFCs anode is constructed as a porous nickel-YSZ cermet. Other conductive oxides such as nickel-ceria cermet anode have been shown to give sufficiently good performance in ceria based SOFCs operating at temperatures as low as 500 °C. In recent years, many ceramic oxides with various crystal structures, such as rutile, fluorite, perovskite, pyrochlore, and tungsten bronze, have been investigated as anode materials. Among them, the perovskite oxides, mainly titanates and chromites, which are chemically stable under anode conditions, have been studied more intensively.

The Energy, Plasma and Electrochemistry Research Centre, at Université de Sherbrooke, has developed a novel planar concept for a reformer-supported thin film SOFCs, called the "spray concept", which is based on radio frequency inductively

coupled plasma spray technology as manufacturing process. Throughout this study, this technique has been adapted to the specific requirements of SOFCs fabrication in terms of liquid precursors such as suspensions and solutions as the feedstock, which has the potential to fabricate the entire thin and nano-structural cell in a single consecutive fast spray process. High material deposition rates promise fast and cost-effective cell production, particularly where large active cell areas are required.

In the following sections, the project objectives will be presented in Chapter 2. In the chapter 3, the current state of the art of SOFCs will be bibliographical reviewed. The experimental results will be reported and discussed in the form of 4 articles published or to be published soon in Chapter 4. Finally, the conclusions and the future works will be summarized in the last chapter.

2. PROJECT OBJECTIVES

The liquid precursor's feedstock plasma spraying process, which is an emerging technology that permits the deposition of adjustable microstructures and compositions, becomes the focus of intensive research around the plasma laboratories in the world. There is an increasing need to gain a better understanding of this spraying process. For this reason, various experimental tests were carried out in this study.

The main objectives of this project are the following:

- To understand the influence of induction plasma spraying parameters on the microstructure and composition of as-sprayed SOFCs components.
- To optimize the shape and operating parameters of a mask system located between the torch and the substrate to improve the coating quality.
- To comparatively study the solution/ suspension plasma sprayed SOFCs electrolytes, as well as to produce dense and thin nano-structured electrolyte.
- To develop the functionally graded and nano-structured electrodes in terms of solution plasma spraying.

3. CURRENT STATE OF THE ART: BIBLIOGRAPHICAL REVIEWS

3.1 Solid Oxide Fuel Cells (SOFCs)

3.1.1 SOFCs history

The solid oxide fuel cell was first conceived following the discovery of solid oxide electrolytes in 1899 by Nernst [Nernst, 1899]. Nernst reported that the conductivity of pure metal oxides rose only very slowly with temperature and remained only relatively low, whereas mixtures of metal oxides can possess dramatically higher conductivities.

Emil Baur, a Swiss scientist and his colleague H. Preis experimented with solid oxide electrolytes in the late 1930s, using such materials as zirconium, yttrium, cerium, lanthanum, and tungsten oxide. The operation of the first ceramic fuel cell at 1000°C, by Baur and Preis [Baur, 1937], was achieved in 1937. In the 1940s, O. K. Davtyan of Russia added monazite sand to a mix of sodium carbonate, tungsten trioxide, and soda glass, in order to increase the conductivity and mechanical strength. Davtyan's design, however, also experienced unwanted chemical reactions and short life ratings. By the late 1950s, research of solid oxide technology began to accelerate at the Central Technical Institute in The Hague (Netherlands), Consolidation Coal Company in Pennsylvania, and General Electric in Schenectady (New York) [Mobius, 1997]. The problems with SOFCs at this time were the relatively high internal electrical resistance, melting, and short-circuiting, due to semi-conductivity. The promise of a high-temperature cell that would be tolerant to carbon monoxide and use a stable solid electrolyte continued to draw a modest attention. Researchers at Westinghouse, for example, experimented with a cell

using zirconium oxide and calcium oxide in 1962 [Draper, 2008]. More recently, climbing energy prices and advances in materials technology have reinvigorated work on SOFCs. A recent report listed about 40 companies working on these fuel cells that include Versa Power, formerly the Global Thermo-electric's Fuel Cell Division, which is developing cells designed at Julich Research Institute in Germany [Tietz, 2006]. Cermatec-Advanced Ionic Technologies is working on units up to 10 kW in capacity, running on diesel fuel, which would be used for mobile power generation. The US Department of Energy announced that a SOFCs micro-turbine co-generation unit has been evaluated, since 2000, by the National Fuel Cell Research Center and Southern California Edison. The fuel cell was built by Siemens Westinghouse and the micro-turbine by Northern Research and Engineering Corporation. In a year of actual operating conditions, the 220 kW SOFC, running on natural gas is achieving an efficiency of 50%. Moreover, a 140 kW peak power SOFCs cogeneration system, supplied by Siemens Westinghouse, is presently operating in Netherlands. Also, a world record for SOFC operation, roughly eight years, still stands, and the prototype cells have demonstrated two critical successes: the ability to withstand more than 100 thermal cycles, and voltage degradation of less than 0.1% per thousand hour. This system has operated for over 16,600 h, becoming the longest running fuel cell in the world [Stambouli, 2002].

3.1.2 Principle of SOFCs

The SOFC is an electrochemical device that converts the chemical energy of a reaction directly into electrical energy. The basic physical structure, or building block, of a fuel cell consists of an electrolyte layer in contact with a porous anode and cathode on either side [Singh, 2001].

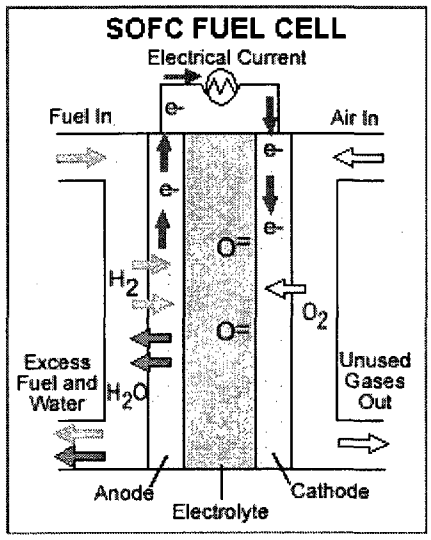

Figure 3.1 Schematic of a solid oxide fuel cell [Haile, 2003]

In a typical SOFC (Figure 3.1), hydrogen is brought into the anode compartment and a gaseous oxidant, typically oxygen, is introduced into the cathode compartment. There is an overall chemical driving force for oxygen and hydrogen to combine and produce water because of the partial pressure difference of oxygen. Direct chemical reaction is prevented by the electrolyte that separates the fuel from the oxidant (O_2) and only allows O^{2-} ions diffusing through it. The electrolyte serves as a barrier to gas diffusion, but permits ion migration across it. Accordingly, half-cell reactions occur at the anode and cathode, producing ions that can traverse the electrolyte. For example, if the electrolyte conducts oxide ions, oxygen will be electro-reduced at the cathode to produce O^{2-} ions and "consume" electrons, whereas oxide ions, after migrating across the electrolyte, will react at the anode with hydrogen and "release" electrons [Haile, 2003].

Cathode: $$\frac{1}{2}O_2 + 2e^- \rightarrow O^{2-} \qquad (3\text{-}1)$$

Anode: $$H_2 + O^{2-} \rightarrow H_2O + 2e^- \quad (3\text{-}2)$$

Overall: $$H_2 + \frac{1}{2}O_2 \rightarrow H_2O \quad (3\text{-}3)$$

The flow of ionic charges through the electrolyte must be balanced by the flow of electronic charges through an external circuit, and it is this electronic balance that generates the electrical power. The only by-product of this process is pure water (H_2O).

3.1.3 Electrochemical basis of SOFCs

Ideal performance of a SOFC: The ideal standard potential (E_{eq}) for a SOFC in which H_2 and O_2 react, can, in principle, be calculated from a knowledge of the thermodynamics of the reaction in question [Laughton, 2002]. One first determines the change in Gibbs free energy, ΔG, for the reaction (3-3) under the given conditions and E_{eq} is then given by $-\Delta G/nF$, where n is the number of electrons transferred in the reaction and F is Faraday's constant. For reaction (3-3), the Gibbs free energy is

$$\Delta G = \Delta G^0(T) + RT \ln \frac{P_{H_2} P_{O_2}^{1/2}}{P_{H_2}O} \quad (3\text{-}4)$$

where $\Delta G^o(T)$ is the Gibbs free energy of the reaction for the case when all species are in their standard states (1 atm, pure gases) and the pressures in the second term refer to the actual pressures in the fuel cell experiment. The term $\Delta G^o(T)$ is tabulated for most reactions of interest (or can be calculated from the formation energies of the species involved). In the case of reaction (3-3), it is−242 kJ/ mol + (45.8 J/mol K) * T, for all components in the vapor phase [Wagman, 1989]. This term alone is used to define the

standard potential (25°C) of a particular reaction. Then, the equilibrium (Nernstian) can be calculated by the following equation:

$$E^0(T) = -\Delta G^0(T)/nF \qquad (3\text{-}5)$$

where $\Delta G^0 = -242\,kJ/mol + \left(45.8\times10^{-3}\,kJ/mol\bullet K\right)\times(273+25)K = -228.4\,kJ/mol$,

n = 2 is the number of electrons exchanged in the chemical equation as written,

F is Faraday's constant (96485 Coulombs/mole).

Thus, for reaction (3-3), the equilibrium potential is 1.18 volts with gaseous water product [Tsipis, 2008].

Actual performance of a SOFC: The actual cell potential is decreased from its equilibrium potential because of irreversible losses, as shown in Figure 3.2. Multiple phenomena contribute to irreversible losses in an actual fuel cell. The losses, which are called polarization, over-potential, or over-voltage, originate primarily from three sources:

- Activation polarization
- Ohmic polarization
- Concentration polarization

These losses result in a cell voltage (V) that is less than its ideal potential, E.

$$V = E_0 - \eta_{act} - \eta_{mass} - iR \qquad (3\text{-}6)$$

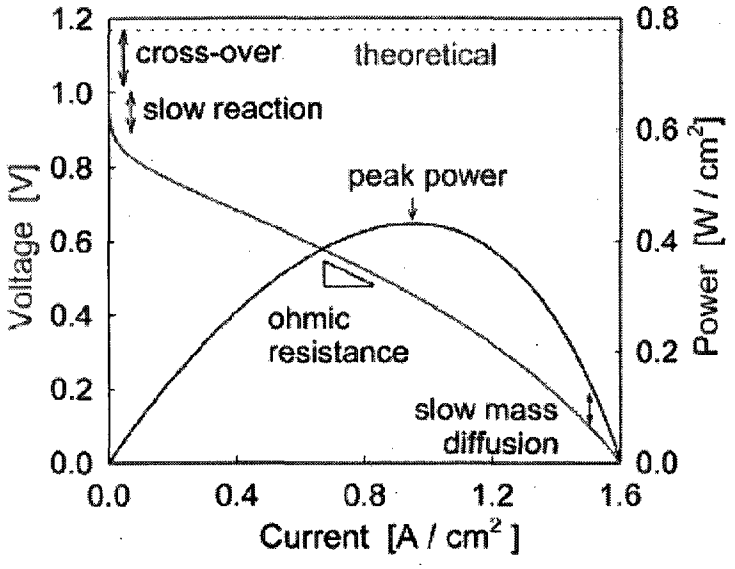

Figure 3.2 Schematic fuel cell polarization and power density curves [Haile, 2003]

The activation polarization losses are dominant at low current density. At this point, electronic barriers must be overcome prior to current and ion flow. Activation losses increase as current increases. Ohmic polarization losses vary directly with the current, increasing over the entire range of current because the cell resistance remains essentially constant. Gas transport losses occur over the entire range of current density, but these losses become prominent at high limiting currents where it becomes difficult to provide enough reactant to the cell reaction sites [Singhal, 2000].

Activation Polarization: Activation polarization is present when the rate of an electrochemical reaction at an electrode surface is controlled by sluggish electrode kinetics. In other words, activation polarization is directly related to the rates of electrochemical reactions [Nozawa, 2008]. There is a close similarity between electrochemical and chemical reactions in that both involve an activation energy that

must be overcome by the reacting species. In the case of an electrochemical reaction with E_{act} > 50-100 mV, it is customary to express the voltage drop due to activation polarization by a semi-empirical equation, called the Tafel equation [Haile, 2003].

Tafel plots provide a visual understanding of the activation polarization of a fuel cell. They are used to measure the exchange current density, given by the extrapolated intercept at $E_{act} = 0$ which is a measure of the maximum current that can be extracted at negligible polarization, and of the transfer coefficient (from the slope).

Ohmic Polarization: Ohmic losses occur because of the resistance of ions in the electrolyte and to the resistance of the electrons through the electrode. The dominant ohmic losses through the electrolyte are reduced by decreasing its thickness and enhancing the ionic conductivity of the electrolyte [Huang, 2001]. Because both the electrolyte and fuel cell electrodes obey Ohm's law, the ohmic losses can be expressed by the equation $E_{ohm} = iR$ where i is the current flowing through the cell, and R is the total cell resistance, which includes electronic, ionic, and contact resistance.

Concentration (mass transfer) Polarization: As a reactant is consumed at the electrode by electrochemical reaction, there is a loss of potential due to the inability of the surrounding material to maintain the initial concentration of the bulk fluid. That is, a concentration gradient is formed. Several processes may contribute to concentration polarization: slow diffusion in the gas phase in the electrode pores, solution/dissolution of reactants and products into and out of the electrolyte, or diffusion of reactants and products through the electrolyte to and from the electrochemical reaction site. At practical

current densities, slow transport of reactants and products to and from the electrochemical reaction site is a major contributor to concentration polarization [Li, 2005].

3.1.4 Ideal Electrolyte and Electrodes for SOFCs

As mentioned above, high power densities (and high efficiencies) can be expected when gas diffusion and electron transport through the electrolytes are slow, electro-catalysis at the electrodes is rapid, the conductivity of each of the components, in particular, the electrolyte, is high, and high mass diffusion through the porous electrodes is favorable. Thus, the ideal fuel cell electrolyte is not only highly ionically conducting, but also impermeable to gases, electronically resistive and chemically stable under a wide range of conditions. Moreover, the electrolyte must exhibit sufficient mechanical and chemical integrity so as not to develop cracks or pores either during manufacture or in the course of long-term operation and cycling [Fergus, 2006].

The requirements on fuel cell electrodes are perhaps even more extreme than those on the electrolytes. The ideal electrode must transport gaseous (or liquid) species, ions, and electrons; and, at the points where all three meet, the so-called triple-phase boundary (TPB), the electro-catalysts must rapidly catalyze electro-oxidation (anode) or electro-reduction (cathode). Thus, the electrodes must be porous, electronically and ionically conducting, electrochemically active, and have high surface areas [Virkar, 2000]. It is rare for a single material to fulfill all of these functions, especially at low temperatures, and consequently a composite electrode, of which the electro-catalyst is one component, is often utilized. For high-temperature solid oxide fuel cells, single component electrodes are, in principle, possible because mixed conducting (O^{2-} and e^{-}) ceramics are known,

and it is precisely such materials which facilitates the electro-catalysis [Cannarozzo, 2007]. Thus, composite systems are suitable.

3.1.5 Types of SOFCs configurations

The SOFCs-stack is a multilayer structure consisting of ceramic and metallic materials. There are different types of SOFCs concepts, basically tubular and planar ones which differ in the single design and arrangement, interconnector materials and gas flow. The advantages of each system configuration depend on the size of the application as well as the composition of the fuel stream. In planar SOFCs, the cell components are configured as flat plates that are connected in electrical series. Planar SOFCs can be classified into two broad categories: an electrolyte-supported cell and an electrode-supported cell.

Conventionally, electrolyte-supported SOFCs use the electrolyte to support thin electrodes on either surface. The advantages of this configuration are relatively strong structural support from a dense electrolyte and little susceptibility to a failure due to anode re-oxidation. In an anode-supported cell, the thin electrolyte layer cracks due to the volume change and sintering of the supporting anode accompanied by the Ni oxidation. However, the electrolyte-supported structure limits the minimum electrolyte thickness to $\sim$200 μm (Figure 3.3) and thereby an operating temperature of about 900–1000 °C is required to minimize the high-ohmic loss due to the thick electrolyte [Will, 2000]. Such a high temperature implies poor long-term stability and high-material costs, particularly for the interconnect materials. The high-temperature limits the choice of interconnect materials to a few ceramics that are thermally stable but expensive [Joo, 2008].

Electrode-supported SOFCs with thin electrolytes can operate at reduced temperatures (600–800 °C). The most common example is the anode-supported SOFCs. However, the disadvantages of this configuration include a mass-transport limitation due to the thick (e.g., 1.5 mm) electrode (Figure 3.3). In addition, to form a dense electrolyte and a porous anode, a careful co-sintering process has to be adopted. As a result, the whole process is both complex and time-consuming [Singhal, 2003].

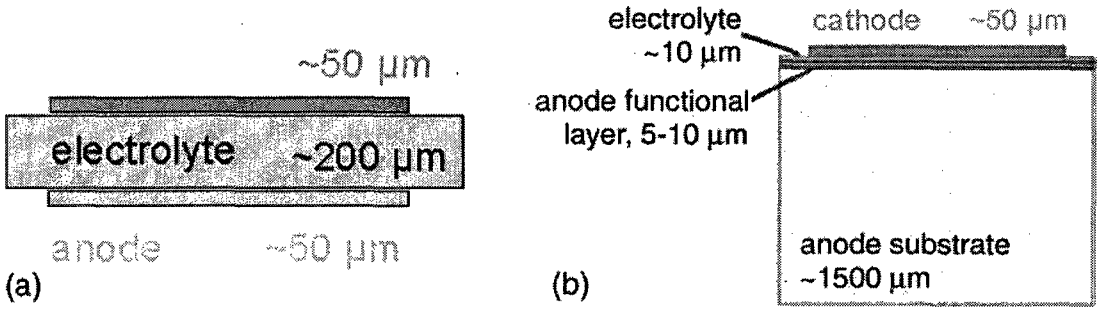

Figure 3.3 Two kinds of planar cell concept: electrolyte-supported (a) and electrode-supported (b) [Will, 2000]

In order to increase stability, lifetime, and economy, the operating temperature of the cells has to be reduced to about 500 to 700 °C. For this purpose, it is necessary to decrease the overall thickness of the SOFCs and particularly of the electrolyte. This means that a relatively thick electrolyte no longer serves as the "backbone" of a cell. With this second generation SOFCs characterized by a thin-film electrolyte, an additional component is required that has the function to mechanically stabilize the cell. A novel concept for a metallic substrate supported thin-film SOFCs [Figure 3.4] has been developed at DLR Stuttgart [Schiller, 2000]. Because of the supporting substrate, the electrolyte layer may have a significantly reduced thickness - only about 30 µm -

compared with conventional self-supporting SOFCs cells. The thicknesses of the cermet anode and the cathode are also in the range of 30 to 50 μm, resulting in a thin-film cell with a total thickness of less than 100 to120 μm.

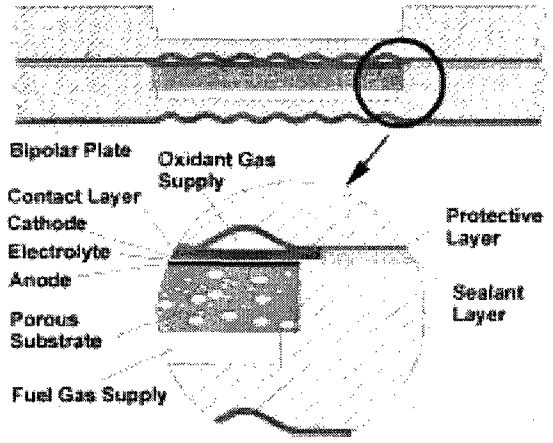

Figure 3.4 Principle of metallic substrate supported thin-film SOFCs [Schiller, 2000]

3.1.6 Advantages and disadvantages of state-of-the-art SOFCs

State-of-the-art SOFCs may be defined as a ceramic multilayer system working at high temperature using gaseous fuel and oxidant. Such characteristics provide a number of advantages over traditional generators and other types of fuel cells [Singhal, 2000]:

- The use of expensive catalysts such as platinum or ruthenium is not necessary.
- The high quality of exhaust heat is very useful for cogeneration applications in industry.
- High efficiency for electricity production (50%) can be achieved in combined cycles.
- Internal reforming of natural gas may considerably reduce costs.
- Electrolyte loss maintenance and electrode corrosion are eliminated, which is not the case for phosphoric acid fuel cell (PAFC) and molten carbonate fuel cell (MCFC).

- CO_2 emission is considerably reduced because of the high conversion efficiency.
- Chemical cogeneration is possible in producing electricity and chemical compounds when appropriate electro-catalytic anodes are used.
- SOFCs can be used as high-temperature water electrolyzers without major modifications.
- Finally, SOFCs provides the flexibility in planning and siting of power generation capacity as a result of their modular nature [Singhal, 2008].

Unfortunately, it is high operating temperature that leads to a number of serious drawbacks, which hamper large-scale commercial applications of SOFCs. On one hand, chemical reactions may occur between cell components to form insulated phase resulting in long-term degradation under high temperature. On the other hand, the cost of cell materials and large-scale manufacturing processes is relatively expensive. Intermediate temperature SOFCs have received much interest recently because reduced-temperature would considerably reduce material and fabrication problems and improve cell reliability during prolonged operation [Zhu, 1998].

In summary, the development of a concept for second-generation SOFCs operated at reduced operating temperature (< 700 °C) need to be addressed. The reduced cell resistances needed for intermediate temperature operation are possibly achievable through a reduction of electrolyte thickness resulting in diminished ohmic losses. Therefore, the novel planar concept has to be developed for a reformer-supported thin film SOFCs. The electrolyte layer should have a significantly reduced thickness - only about 10 to 20 μm. The thicknesses of the cermet anode and the cathode also should be in

the range of 20 to 30 μm, resulting in a thin-film cell with a total thickness of less than 80 μm.

3.2 Materials for SOFCs

During the last decades, many novel types of electrolyte and electrode materials have been developed. Most of these materials work very well at high operating temperature. However, when the temperature is reduced their performance is degraded, and their applications for intermediate temperature solid oxide fuel cells (IT-SOFCs) are limited. Recently, many efforts have been addressed to the development of novel materials and technology for IT-SOFCs. There are a number of comprehensive materials reviews for the electrolyte [Brandon, 2006] [Huang, 2001], the cathode electro-catalyst [Adler, 2004] [Tietz, 2004], and the anode electro-catalyst [Atkinson, 2004] [Jiang, 2004].

3.2.1 Electrolyte materials

Electrolyte should satisfy numerous requirements, including fast ionic transport, negligible electronic conduction, and thermodynamic stability over a wide range of temperature and oxygen partial pressure. In addition, it must be thermal expansion compatible with electrodes and other construction materials; it must have a negligible volatilization of its components, suitable mechanical properties, and negligible interaction with electrode materials under operating conditions.

The most common solid electrolyte material used in solid oxide fuel cells is yttria-stabilized zirconia (YSZ). Yttria (Y_2O_3) is added to stabilize the conductive cubic fluorite phase, as well as to increase the concentration of oxygen vacancies, and thus increase the

ionic conductivity [Han, 2007]. It is also abundant, relatively low in cost and is easy to fabricate.

ZrO_2, in its pure form, does not serve as a good electrolyte, primarily because its ionic conductivity is too low. At room temperature, ZrO_2 has a monoclinic crystal structure. The monoclinic structure changes to a tetragonal form above 1170 °C and a cubic fluorite structure above 2370 °C. Yttria (Y_2O_3), along with some other aliovalent oxides (CaO, MgO, Sc_2O_3) and various rare-earth oxides (Sm_2O_3 and Yb_2O_3), show a high solubility in ZrO_2 and stabilize the zirconia in the cubic fluorite structure from room temperature to its melting point (2680 °C), and at the same time increase the concentration of oxygen ion vacancies, which significantly enhances the ionic conductivity, making stabilized ZrO_2 suitable for use as an electrolyte in SOFCs. Although yttria-stabilized zirconia is the most widely used electrolyte material in SOFCs, yttria does not yield the highest conductivities (Table 3.1). For reasons of cost, availability and stability in oxidizing and reducing atmospheres, and its chemical inertness towards other components in the SOFC Yttria is however preferred [Choudhary, 1980]. Typically the concentration level of Y_2O_3 present in YSZ is around 8 mol%.

Table 3.1 Conductivity Data for Stabilized ZrO, Doped with Rare-Earth Oxides [Choudhary, 1980]

Dopant	**Composition** (mol %)	**Conductivity (1000°C)** (X 10^{-2} .cm^{-1})	**Activation energy** (kJ/mol)
Y_2O_3	8	10.0	96
Nd_2O_3	15	1.4	104
Sm2O3	10	5.8	92
Yb_2O_3	10	11.0	82
Sc_2O_3	10	25.0	62

However, the ionic conductivity of YSZ does not fulfill the requisite for the recent demands of intermediate- or low-temperature SOFCs, because the ionic conductivities of YSZ are 0.1 S/cm at 1000 °C, and 0.03 S/cm at 800 °C. So high temperatures around 800-1000 °C are considered for YSZ. Such a high operating temperature results in many unfavorable influences on the fuel cell and/or stack performance due to the degradation of its constituent components and undesirable interfacial reactions [Guan, 2008]. There is therefore considerable interest in lowering the operating temperature of SOFCs to below 700 °C and to enable the use of cheaper materials, such as stainless steel, and reduce fabrication costs, whilst maintaining high power outputs.

The discovery of alternative solid electrolyte materials has been an active research area for many years. At present the two most promising alternative electrolytes to YSZ, which have been intensively studied in recent years, are ceria based [Steele, 2000] and lanthanum gallate based electrolytes [Steele, 2001]. Both these electrolytes offer the possibility of lower temperature operation of SOFCs between 500 °C and 700 °C.

Ceria-based electrolytes show an ionic conductivity at 700 °C similar to YSZ at 1000 °C [Yahiro, 1989]. Usual doping ions for CeO_2 are Gd^{3+}, Sm^{3+} and Y^{3+}. Substitution of the Ce^{4+} cations in the lattice results in the formation of vacancies and enhances the ionic conductivity [Inaba, 1996].

Doped CeO_2, has been proposed as a potential candidate for SOFC electrolyte. However, the material undergoes large departures from stoichiometry at elevated temperatures in a reducing atmosphere, such as that present at the anode. Indeed ceria undergoes partial reduction to Ce^{3+}, which leads to electronic conductivity, which significantly lowers the

efficiency of the SOFCs, and also an undesirable structural change. Considerable effort has been devoted to minimizing the electronic conductivity of doped ceria under reducing conditions. One solution is to use an additional ultra-thin interfacial electrolyte layer which prevents electronic transport [Wachsmann, 1997], and can suppress the reduction of ceria under reducing conditions [Virkar, 1991]. Another approach to suppress the reduction of CeO_2 under reducing conditions is to coat the CeO_2 based electrolyte with a stabilized ZrO_2 layer [Yahiro, 1988].

Doped lanthanum gallate, $La_{0.9}Sr_{0.1}Ga_{0.8}Mg_{0.2}O_3$ (LSGM), has attracted considerable attention those recent years as a promising alternative electrolyte for lowering the operating temperature of SOFCs. Compared to the other electrolytes (Figure 3.5), LSGM has the advantages of stability and significantly higher oxygen-ion conductivity at lower temperatures. Although scandia-doped zirconia also has high conductivity, its conductivity is known to decrease with time at temperature (aging effect) [Badwal, 2000]. LSGM is very similar to YSZ in terms of its chemical stability. LSGMs stability towards reduction in the oxygen partial pressure (P_{O2}) range of $0.21–10^{-35}$ atm; conditions which are relevant to SOFCs operation and which have been investigated by Kim and Yoo [Kim, 2001]. They have reported that LSGM is stable and has an ionic transference number close to unity (>0.99) under these conditions.

However, there are problems associated with material costs, Ga volatility, lower mechanical strength compared to zirconia-based electrolytes, and the stability of LSGM which still need to be addressed.

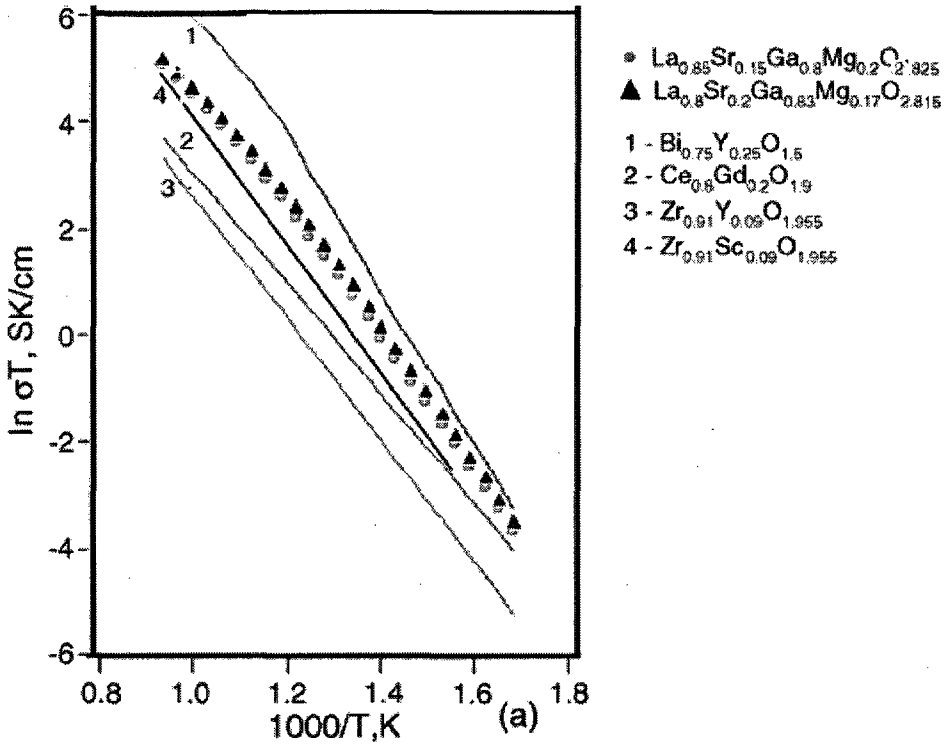

Figure 3.5 Comparison of conductivities as a function of temperature of various oxygen-ion-conducting solid electrolytes [Badwal, 2000]

3.2.2 Electrodes materials

The electrode materials should exhibit a high catalytic activity for the desired chemical and electrochemical reactions. The microstructure of the electrodes should display a large number of active reaction sites. All materials and components have to show chemical stability in the prevailing atmospheres. The compatibility in-between the different materials, that is a well-adjusted thermal expansion behavior, chemical compatibility, and good adhesion at the interfaces has to be fulfilled.

Cathode: Because of the high operating temperature (1000 °C) of the YSZ-based SOFCs, only noble metal or electronic conducting oxides can be used as cathode materials. Noble metals, such as platinum, gold, silver and palladium have been studied

as electrode materials for YSZ-based SOFCs. However, these metals are too expensive and impractical for commercial applications (and insufficient long-term stability due to vaporization of silver). Thus, electronically conducting oxides are exclusively used [Tsai, 1997]. In addition to possessing sufficiently high electronic conductivity, the oxide must have a thermal expansion coefficient comparable to that of the solid electrolyte. At present, strontium-doped lanthanum manganite (LSM) is the most commonly used cathode material in YSZ-based SOFCs. It has also been shown that the performance of LSM for SOFC's operating at 1000 °C can be improved by addition of YSZ [Hayashi, 1997] which results in suppressing the growth of LSM particles therefore sustaining the porosity and increasing the triple phase boundary length (TPBL). The polarization resistance of the composite electrode was decreased by extending the TPBL which resulted in a much lower over-potential toward oxygen reduction in SOFCs application than the pure LSM [Ostergard, 1995]. A problem with LSM is its chemical compatibility with the YSZ-based electrolyte, which generally restricts sintering temperature to below 1300 °C. Above these temperatures, manganese can diffuse into the YSZ-based electrolyte, detrimentally affecting both the cathode and the electrolyte [Yamamoto, 1987].

$La_{1-x}Sr_xCo_yFe_{1-y}O_{3-d}$ (LSCF) doped perovskites based on $LaCoO_3$ have attracted considerable attention over the last twenty years as an alternative material for intermediate-temperature solid oxide fuel cells (IT-SOFCs) electrodes. However, LSCF cathode cannot be used in conventional SOFCs because of the formation of strontium zirconate when applied on YSZ electrolytes [Figueiredo, 1997]. In contrast, LSCF does not react with doped ceria, and hence it is a promising material for IT-SOFCs based on

this electrolyte [Steele, 2000]. In addition, LSCF has a high electrical conductivity at 600 °C for the composition $La_{0.6}Sr_{0.4}Co_{0.2}Fe_{0.8}O_{3-d}$ and high ionic and electronic conductivity, with high catalytic activity for oxygen reduction. LSCF is also chemically and thermally compatible with the gadolinium-doped ceria oxide (GDC) electrolyte, which exhibits nonstoichiometry at high temperatures and at low P_{O2}, and displays high oxygen surface and tracer diffusion coefficients, all of which meet the requirements for an SOFC cathode [Anderson, 1992].

Anode: In the SOFCs, the fuel arriving at the anode is reducing in nature. Thus, metals can be used as the anode material. However, the metal must not be oxidised under the operating conditions of the SOFC, in particular at the fuel outlet where the gas composition is more oxidising. At the elevated operating temperatures of SOFCs this effectively limits the choice to nickel, cobalt and the noble metals. Nickel is most commonly used because of its low cost compared to cobalt and precious metals [Sun, 2007]. To maintain the porous structure of nickel over long periods at 1000 °C, nickel metal is often dispersed with the solid electrolyte material YSZ to form a cermet, which maintains the porosity by inhibiting sintering of the nickel particles at the fuel cell operating temperature, and also provide an anode thermal expansion coefficient acceptably close to those of the other cell components [Fergus, 2006].

The Ni/YSZ anode cermet is generally made by physically mixing NiO and YSZ powders. Because NiO and YSZ do not form solid solutions, even at high temperatures, this green body can be sintered to form a NiO/YSZ composite and then is reduced to form a porous Ni/YSZ cermet. As shown in Figure 3.6, the amount of Ni is typically at

least 30 vol. % to achieve the percolation threshold for electronic conductivity [Dees, 1987]. This material fulfils most requirements of the anode. The disadvantages of this material are its poor redox stability, low tolerance to sulphur [Matsuzaki, 2000], carbon deposition when using hydrocarbon fuels and the tendency of nickel agglomeration after prolonged operation. Especially, the low tolerance for carbon deposition makes this material inappropriate for operation with available hydrocarbon fuels [Atkinson, 2004]. Since nickel is an excellent catalyst for both steam reforming and hydrogen cracking, carbon deposition occurs rapidly when hydrocarbon was used as the fuel, unless excess steam is present to ensure steam reforming. The composition of the anode, particle sizes of the powders and the manufacturing method are crucial to achieving high electronic conductivity, adequate ionic conductivity, and high activity for electrochemical reactions, reforming and shift reactions.

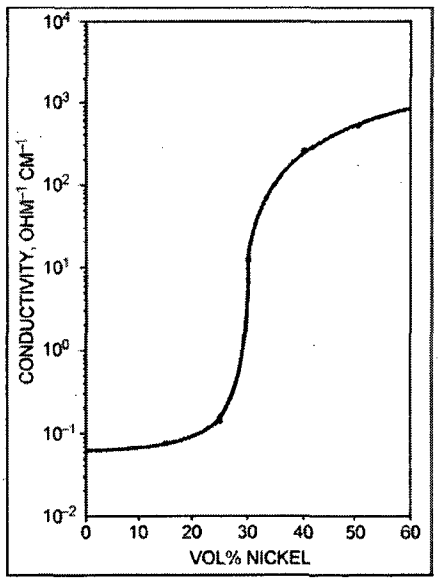

Figure 3.6 Electrical conductivity of a nickel/yttria-stabilized zirconia cermet anode as a function of nickel content [Dees, 1987]

Other materials such as conductive oxides have been proposed as possible SOFCs anode materials. A number of researchers have studied nickel/ceria cermet anodes for zirconia-based SOFCs, in addition to being used for ceria–gadolinia based SOFCs [Tsai, 1998]. Nickel/ceria cermet anodes have been shown to still give sufficiently good performance in ceria based SOFCs operating at temperatures as low as 500 °C. Ceria has also been added to nickel/YSZ anodes to improve both the electrical performance and the resistance to carbon deposition. Although cobalt and ruthenium offer potential advantages over nickel, including high sulfur tolerance, and in the case of ruthenium, higher reforming activity and greater resistance to sintering, and cobalt/YSZ and ruthenium/YSZ anodes have been developed, the cost of these materials effectively precludes their use.

Electrically conducting oxides also have been investigated as possible anode materials include materials based on lanthanum chromite, $LaCrO_3$, and strontium titanate, $SrTiO_3$. Doped lanthanum chromite and doped strontium titanate have also been studied. Mixed conducting oxides such as ytterbia- and titania-doped YSZ and yttria-doped ceria have also attracted some interest as potential anode materials [Han, 1995]. Such materials can significantly lower over-potential losses at the anode.

Much attention has been given to overcoming problems associated with the thermal expansion mismatch, for example by minimizing any processing flaws in the electrolyte, improving its fracture toughness, using graded anodes of different compositions and altering the thickness of the electrolyte and anode layers. This will be discussed in Chapter 4.

3.2.3 Interconnect materials

The interconnect in SOFCs is the component which electrically connects the single cell and separates the gas compartments. In an SOFC system, a number of demands are made on the interconnect, which ultimately determine the material selection. Important requirements are good electrical conductivity, gas tightness, chemical compatibility with the adjacent components of the fuel cell, chemical stability in reducing and oxidizing atmospheres, matched thermal expansion and last but not least reasonable costs. In order to meet these requirements, two classes of materials are commonly used for the interconnect, namely, ceramic and metallic materials. Whereas ceramic interconnects played a dominant role in the early SOFCs developments and are still essential in tubular designs, metallic interconnects have been frequently used in recent developments. Both variants have benefits and disadvantages and the final choice is therefore always a compromise depending, among other aspects, on the design, the operating temperature, and the required service life as well as on the material and production costs of these components [Tietz, 2002].

The requirements severely restrict the choice of materials for the interconnect. The vast majority of SOFCs use lanthanum chromite, $LaCrO_3$, as the interconnect. $LaCrO_3$ has a perovskite structure and is a p-type conductor, and satisfies all the above criteria. It is refractory and is oxygen deficient under very reducing conditions, but otherwise is stoichiometric. The electrical conductivity of $LaCrO_3$ can be enhanced by substituting the La^{3+} with a divalent cation, such as strontium, calcium or magnesium. However, the materials cost of perovskites are rather high and their application as ceramic interconnect

is only meaningful as long as the stack design requires only small amounts of the materials [Mark Ormerod, 2002].

Whereas practically all activities are related to $LaCrO_3$ modifications for the ceramic interconnects, clearly more material systems are under development for the metallic interconnects. The $Cr_5FeY_2O_3$ alloy developed by Plansee in cooperation with Siemens shows excellent behavior at temperatures up to 950 °C. A disadvantage of the alloy produced by powder metallurgy is the currently high price which could be drastically reduced by suitable production techniques [Thierfelder, 1997].

From the aspect of costs, ferritic chromium steels are attractive candidates for metallic bipolar plates. On the one hand, they form chromium oxides, have a lower thermal expansion compared to austenitic alloys and can be mechanically easily deformed and machined. On the other hand, they have a number of properties limiting their application such as lower high-temperature strength, insufficient corrosion protection at high temperatures and brittle phase formation. R&D work on ferritic steels therefore concentrates on application temperatures <800 °C. The application range of interest for this material class coincides with the development goals for planar anode-supported fuel cells. For this reason, such materials are being used or developed by all companies and research institutions working on this concept (e.g. Sulzer, CFCL, Plansee, Sanyo, FZJ) [Tietz, 2002]. In general, it can be stated that the long-term corrosion behavior of commercially available materials is not yet sufficient. Recent developments have attempted to achieve acceptable long-term behavior by selected doping with reactive elements (Ti, Y, La) and spinel formers [Quadakkers, 2000].

3.2.4 Nano-materials for SOFCs

Current developmental targets for SOFCs include increased volumetric power density, lower operating temperature, increased reliability and durability, and reduced cost. In response to these goals, the need for materials with improved physical and mechanical properties for demanding applications is becoming increasingly apparent. Advances in powder-based processing have been focused on reducing particle size and improving the particle uniformity. Nano-scale powders, approximately 1–100 nm in size, are becoming increasingly critical to the innovations in numerous applications, including catalysis, coatings, cosmetics, electronics, sensors, and drug delivery.

Nano-materials in particular are of considerable interest for use in SOFCs due to their potential to increase the surface area of active sites on which the electrode reactions take place, thereby improving reaction kinetics. There is a demand to decrease the SOFCs operation temperature in order to improve the system reliability, durability, and cost. One problem created by reduced operation temperature is the decreased electrode reaction rate, which may result in large polarization losses. SOFCs electrode reactions occur mainly at the interfaces between phases that conduct oxygen ions, gases, and electrons, commonly referred to as Tripe Phase Boundary (TPB). Therefore, an extended reaction surface area with an optimized porous microstructure will enhance the electrode performance. In addition, nano-materials with dimensions down to the atomic scale (10^{-9} m) represent a new generation of advanced materials with improved physical, chemical and mechanical properties [Gleiter, 1992]. A feature of such nano-materials is the high fraction of atoms that reside at grain boundaries and grain surfaces, largely enhancing the chemical activity. Nano-structured materials provide unprecedented

opportunities for significantly improved materials performance [Lau, 1996]. Nano-structured materials also have the enhanced electrical conductivity that is required for SOFCs components, either ionic or electronic conductivity [Schoonman, 2000]. Nano-structured ceramic powders are characterized by the relatively high specific surface area which acts as a primary cause in low temperature sintering and shrinkage of the nano-material compacts. Nano-scale electrolyte powders can be sintered at decreased temperatures compared with micron-scaled powder to avoid the chemical reactions between different components at high-sintering temperatures. Some attempts have been done to lower sintering temperature [Moskovits, 1999], minimize component shrinkage [Hellmig, 2001], and achieve highly sinter-reactive ceramics [Ohrui, 1998].

Nano-technology for preparation of the electrolyte composite powders is of high value, especially in a good controlling level both for the microstructure and for the molecule. The host oxide structure-dependent properties of the composites prepared by the nano-technology are significantly different from those of the conventional bulk materials in many cases. High defect concentration existing in the nano-structured host oxide phase can provide a large number of active sites for ion conduction as well as gas-solid catalysis. In addition, high diffusivity through nano-metersized interphase boundaries promotes fast kinetics of catalyst activation and ion transportation [Zhu, 2005]. Nano-structures have much promise for enhancing the ionic conductivity through the electrolyte [Zhu, 2003]. In a recent study [Mori, 2005], a new conduction pathway is created through nano-structured electrolytes to improve the conducting property. Moreover, nano-powders are expected to facilitate thin-film deposition of dense electrolyte layers to decrease ohmic losses and polarization losses.

In summary, the different inorganic materials used as electrolyte, anode, cathode and interconnects in SOFCs, and the strategy behind their selection and choice in terms of their chemical properties and the function they fulfil, with an emphasis on their chemistry need to be focused. The development of new and novel materials with improved properties needs to be evaluated. These include improvements in their electrochemical and catalytic properties, in their chemical and physical stability, and their ability to withstand more rapid temperature fluctuations. Furthermore, since the nano-structured SOFCs components offer superior mechanical and physical improvement, for example, higher ionic conductivity, higher surface area, lower electrode/electrolyte interfacial polarization resistances, better coherency and longer triple phase boundary length, the preparation of nano-materials for SOFCs need to be addressed as well.

3.3 Fabrication of SOFCs by Thermal Spray

3.3.1 Advantages of Thermal Spray

Thermal spraying is the family of coating deposition processes in which molten, semi-molten or solid particles are deposited onto a substrate. The processes use hot gas, flame or plasma to accelerate the particles and to heat them up. Obtained coatings have a lamellar microstructure, which determines many of coatings properties. The microstructure of the coatings results from their solidification and sintering.

Plasma spraying is part of thermal spraying, a group of processes in which finely divided metallic and non-metallic materials are deposited in a molten or semi-molten state on a prepared substrate. Plasma spraying is a well-established manufacturing technique first developed in the 1960s to produce value added coatings to enhance wear resistance,

temperature resistance, and to repair parts [Fauchais, 2004]. Plasma sprayed coatings are most commonly used as thermal barrier coatings in gas turbines and diesel engines. The thermal plasma heat source (direct current (DC) arc or radio frequency (RF) discharge) with temperatures over 8000 K at atmospheric pressure allows the melting of any material. However, to avoid too low a deposition efficiency, the melting temperature must be at least 300 K lower than the vaporization or decomposition temperature. Powered materials are injected within the plasma (RF discharges) or the plasma jet (DC arcs) where particles are accelerated and melted, or partially melted, and then impact with a substrate and rapidly solidified, forming lamellae or solid splat. Subsequent splats form on previously deposited ones to produce coatings. Fully sintered coatings may be produced rapidly without the need for post-deposition heat treatments.

Although SOFCs offer attractive potentials in different areas of energy conversion, there are still obstacles which prevent a wide-spread use of SOFCs based systems up to now. Besides the high degradation rates, a major obstacle are the high production costs of the cells. Different technology have been investigated in the past which can be summarized under the topic ''Wet Ceramic Techniques'' based on tape casting, screen printing, and co-sintering of layers. The relatively new process family, representing the topic of "Thermal Plasma Spray Processes", e.g., plasmas generated by DC and RF discharges either for spraying of powders or for synthesizing and subsequent deposition of materials.

- Comparing both process families it can be stated in a simplified way, that the Wet Powder Processes are well-established and relevant equipment and knowledge is available, in principle. But, these processes need high-process temperatures for

relatively long periods which can cause material and structure alterations and which limit material selection particularly for the substrates.

- Thermal plasma spray processing, in contrast, potentially provides a much simplified and cost-effective choice for fabricating SOFCs components and integrated cells. Low melting point and highly active electrode materials can be deposited directly onto the electrolytes without detrimental inter-reaction. Plasma spray processing allows the entire multilayer SOFCs to be processed in a consecutive spray process using only one piece of equipment and within a few minutes. The ability to rapidly produce ceramic layers without post-deposition sintering processes can allow metal-supported SOFCs to be manufactured rapidly and relatively inexpensively. Plasma spray processing also has the ability to achieve considerably higher deposition rates than those obtained through conventional physical or chemical vapor deposition techniques. Moreover, plasma spray processing is easily scaled up in terms of individual cell size and volume of production. Plasma spraying is also of potential interest for the improved control of composition, porosity, and microstructure within the electrodes because functionally graded and consecutively adjusted microstructures can be easily deposited, which are difficult to realize using wet ceramic processing [Kesler, 2007].

Most of the original plasma sprayed SOFCs work used vacuum plasma spraying (VPS) techniques. German aerospace center (DLR) has produced VPS SOFCs for many years [Franco, 2007]. VPS operates in low pressure atmospheres, which enable a longer and less turbulent plasma flame to be formed. Unfortunately, VPS systems require more

equipments and are more expensive to operate [Fauchais, 2004] and thus much recent interest has arisen in developing methods to produce plasma sprayed SOFCs using atmospheric plasma spray (APS) systems that operate at atmospheric pressure [Hui, 2007].

Plasma spray systems usually use feedstock powders that are typically 10–100 μm in diameter. The powders are typically delivered by suspending them in a flowing gas, and most plasma spray SOFCs research has focused on using these conventional powder spraying routes to produce fuel cell layers [Ma, 2005]. However, it is challenging to produce fuel cell microstructures with the required properties, since it is difficult to feed powders <5 μm in diameter and due to the horizontal splat orientation of the microstructure. It is also quite challenging to find spraying conditions to produce the porous, high surface area microstructures required for high performing SOFC composite electrodes or thin (<10 μm), fully dense microstructures required for electrolytes.

Recently, plasma spray systems have been modified in order to use nano- to micro-sized powders suspended in a liquid as feedstock. These smaller powders improve the ability of plasma spraying to produce finer microstructures and controlled porosity. However, much work remains to be done to develop methods to deliver and atomize the suspension, to deal with the liquid effects on the plasma, and to find optimal spraying conditions to produce layers with the desired microstructures.

Many suspension plasma spraying (SPS) SOFCs studies have used relatively low powered plasma torches and have injected the feedstock suspensions radially. Low torch power limits the ability to use high solid content suspensions and often requires

suspensions to be alcohol based [Rampon, 2008] to lower the energy required to vaporize the suspending liquid. The low solid content limitations reduce coating deposition rates, and non-aqueous suspensions are typically more expensive and less environmentally friendly than water based ones. Radial injection of feedstock suspensions makes suspension atomization, droplet size, and velocity extremely important parameters, because it is very difficult to achieve good penetration of nano- to micro-sized suspended powders from the periphery to the center of the plasma plume. Axial injection of feedstock suspensions simplifies a number of injection issues, as the suspension is fed directly into the center of the plasma plume and thus does not have to pass through the more turbulent outer fringes of the plasma. However, axial feedstock injection increases the complexity of the plasma torch and limits the size of suspension feeding lines, since the lines have to pass between the torch electrodes.

3.3.2 Production of electrolytes

Electrolytes for SOFCs require the highest demand on quality and production. They should be very thin in the range of some meters up to few tens of microns to keep the internal resistance for conducting the oxygen-ion low, but still being dense enough for avoiding the permeation of reacting gases which would not only reduce the performance, but also in the case of H_2-transfer lead to H_2O formation at the cathode side causing increased degradation effects by destroying the cathode with time. Also, a well-developed fine-grained structure at the interfaces to the two electrodes with graded material and porosity transition showing an extended triple-phase boundary zone should exist.

Conventional plasma spraying is blamed for its drawback that the production of fully dense ceramic layers is almost impossible with it, and particularly, as already described, when most present SOFCs electrolytes consist of relatively high melting ceramic materials, e.g., YSZ. Nevertheless, means have to be developed to make those layers as dense as possible either by process improvement or by post-processing. Various processing improvements are currently being developed to obtain more homogeneous, denser, and thinner electrolytes through the use of solution, suspension, fine powders, or reduced pressure during spraying, in order to minimize or eliminate the need for post-deposition heat treatments.

To produce electrolyte coatings by thermal spray techniques, three routes have been suggested:

1. to spray 10-100 μm sized powder feedstock into the high temperature, high velocity plasma jet to melt and produce fine-grained (0.5 to 5 μm) electrolyte deposits;
2. to spray sub-micron-sized or nano-sized particles via a suspension;
3. to spray solutions precursors.

Atmospheric plasma spray: APS has been widely investigated for the production of dense electrolyte layers. It is difficult to fabricate dense electrolyte layers by single-step deposition by thermal plasma spraying. The reason for these problems is the fact that thermally sprayed coatings of ceramics like YSZ typically form cracks and pores during the spray process and the cooling to room temperature. Therefore, additional post thermal treatments are often necessary to achieve a sufficiently high gas tightness of the

electrolyte layer, such as spark plasma sintering [Khor, 2003], high-temperature vacuum sintering [Scagliotti, 1988], and chemical impregnation densification [Rose, 2007]. However, these post-spraying treatments increase the process complexity. For example, high-temperature vacuum sintering requires a complex furnace and firing at a temperature as high as 2000 °C, while the impregnation densification generally requires repeated cycles of wet coating, drying, and firing.

Another major challenge in the development of dense electrolytes through APS is the avoidance of cracks, typically generated during the spraying process [Vaßen, 2007]. The major influencing factors are the particle properties in the plasma jet, the substrate temperature, the movement of the gun during deposition, the particle size distribution of the feedstock powder, and the powder feeding rate. The spray gun used can also play a major role.

In the paper by Stöver et al. [Stöver, 2006], the authors describe that the formation processes of micro and segmentation cracks and pores in the ceramic coatings. A three-cathode gun Triplex II (Sulzer Metco, Wohlem, Switzerland) is used to inject YSZ powders to produce the electrolyte coatings. The specific spray conditions, for example, higher Ar/He ratio, lower spray distance and higher substrate temperature, have been developed which largely reduce number and size of the cracks in the coatings. The produced YSZ coatings with a thickness below 50 μm (Figure 3.7) are gastight (OCV > 1.02V) in the as-sprayed condition and no additional thermal treatment is necessary.

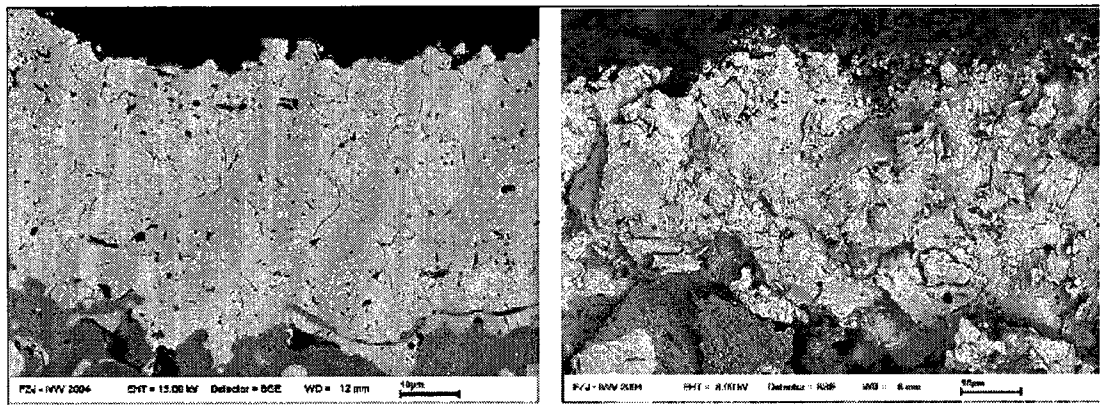

Figure 3.7 SEM micrographs of a metallographical section (left) and of a fracture surface (right) of a dense APS YSZ coating [Stöver, 2005]

Generally, for APS process, the flowable powders with a typical size range between 10 and 100 μm are used as starting materials. Nano-scaled powders cannot be directly used in this process due to their low flowability. This leads to a limitation of the resulting splat size and the achievable microstructure. One possible method to process nano-scaled particles is the use of agglomerated nano-powders. However, these agglomerates have a size from 10 to 200 μm. In contrast, suspension plasma spraying (SPS) process is an emerging technology that permits the projection of much finer starting powder and allows the formation of thinner coatings. In this process, a suspension precursor is injected directly into the plasma flame. The plasma-liquid interaction atomizes the suspension into a fine mist and evaporates the suspension medium, thereby concentrating the solid content into micro-sized particles. The small particles are then nearly immediately accelerated to the plasma gas velocity. At impact on the substrate, these particles form thinner lamellae with rapid solidification rates. Thin coatings (3-20 μm) with a more refined microstructure and grain size than in conventional thermal spraying are thereby created [Fauchais, 2008].

Considering DC plasma spraying, the suspension is commonly injected radially into the plasma jet externally to the torch, either as a straight jet or as an atomized one. It has been shown that the coating density is improved by enhancing the penetration of the liquid feedstock within the plasma jet, either by optimizing the injection system (from a nebulized to a liquid or droplet jet) or by adjusting both the plasma jet and the liquid characteristics (suspension momentum density, injection angle, plasma gas mixture and mass rate, etc.) [Delbos, 2003]. A mechanical injection (single precision hole injector with pressurized tanks or continuous ink jet printer) is often preferred because it provides a stream of drops of homogenized size and velocity which should then be more homogeneously treated in the plasma flow. Considering SPS conditions (i.e., radial injection of the suspension), it was shown that the liquid velocity as well as location and injection angle are critical to ensure effective heat and momentum transfers to the droplets which seem to lead to dense ceramic coating [Fazilleau, 2006].

Fauchais et al. reported in 2005 about their work to synthesize dense and thin (30 μm in thickness) YSZ coatings for the electrolyte of SOFCs by radial injection of suspension (Figure 3.8) [Fauchais, 2005]. In this context, information was also given about characterization of the injection, in-flight phenomena and formation of coatings. They used a suspension of sub-micron with narrow size distribution (0.5-3 μm) YSZ powders in ethanol. Suspension was dispersed by phosphate ester to reduce the viscosity and stabilize the suspensions. As plasma source, Sulzer Metco PTF4 plasma torch was applied in atmosphere. The suspension plasma spraying process had a deposition efficiency ranging from 50% to 60%. The operating parameters had a strong influence on density where a fully dense YSZ coating in the cubic phase was obtained (Figure 3.9).

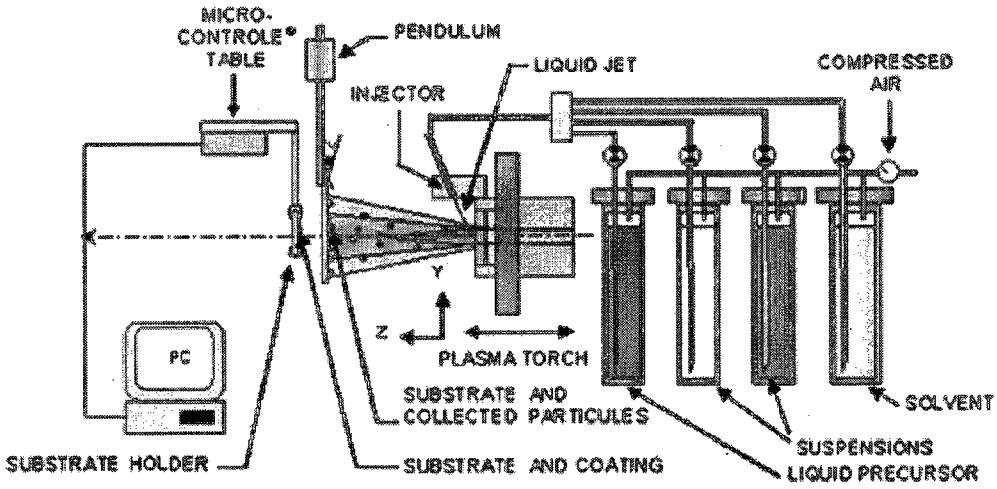

Figure 3.8 APS suspension plasma spraying setup [Fauchais, 2005]

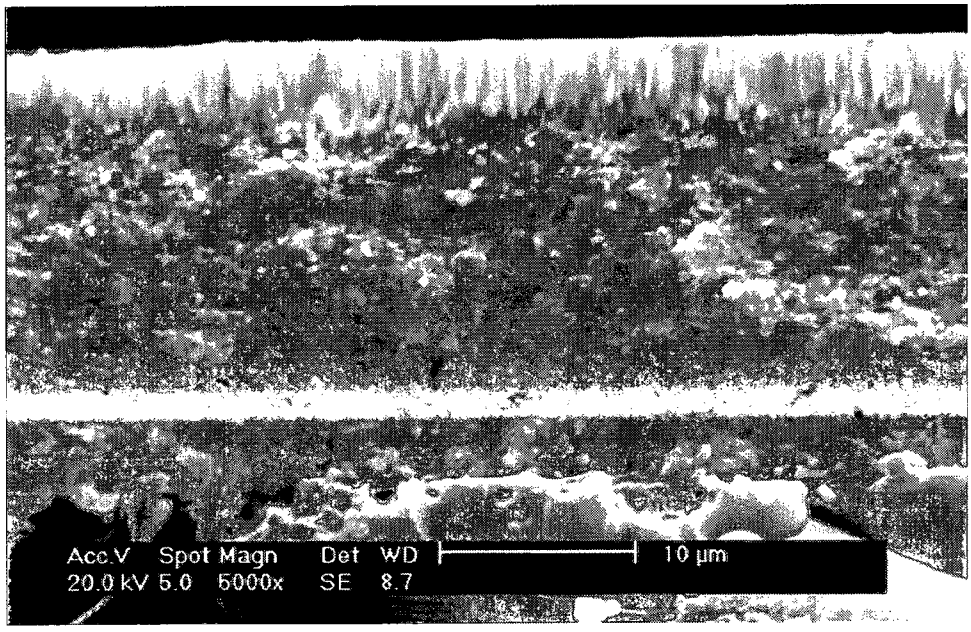

Figure 3.9 YSZ electrolyte coating deposited by SPS using a radially injection DC torch [Fauchais, 2005]

In order to produce the dense coatings, the suspensions or powders need to be injected into the centre of the plasma flame to be fully melted before impacting to the substrate.

However, it is very difficult to control the radial injection parameters to inject the all particles into the flame centre. Berghaus et al. used an axial injection DC torch to solve this problem [Berghaus, 2007] [Wang, 2008]. In their work, the Mettech Axial III torch equipped with an internal injection/atomization module was applied. This torch consists of three cathodes that can reduce the average arc voltage fluctuations. With this torch, a higher particle velocity of 691 m/s was achieved at short spray distance (50 mm) to synthesize the dense (porosity of 1.5%), thin (20 μm) and non-fractured samarium doped ceria (SDC) electrolyte using SPS process (Figure 3.10).

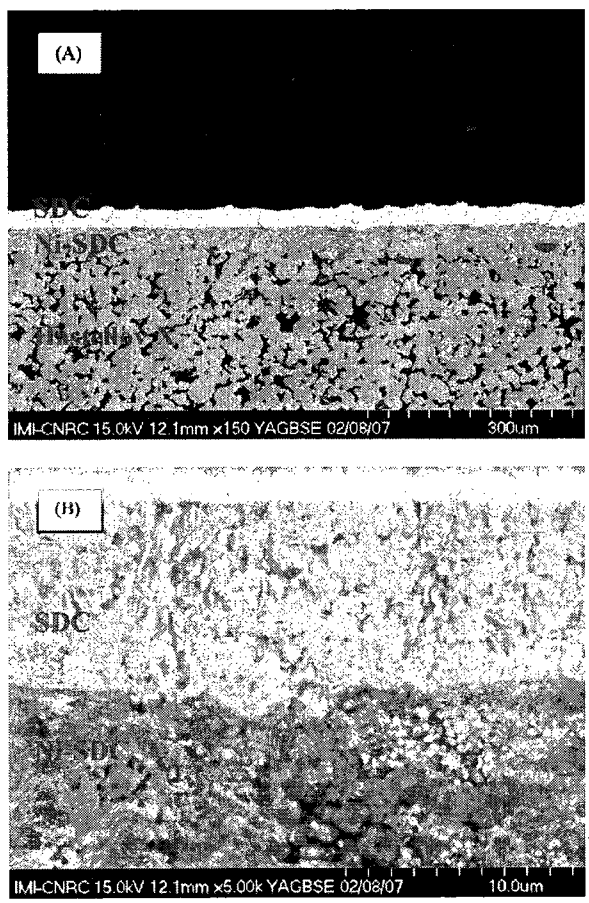

Figure 3.10 SDC electrolyte coating deposited by SPS using an axially injection DC torch [Berghaus, 2007]

Recently, US Nanocorp has been developing two plasma spray routes for the production of SOFCs electrolytes: (1) APS process for producing strontium- and magnesium-doped $LaGaO_3$ perovskite oxide (LSGM) electrolyte [Ma, 2005] [Ma, 2003], and (2) solution plasma spray for producing a dense 20YSZ electrolyte [Ma, 2003]. In their work, the LSGM electrolyte layer was deposited onto the LGM cathode layer by APS process. APS is proven to be capable of producing a thin layer as 50 μm which keeping the microstructure, continuity and uniformity of the deposit under the optimized plasma condition (Figure 3.11). The high OCV of the electrolyte was measured 1.045 V at 700 °C which indicates that the plasma sprayed electrolyte layer has a satisfactory gas tightness, and thus can isolated hydrogen and air effectively.

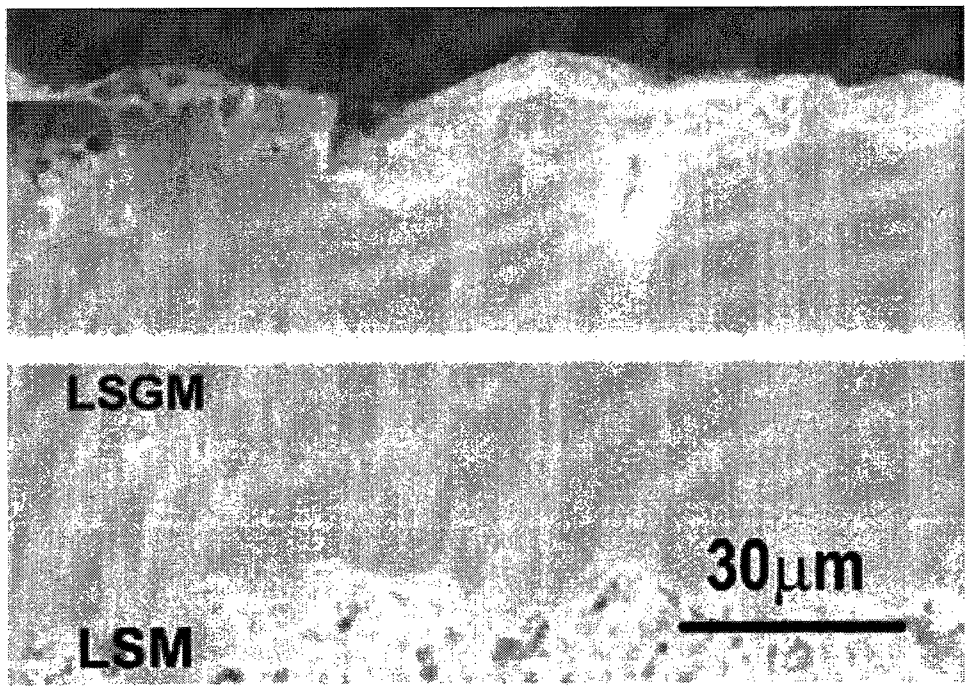

Figure 3.11 US Nanocorp APS sprayed LSGM electrolyte layer with a high coating density [Ma, 2003]

US Nanocorp and University of Connecticut have collaborated in a cooperative research endeavor to develop a solution plasma spray (SolPS) process for the deposition of dense YSZ (yttria-stabilized zirconia) coatings. In the SolPS process (Figure 3.12), liquid-precursor solutions are injected directly into the plasma jet. The atomized droplets undergo a series of physical and chemical reactions before deposition on the substrate as a coating. The SolPS process for the deposition of ceramic coatings offers several advantages over the conventional plasma spray method, such as circumvention of the powder-feedstock preparation step, better control over the chemistry of the deposit, the ability to deposit compositionally graded coatings with ease, the ability to deposit coatings that are inherently nano-structured (nanometer-scale grain sizes), and processing versatility. These advantages and the potential to deposit a wide range of ceramics (oxides and nonoxides) make the SolPS method attractive [Ma, 2004].

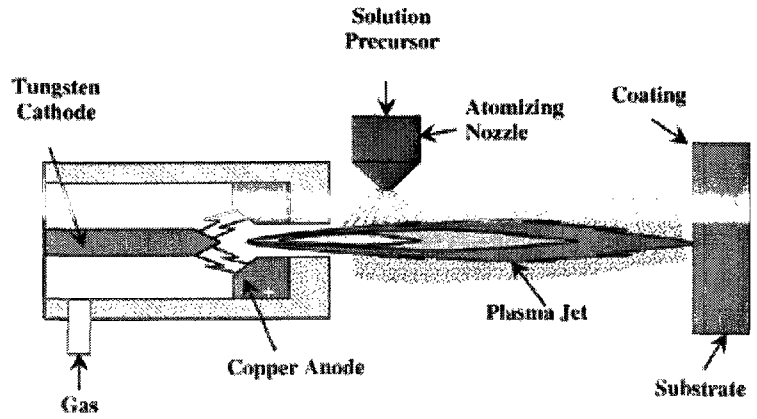

Figure 3.12 Schematic illustration of US Nanocorp solution precursor plasma spray process [Ma, 2004]

The work at US Nanocorp is directed towards SOFCs and addresses technical issues related to the formation of the ZrO_2 - 20 wt% Y_2O_3 coatings using SolPS with controlled

micro-structural features, especially coating porosity. According to their report, the YSZ coating was formed from a pyrolysis reaction of the solution precursor. They believe that the precursor droplets experienced sequential steps of droplet breakup, evaporation, pyrolysis, partial and /or full melting during droplet flight in the plasma. Thereafter, flattening, solidification and even sintering occurred while this combination impinged on the substrate. Consequently, the SolPS coating structure is highly dependent on those process parameters, which are adjustable by controlling the main factors which influence plasma flame and substrate temperatures. In conjunction with the plasma condition, other process parameters with liquid delivery and feeding were optimized enabling production of high density (98%) YSZ coating with a thickness of 690 μm using the SolPS process [Ma, 2005].

Vacuum plasma spray: As mentioned above, local overheating of substrates represents a severe problem with plasma spraying of SOFCs. Therefore, means have to be applied with which the cross section of the plasma jet is extended in order to reduce the thermal load. This requires special nozzles for the plasma source and adapted parameter conditions. Also the spray distance has to be enlarged, where nevertheless the spray material should stay hot enough to hit the target in molten state. One possibility to meet these demands is to spray in an environment with reduced pressure and with nozzles allowing for supersonic plasma jets when a sufficient pressure gradient between the plasma source and the spray reactor exists. DLR has long experience with the design of supersonic nozzles for VPS and its application for SOFCs [Schiller, 2000]. Novel plasma torches with Laval-like nozzle contours for supersonic plasma jet velocities of up to 2000 to 3000 m/s have been developed, resulting in enhanced spray particle velocities of up to

600 to 700 m/s (Figure 3.13). This leads to an increase of the heat and momentum transfer to the ceramic particles, thereby resulting in completely molten particles with high velocities. Therefore, the formation of a dense lamellar micro-structured electrolyte layer with high inter-particle bonding can be achieved [Lang, 2001].

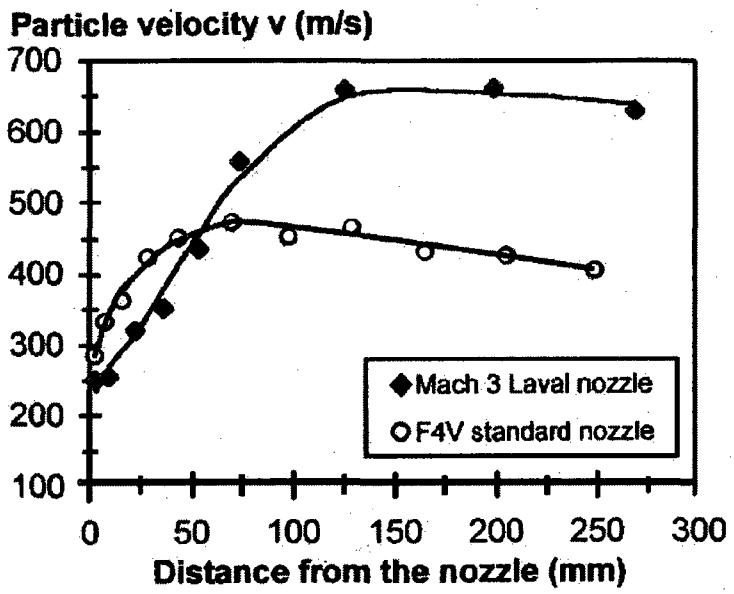

Figure 3.13 Velocities of the YSZ powder, sprayed with different DLR-VPS plasma nozzl [Schiller, 2000]

With VPS such nozzles can generate an extended hot cross section of the plasma jet where more powder particles are becoming involved (Figure 3.14). This means higher deposition efficiency, reduced peak temperature in the jet center and lower local thermal load for the substrate (8 µm/pass at a distance from the nozzle of 220 mm). The jets show reduced gradients at the rim. Also the cold gas entrainment is delayed. The extended spray area allows for a better overlap at scanning over the substrate. With VPS further improvements, the velocity of plasma jet and sprayed material can be increased, resulting

in denser coatings, reduced entrainment effect and the advantage for extended spray distance reducing further thermal loads and gradients.

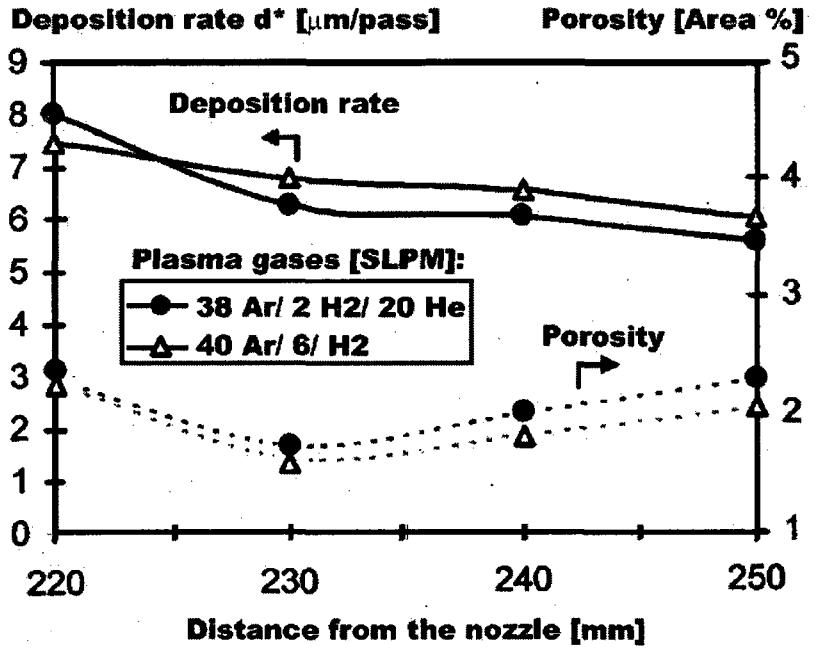

Figure 3.14 Deposition rate and porosity of DLR-VPS plasma-sprayed YSZ electrolytes [Schiller, 2000]

Renouard-Vallet et al [Renouard-Vallet, 2004] separately elaborated the SOFCs' electrolytes by using APS and VPS, to compare produced electrolytes' properties. In their study, the plasma is generated using a Sulzer Metco F4V8 plasma gun for both APS and VPS experiments. A supersonic "de Laval" nozzle Mach 2.5 with an axial plasma forming gas injection and an in internal powder injection to lead to high particle velocities (350 m/s) at the atmospheric pressure with high surface temperature (T = 3170 °C). For VPS experiments, a VPS nozzle (Medicoat AG, Switzerland) and an internal injection were used. The authors described that the electrolyte porosity controls not only

the mass of gas diffusion, but together with the quality of the internal structure of the lamellas also the oxygen-ion conductivity and hence the internal polarization losses. For APS and VPS the relationships between spraying conditions and the in-flight properties of the particles upon impact were studied in addition to the resulting coatings. It turned out that in general the oxygen-ion conductivity of optimized VPS-YSZ layers overcame the values of APS-produced layers. Moreover, a rise of the substrate temperature also improves the conductivity due to better inter-lamellar contacts.

High velocity oxy-fuel (HVOF): The small particles created in SPS carry little momentum and low thermal inertia. They generally have to be heated far above their melting point in the high-temperature plasma ($T_{\text{flame}} > 8000$ °C) to retain melting phase and high velocity further downstream at the impact on the substrate to form a dense coating. For ceria, this high superheating in the chemically reducing plasma can lead to an undesirable transformation of CeO_2 to Ce_2O_3, which is associated with a lowering of the melting and boiling points [Sodeoka, 19971]. The decomposition and resulting vaporization can limit deposition efficiency, electrochemical performance, and mechanical integrity of the electrolyte. Employing a much lower flame temperature of a high-velocity oxy-fuel (HVOF) system (2600-3200 °C) may alleviate these effects, under the condition that the ceria particles are still heated to at least their melting point (~2730 °C) [Sodeoka, 1997]. Maximum particle temperatures in HVOF depend on a number of factors, including the torch design, the fuel and fuel-to-oxygen ratio, the feedstock and feed rate, and the position in the flame. Advantages of HVOF spraying of conventional feedstock powders for SOFCs production were demonstrated at University of Stuttgart [Gadow, 2007]. Berghaus et al. reported HVOF suspension spraying for the

production of ceria-based electrolyte coatings and the role of operating parameters on the in-flight particle states and microstructure are discussed [Berghaus, 2008].

Suspension spraying (suspension of 2.5 wt.% SDC with particle size of approximately 20 nm were prepared in a mixture of ethanol and ethylene glycol) for the SDC coatings was implemented using an HVOF DJ-2700 hybrid gun (Sulzer- Metco, Westbury, NY) using propylene fuel (C_3H_6). The system was equipped with an internal injection/atomization module inserted into the standard powder feeding port, thereby intimately contacting the coaxially fed suspension droplets with the fuel inside the HVOF combustion chamber. Optimum spray parameters in terms of fuel-to-oxygen ratio, feedstock/suspension conditions, and standoff distance were established using in-flight particle diagnostics (Figure 3.15). The HVOF flame was found to limit evaporation and decomposition of the feedstock and to favorably affect the coating stresses, resulting in low-porosity (no visible open porosity and closed porosity <2% as estimated from cross-section SEM image analysis), smooth, and virtually defect-free coatings of 20μm thickness (Figure 3.16).

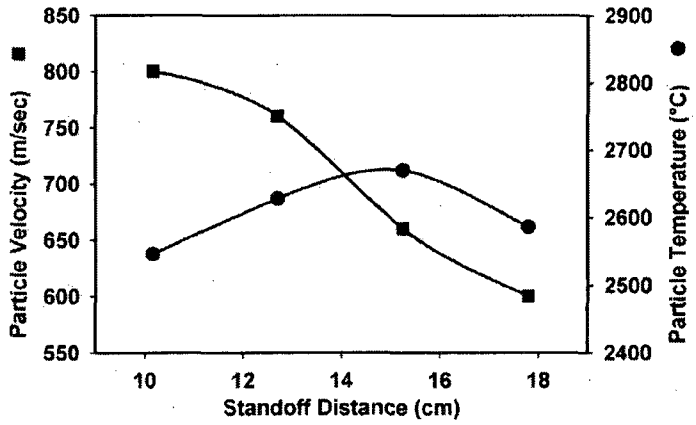

Figure 3.15 Axial T-V profile for SDC electrolyte deposited by HVOF process [Berghaus, 2008]

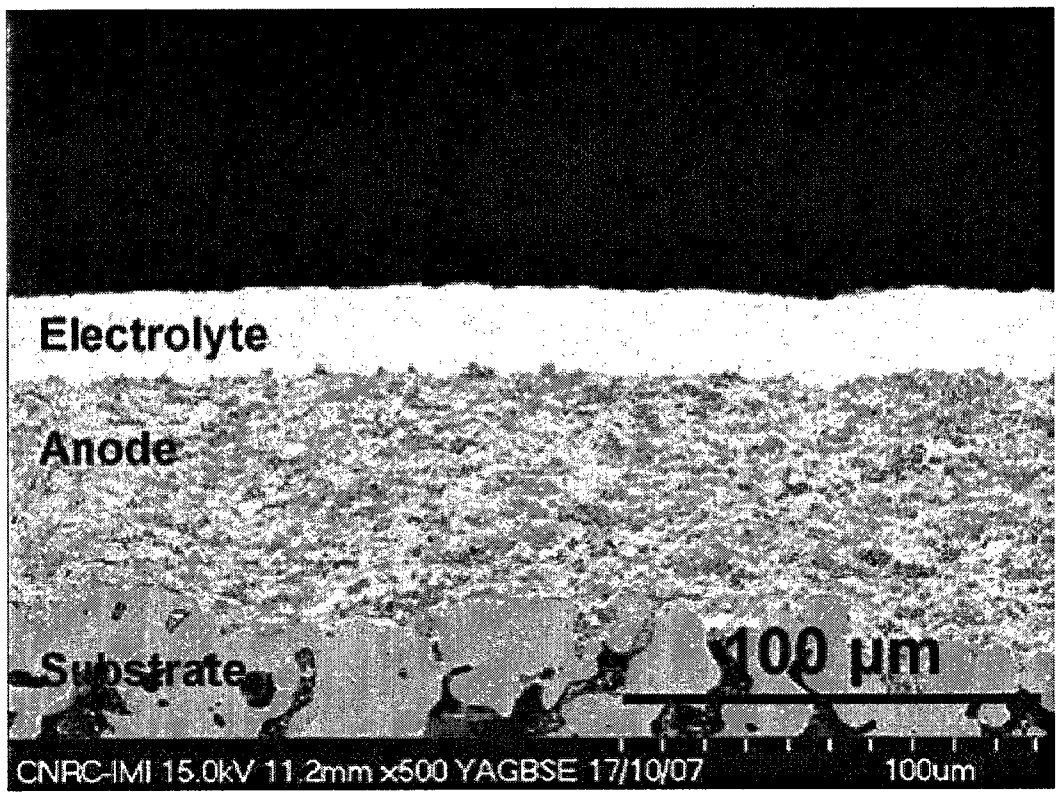

Figure 3.16 Microstructure of HVOF sprayed half cell [Berghaus, 2008]

High velocity suspension flame spray (HVSFS): Spraying nano-oxide ceramic suspensions by means of high velocity suspension flame spraying (HVSFS) developed at Institute for Manufacturing Technologies of Ceramic Components and Composites (IMTCCC) (University of Stuttgart, Germany), proven to run as a stable process. Thanks to the very high particle velocity generated by the modified HVOF torch, it is possible to produce very dense coatings [Rauch, 2009]. The suspension is axial suspension injection of the HVSFS process overcomes many of the injection problems encountered in suspension plasma spraying processes, where the suspension is fed radically to the plasma jet. New nozzle/combustion chamber designs also have developed to reduce the strong turbulences that occur in the combustion chamber interfere with the small particles

of the suspensions (Figure 3.17). The YSZ suspension is flame sprayed with a suspension feeding rate of approx. 9.5 g/min using a 0.7 mm conical nozzle. Ethane is generally chosen as the fuel gas to achieve a high flame temperature (2924°C). The deposition rate is in the range 8 -10 μm/cycle. Fully dense YSZ coatings with a refined microstructure and a layer thickness typically ranging from 20-50 μm can be achieved (Figure 3.18).

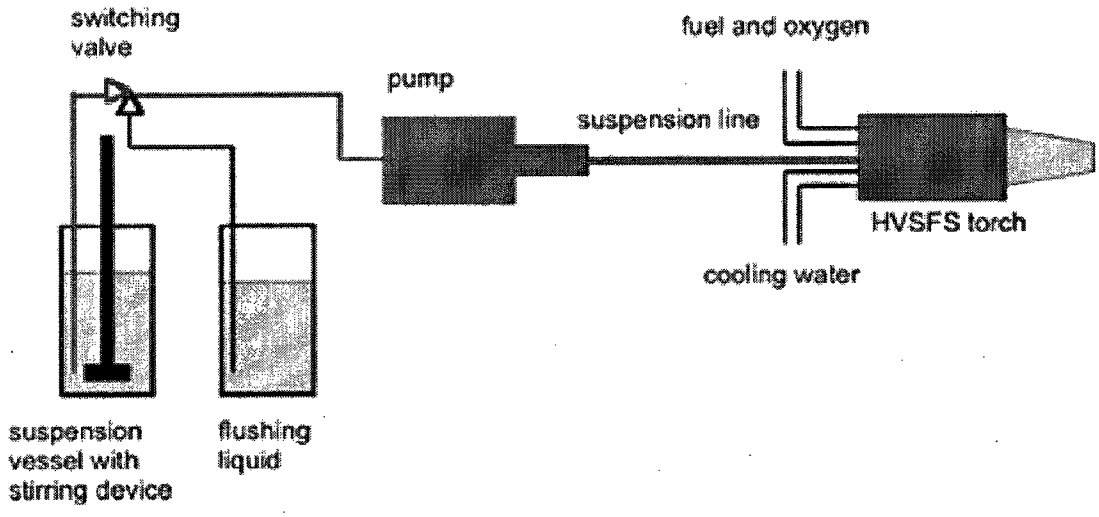

Figure 3.17 Outline of the HVSFS process [Rauch, 2009]

The main challenge of this application is the prevention of micro cracks in the coating that decline the necessary gas-tightness of the 8-YSZ electrolyte layer of the SOFC. Further process development has to be accomplished to abolish this critical circumstance and make a serial production possible.

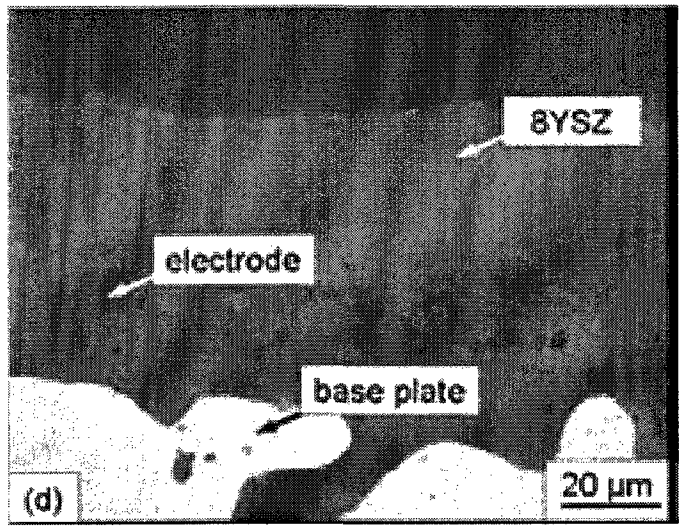

Figure 3.18 Microscope images of 8YSZ layer sprayed by HVSFS process [Rauch, 2009]

Radio frequency plasma spray (RFPS): Radio Frequency plasma spraying (also known as Induction Plasma Spraying, RF-ICP) applied in a reduced pressure environment seems also to be promising because the spray material (powder, suspensions or liquids for plasma synthesis) can be centrally injected (Figure 3.19), not more or less in radial direction as with standard DC equipment. This means better process conditions, in principle. Also higher spray material inertia with less material evaporation due to higher velocity is possible due to shorter dwell time. With larger spray distance also a reduced area specific thermal load can be obtained.

In the paper of Mailhot et al. [Mailhot, 1998], the influence of the different process parameters on porosity with supersonic induction plasma spraying of yttria stabilized zirconia films was investigated, showing that high density layers could be obtained using a supersonic Laval nozzle integrated on a standard torch. 50 to 100 µm YSZ coatings with porosity of near 1% could be obtained using this technique at relatively high

deposition rates (10 g/min). In a recent paper of Renouard-Vallet et al. [Renouard-Vallet, 2003] further progress with this process-type was reported.

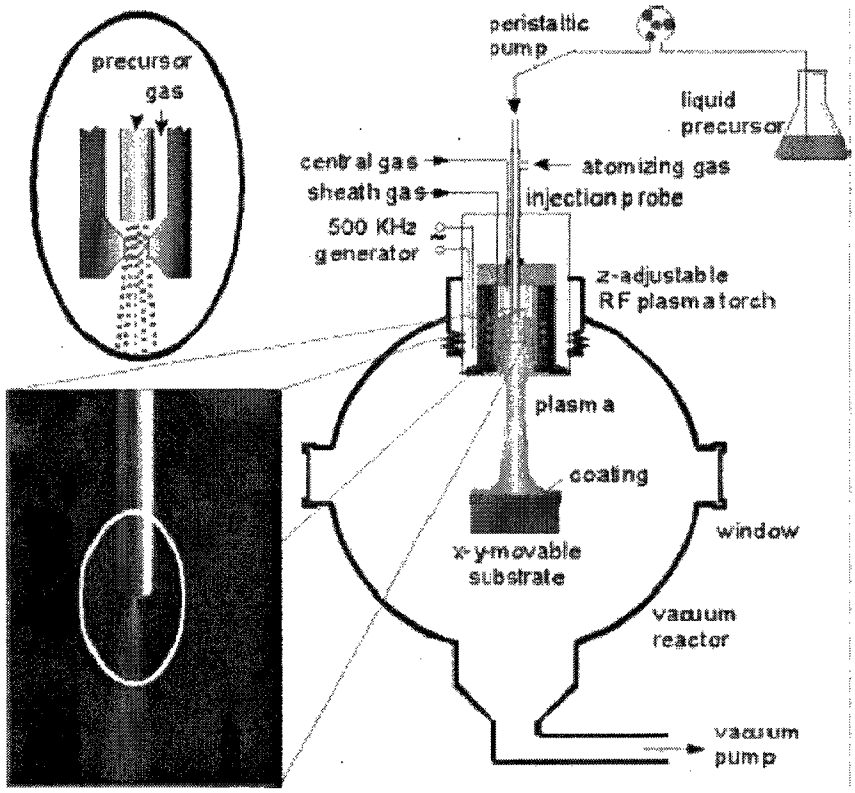

Figure 3.19 Experimental set-up for RF-IPS system [Schille, 2004]

Hybrid plasma spray (HYPS): The study of Yoshida et al [Yoshida, 1992] was aimed at developing an integrated fabrication process for solid oxide fuel cells (SOFC) with radio-frequency plasma spraying (RFPS) and/or hybrid plasma spraying (HYPS). Fundamental studies concerning particle velocity and deformation showed that the novel plasma spraying processes were mainly characterized by their superior capability for homogeneous heating and spraying of large size powders with relatively low particle velocity. The lower particle velocities in RFPS (20 m/s) and HYPS (40-70 m/s) compared

with those in direct current plasma spraying (200 m/s) were found to be sufficient for deformation of impinging molten particles on the substrate. However, RESP imposed a severe limitation on the substrate position because it led to a short flying distance for the molten particles. In this respect, HYPS was considered to be superior to RFPS. With 75 μm YSZ powder, using of HYPS made it possible to get not only dense YSZ coating with relative density higher than 98%, but also good gas permeability, lower than 5.7×10^{-7} cm $g^{-1}s^{-1}$.

Triple torch plasma reactor: Heberlein et al [Heberlein, 2000] developed a new approach to produce electrolyte. This approach is based on different plasma deposition processes performed successively in the same chamber. A schematic of the triple torch plasma reactor (TTPR) is shown in Figure 3.20. Three DC plasma torches are mounted on the top flange of a controlled-atmosphere chamber. The jets of the three torches coalesce to form one enlarged plasma jet. To deposit the YSZ electrolyte layer, fine YSZ powder suspended in argon carrier gas, is injected axially through a central probe into the region where three plasma jets merge. The chamber pressure remains at 100 Torr. The center injection-low pressure plasma spray process (CI-LPPS) results in a 70 μm thick and dense layer (OVC = 1.08 V).

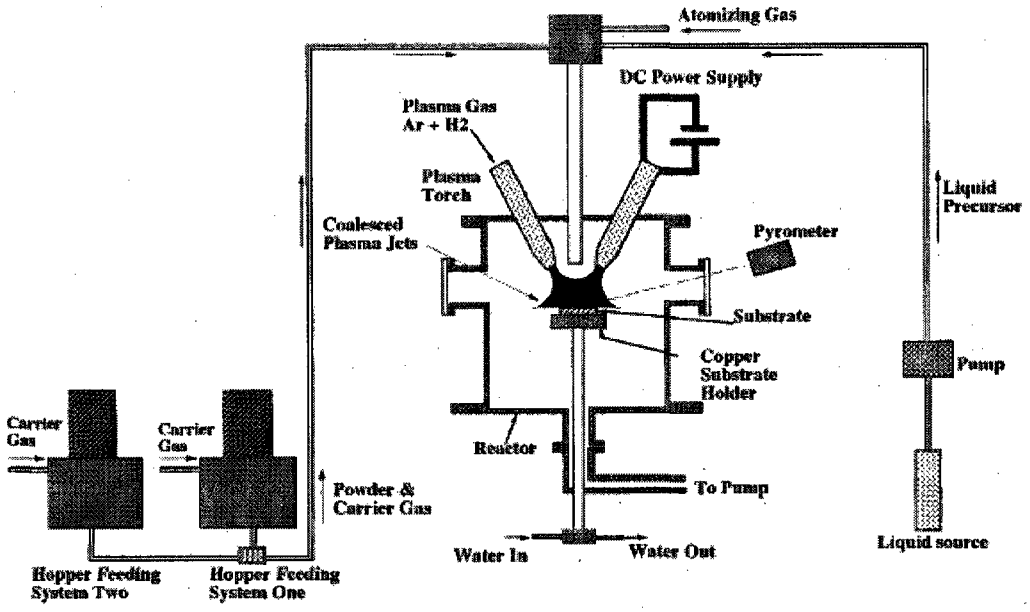

Figure 3.20 Schematic of triple torch plasma reactor setup [Heberlein, 2000]

Moreover, a comparative study of the film obtained with the CI-LPPS in the triple torch reactor with YSZ films obtained with the same powder under APS conditions has been performed in their paper. A double layer has been prepared in which an YSZ has deposited using the CI-LPPS process on top of an YSZ film deposited under APS conditions. According to their report, the APS-YSZ layer exhibits a delaminating type fracture with columnar grains visible inside the lamellae and with laminar porosity or micro-cracks along the lamellae. Therefore, the lamellae in the APS layer are bonded together by mechanical interlocking. In contrast, the CI-LPPS layer shows a translamella type of fracture resulting from inter-lamellar chemical bonding brought about by a liquid sintering effect and higher velocities of the particles involved in the film preparation (Figure 3.21). They concluded that the following combination of conditions is unique to

the CI-LPPS process: (a) all particles pass through the hot plasma region created by the coalescence of the three plasma jets, and all are in a molten state when they impinge on the substrate; (b) the heat flux from the three plasma jets in combination with the low thermal conductivity of the porous substrate will result in higher substrate temperatures than one usually encounters in spray deposition; and (c) there is additional deposition from the vapor phase because some of the material from the particles is vaporized. These factors allow liquid sintering to occur, resulting in the very dense coating without visible lamellar structures.

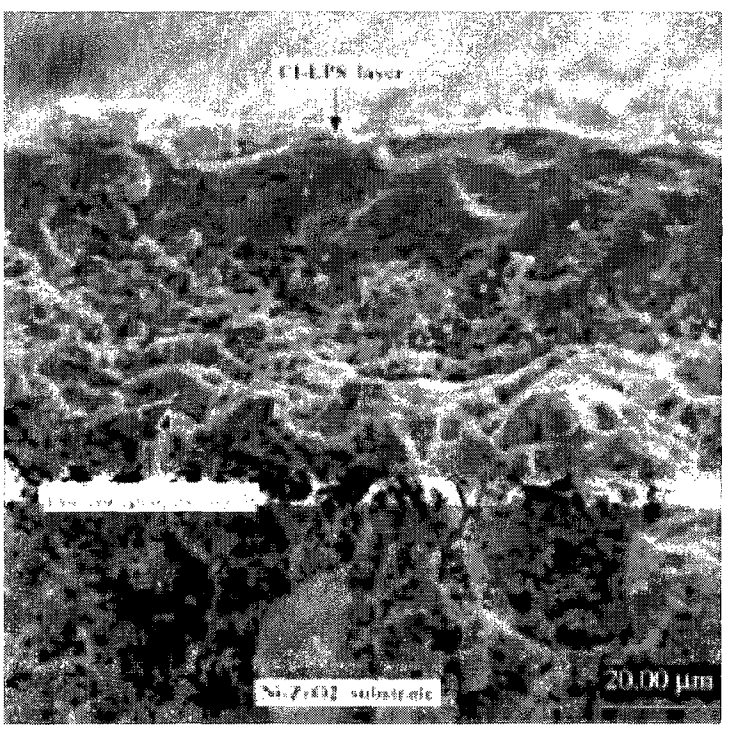

Figure 3.21 Comparison of YSZ electrolyte layer deposited by CI-LPS process to APS-deposited YSZ layer [Heberlein, 2000]

Low pressure plasma spray-thin film (LPPS-TF): Low pressure plasma spray-thin film (LPPS-TF) is a vacuum plasma spray technology recently developed by Sulzer Metco AG (Switzerland) to coat out of the vapor phase (Figure 22). In comparison to conventional vacuum plasma spraying (VPS) or low pressure plasma spraying (LPPS), LPPS-TF uses a working pressure below 2 mbar and a high energy plasma gun. This leads to unconventional plasma jet characteristics which can be used to obtain specific and unique coatings. An important new feature of LPPS-TF is the possibility to deposit a coating not only by melting the feed stock material which builds up a layer from liquid splats but also by vaporizing the injected material. Therefore the LPPS-TF process fills the gap between the conventional PVD/CVD technologies and standard thermal spray processes. The vaporizing of coating material and producing layers out of the vapor phase result in new and unique coating microstructures.

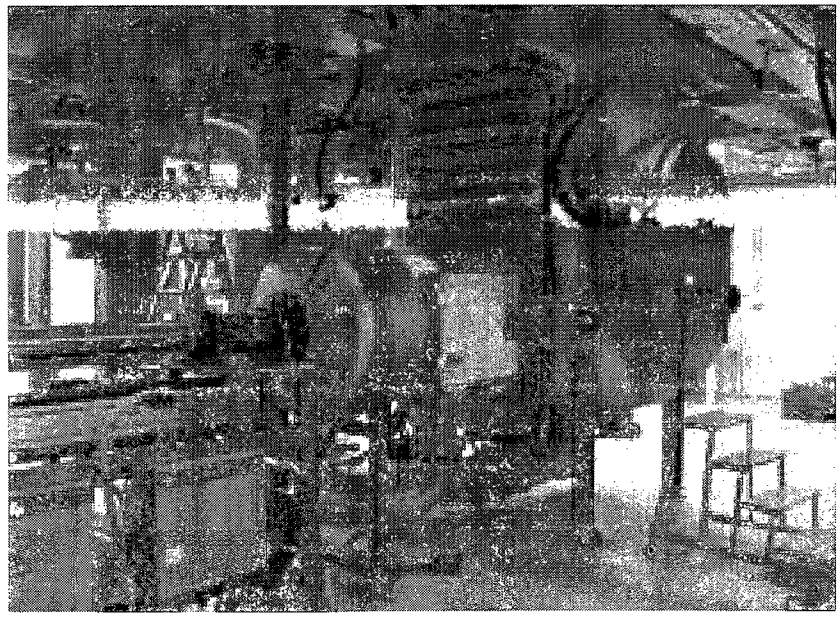

Figure 3.22 LPPS-TF system with large vacuum chamber and horizontal sting manipulator [Refke, 2007]

A considerable progress promises to produce SOFCs electrolyte in terms of LPPS-TF process [Refke, 2004]. The O3CP-torch of Sulzer Metco was applied to generate the high power up to 180 kW in combination with the reduced work pressure range between 1 and 20 mbar. This creates a high enthalpy plasma stream with increased jet dimensions of 1-2 m length and 20-40 cm diameter. In this way, the spray pattern is enlarged reducing thermal gradients and promising a more homogeneous material deposition. It is reported that using an $Ar/He/H_2$ gas mixture at a chamber pressure of 1.5 mbar, an input power of 125-150 kW with a powder feed rate of 90 g/min a typical deposition efficiency of 40-45% can be obtained. The torch can be rapidly moved and the spray plume passes therefore very quickly over the substrate to control the heat load. Typically, about 1 μm is deposited per pass. According to the report 40 μm are necessary to get a dense electrolyte [Refke, 2007]. If post-sintering is allowed the required layer thickness for the necessary density could perhaps be reduced toward 30 μm (Figure 3.23).

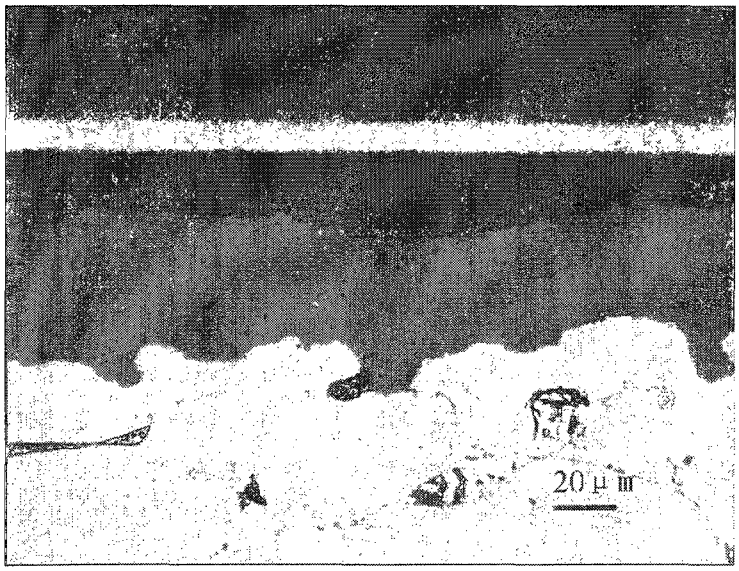

Figure 3.23 40 μm YSZ electrolyte coating deposited by LPPS-TF process [Refke, 2007]

3.3.3 Production of anodes

The anode has to provide the reaction sites for the electrochemical oxidation of the fuel gas such as hydrogen and carbon monoxide (H_2 and CO, respectively) to water (H_2O) and carbon dioxide (CO_2). Thus, the layer must have a high open porosity, represented by a low flow resistance, to guarantee a sufficient supply of fuel gases and the disposal of reaction products. To obtain a highly efficient fuel cell, the anode has to fulfill the following requirements: homogeneous pore and material distributions provide an increase in electrochemical active areas and reduce polarization resistance. The thermal expansion coefficient of anode should be close to that of electrolyte to ensure a good adhesion between these two compartments. The anode layer must show a high stability under reducing and oxidizing conditions and has to demonstrate high electronic and ionic conductivity as well as a high catalytic activity for the electrochemical reaction under operating conditions. The minimization of the electrode resistance (polarization and ohmic) represents one of the greatest challenges in obtaining high, stable power densities [Mizusaki, 1995]. Porous Ni-YSZ cermets are the most frequently applied anode materials, at present, processed conventionally by plasma spraying processes.

Atmospheric plasma spray: As with all plasma spraying experiments of mixtures of YSZ with Ni or NiO, a strong influence of plasma power on layer density and as well as on the fractions of Ni and YSZ within the resulting deposit has been observed. Recently, Hathiramani et al. [Hathiramani, 2006] carried out the experiments using different types of powder feedstock in order to develop anode layers by atmospheric plasma spraying. The different feedstock comprised NiO or Ni powders mixed with YSZ as starting material, agglomerates of NiO and YSZ premixed on a sub-micrometer range, blended

NiO/YSZ powder and of individual NiO and YSZ powders, separately injected. The performance of the produced APS anodes were subsequently investigated in single fuel cell tests. The results showed the importance for getting a large three-phase boundary that NiO and YSZ phases are homogeneously mixed on a sub-micrometer range. Under this condition almost all the compared procedures gave comparable electrochemical results. But, the anodes made by separate injection of NiO and YSZ into the plasma plume revealed a better thermal cycling behavior. With this type of anode, operated at 800 °C and H_2 as fuel, a cell voltage of 0.7 V and a power density of about 500 mW/cm^2 could be obtained according to this article.

An alternative way to make porous anodes is the use of Ni-coated graphite powder (Ni-C) together with YSZ with the idea to get the porosity by burning-away the carbon content during and after the deposition process. Weckmann et al. [Weckmann, 2005] studied the influence of the parameters on microstructure, porosity, roughness, triple phase boundary and electrochemical behavior of the products with a Triplex II system at the site of Sulzer Metco AG, Wohlen, Switzerland. The results shown that using a fine Ni-graphite powder fraction (Ni(C)) denser layers with smoother surfaces and a higher share of YSZ within the layer were obtained with increasing the torch power.

As mentioned above, one of the greatest challenges of electrode is to minimize the electrode resistance (polarization and ohmic). The novel method now to reduce the energy losses from anode is to use nano-structured composite anode [Virkar, 2003]. The nano-structured composite anode is expected to provide longer triple-phase boundaries (TPB) that extend well into anode so that catalytically assisted electrochemical reactions

in anode can be enhanced. In order to minimize anode resistance, Huang et al [Hwang, 2008] injected YSZ-NiO powders which containing nano-YSZ and NiO powders into the APS high temperature plasma flame to deposit the porous YSZ-NiO coating (Figure 3.24). The nano-scaled NiO particles are wrapped by the nano-structured YSZ network, and NiO and YSZ networks interlace. The nano-structured YSZ-NiO anode coating produced herein can provide significantly longer triple phase boundaries for hydrogen oxidation reactions than those in the micro-structured YSZ-Ni coating. Moreover, from analyzing measured ac impedance data at 800 °C by equivalent circuit fitting, it is found that anode resistance $0.024\Omega cm^2$ is smaller than electrolyte resistance $0.11\Omega cm^2$ and cathode resistance $0.11\Omega cm^2$ according to this article.

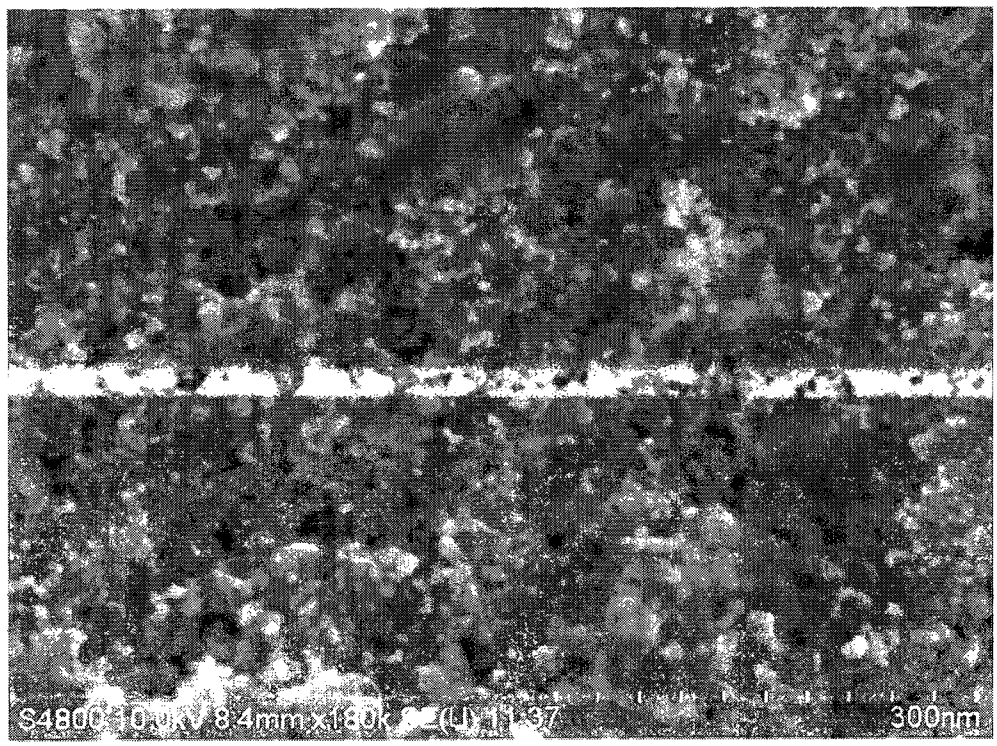

Figure 3.24 Nano-structured surface of APS deposited anode [Hwang, 2008]

At present, conventional SOFCs anodes are made of an active electro-catalytic Ni-YSZ cermet. Such anodes are most appropriate for SOFCs running on hydrogen than for those fed directly with methane. That is because problems of carbon anode poisoning, sintering of anode particles and thermal phenomena management at the anodic compartment. A search is under way for replacing the Ni by either Ni-based bimetallic compounds or mixed metal oxides of perovskite type anode material.

To improve the internal reforming reactions at SOFC anode, Benyoucef et al. [Benyoucef, 2008] coated alternative (Ni, Cu, Co) –YSZ and Cu-Co-YSZ anode cermets at different weight ratio by APS. It is found that the nature and the percentages of metals have a considerable influence on both monometallic and bimetallic cermets porosities. Co-YSZ cermet of (2:3) weight ratio coating reaches a maximum porosity of 21.57%. The metal content in the cermets have a negligible influence on the crystalline phase structure and that for the bimetallic cermets Co diffused in Cu lattice offering the best electronic conductivity, carbon tolerance and thermal stability [Lee, 2005]. Such bimetallic materials anode are very interesting because carbon formation due to electrochemical anodic reaction, can often be avoided by replacing Ni with an electron conductor such as Cu that does not catalyze carbon formation, and Co as second metal that provides thermal stability.

Vacuum plasma spray: An extended work on the plasma spraying of thin and porous Ni-YSZ anodes under reduced pressure was performed by Lang et al. at German Aerospace Center (DLR) [Lang, 2001]. In their study, the high melting YSZ ceramic powders were injected internally, which the lower melting NiO powder was fed

externally of the laval-like nozzle into the plasma. It has been proven that the particle velocities depend strongly on the spray parameters such as type of torch nozzle, gas composition, chamber pressure, and torch power. With the optimized spray parameters, particle velocities between 380 m/s at a distance of 50 mm and 250 m/s at a distance of 240 mm were measured under the reduced pressure of 200 mbar for the spraying of the anode layer. The relatively low velocity of the particles at impact on the substrate leads to the desired formation of porous anode with porosity of 21 vol. %, which ensures sufficiently high gas diffusion. With this type of anode, the cells show very good electrochemical performance and low internal resistances. Power densities of 300 to 400 mW/cm^2 at low operating temperatures of 750 to 800 °C were achieved.

Low pressure plasma spray: LPPS showed some advantageous properties for spraying of anodes [Refke, 2004]. Refke et al. used the LPPS equipment for processing of mixtures of Ni(C) with YSZ and reached the desired layer porosity of about 30% with a deposition efficiency of 40-50%. Also in the case of LPPS a specific adjustment of the spray parameters was necessary because of the different melting and deposition behavior of both powder components.

Solution or/and Suspension plasma Spray: In conventional plasma spray of SOFC anode, the large NiO and YSZ particles used, about 50-150 microns for high-porosity coating, to reduce the density of three-phase sites for electrode reaction. In addition, NiO and YSZ powders for conventional plasma spray cannot be homogenously mixed due to the large density difference of the two powders, resulting in inhomogeneous distribution of the two phases in the fabricated coatings. Recently, suspension or/and solution plasma

spraying processes have been developed due to the potential to deposit a highly efficient Ni-YSZ anode. In the application of Fauchais et al. [Fauchais, 2007], Ni was introduced as a nitrate solution in ethanol according to the reaction:

$$6NiNO_3 + 2CH_3CH_2 - OH \rightarrow 6NiO + 3N_2 + 4CO_2 + 6H_2O \qquad (3\text{-}7)$$

The Ni solution and the YSZ suspension were injected simultaneously to Sulzer Metco PTF4 plasma torch, a porous coating has been obtained with a uniform distribution of Ni within zirconia (Figure 3.25). The solution is fragmented into droplets where the NiO droplets are vaporized and NiO re-condenses on YSZ particles. Works are still in progress to develop these anodes in Limoges University.

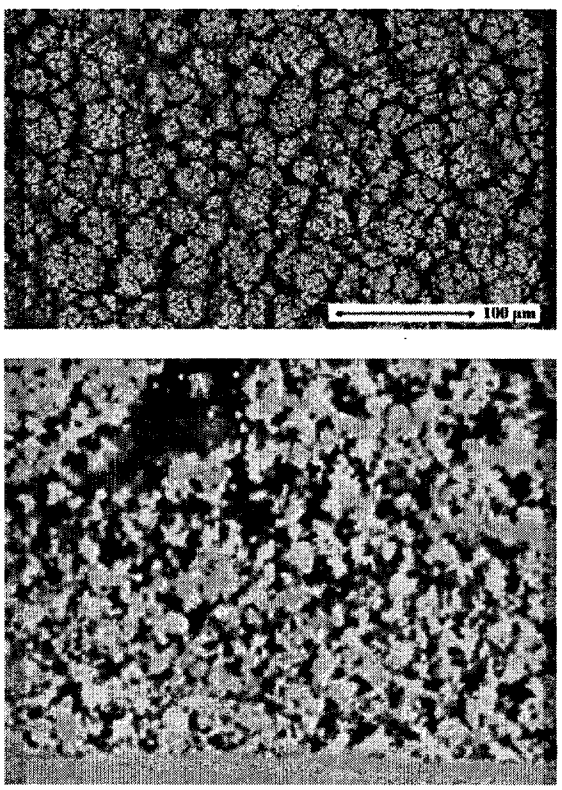

Figure 3.25 Anode coating co-sprayed with YSZ suspension and solution of nickel nitrate [Fauchais, 2007]

Solution plasma spraying process also has been developed by US Nanocorp to produce 40 mol% La_2O_3-doped CeO_2 + 50 mol% NiO anodes. Lanthanum, cerium and nickel salts were dissolved in distilled water according to stoichiometric compositions, and then APS deposited to form highly porous (porosity 40-50 vol. %) and thin (with a thickness of 20 to 50 μm) SOFCs anode by controlling the chemical concentration in the solution precursors and the flow rate. The deposition mechanism of the formation of a SolPS coating was discussed by Ma et al. [Ma, 2005]. In the SolPS process, it has been verified that a film or coating is formed in sequential multiple steps involving a series of physical and chemical reactions of precursor droplets. The multiple steps consist of (a) generation of liquid droplets via a liquid injector, and then radially liquid feeding into the plasma flame that has a high temperature and velocity; (b) breakdown of original droplets into ten times smaller droplets simultaneously when penetrating into the torch due to the dynamic interaction between droplets and the plasma torch; (c) evaporation of solvent in the hot plasma, and formation of gel-like stuff due to heating and concentrating of the chemical precursor; (d) thermal decomposition of the precursor occurs in pyrolysis reaction; (e) formation of solid state particles (nano-meters or micrometers in diameters); (f) partially or/and fully melting of the particles with the residence of several milliseconds; (g) flattening of melted particles upon impacting the substrate forms splats; and (h) final building up of a film or coating. The microstructure of a SolPS coating will be determined by those critical parameters including original droplet momentum, plasma and heat transfer, flight trajectory and residence time of droplets in plasma and substrate temperature as well. As a result, fine splats with a typical size of less than 0.8 μm are produced in the SolPS process.

Results of further relevant investigation were added by Wang et al. in 2007 [Wang, 2007]. The solution precursor made by adding distilled water to the mixture of $ZrOCl_2 \cdot 8H_2O$, $Y(NO_3)_3 \cdot 6H_2O$ and $Ni(NO_3)_3 \cdot 6H_2O$ was sprayed with Miller SG-100 torch (Miller Thermal, Appleton, WI, USA) in atmosphere. The as-sprayed anode coatings consisted of a continuous Ni matrix and Ni-YSZ composite. The coatings have 30-50 % porosity.

Functional Graded Anodes: Generally, intermediate-temperature SOFCs operate under high-temperature conditions (~800 to 1000 °C). The strict bonding among each cell component results in mechanical constraints; thus a slight mismatch in the coefficient of thermal expansion (CTE) of cell components causes large thermal stress [Yakable, 2004]. As a consequence, CTE matching among the cell components is indispensable to reduce the internal stress. In addition, the contact state of the interfaces between electrodes and electrolyte severely influences the output power of the SOFCs. Functionally graded layers provide a solution to meet these requirements.

In general, the anode graded layers of a few micrometers thickness is prepared to enhance the electrochemical performance. Thermal plasma process facilitates the deposition of graded layers with changes in composition or microstructure as a function of distance across the deposited layer. Traditional wet ceramic techniques can deposit only discrete layers of a fixed composition and powder particle size distribution. Therefore, if a spatial variation in microstructure and composition is desired, multiple depositions of discrete layers must be performed to obtain the functionally graded electrodes, by utilizing a series of different slurry feedstock. In contrast, thermal plasma process can introduce

compositional gradients in microstructure in a coated layer by spraying the two components from separate reservoirs, and gradually changing the relative amounts of each as the coating is deposited [Giannakopoulos, 1995]. Moreover, both the porosity and particle surface areas can be controlled during deposition in order to obtain microstructures ranging from a high-reaction surface area and TPB length near the electrode-electrolyte interfaces to a higher porosity near the electrode-interconnect boundary. These micro-structural gradients can be achieved during deposition by varying the spray parameters while building the layers, or by changing to a different feedstock reservoir with different powder particle size distributions during spraying. Additionally, higher electronic conductivity phases for current collection can be deposited at higher volume fractions towards the electrode-interconnect boundary. Such compositional gradients have been shown to significantly reduce thermal stresses caused by the changes in operating temperatures, relative to the thermal stresses present at the sharp interface between two adjacent but dissimilar materials [Stöver, 2004].

APS recently has been demonstrated by Xia et al. [Xia, 2009] to prepare functionally graded layers of SOFCs by gradually changing the compositions of powders. Anode graded layers were deposited by a Metco 9 MB gun. YSZ-Ni-C premixed powders and YSZ powders injection flow rate were adjusted using a specially developed three hopper powder feeding system. Carbon powder was added as a pore forming agent. Following the adjustment of the spray parameters and the addition of carbon powder into anode powder, the porosities of the anode were changing from 32.74 % at the anode side to 3 % at the electrolyte side, which is sufficient to the operation requirements of SOFCs (Figure 3.26). The graded anodes have far lower interface resistance than those without graded

layers. They also exhibit much higher electrochemical performance, which can be attributed to the grading of composition and microstructure leading to improved functionality of the individual layers.

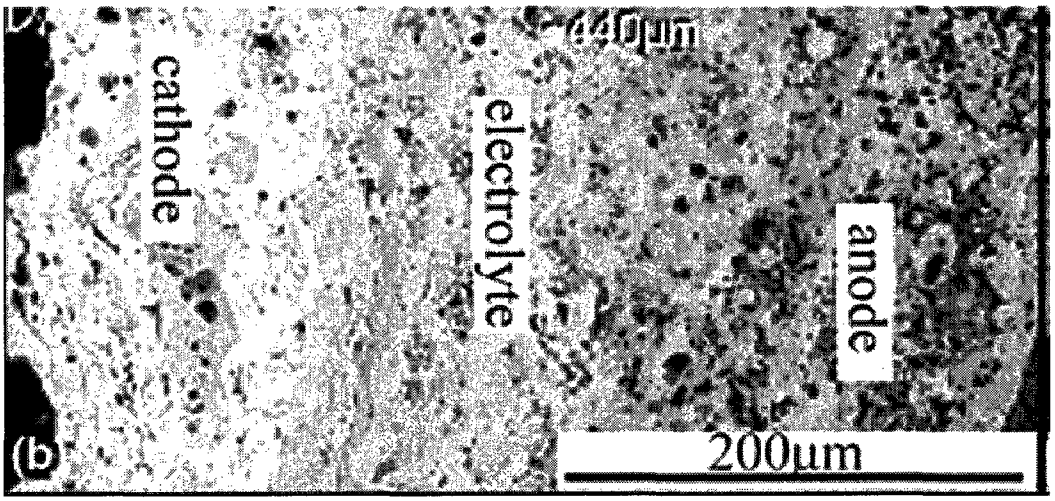

Figure 3.26 Functionally graded anode produced by APS [Xia, 2009]

Thermal plasma deposition methods show a high potential for producing such graded structures for improved anodes. More work in this direction should be done in future to take further advantage of this potential. RF plasma application in this field will be discussed in more detail in Chapter 4.

3.3.4 Production of cathodes

SOFCs make use of a dense ceramic solid electrolyte exhibiting a high ionic conductivity and a low electronic conductivity. Porous electrode catalysts are deposited on both side of the electrolyte. At the cathode, oxygen reduction occurs and the ionic species pass through the electrolyte to the anode where oxidation of the fuel occurs. Therefore, the cathode must show high electronic and ionic conductivity, sufficient thermal and

chemical stability at high temperatures in air and good compatibility with the electrolyte. Electrochemical activity in an SOFCs cathode occurs at triple phase boundary (TPB), where gaseous oxygen and ionic and electronic conducting phases come into contact. The greater the length of the triple phase boundaries, the greater the cathode activity and the better the cell performance is. Thus, two main approaches can be adopted to improve the cathode performance: (a) changing material composition or components, such as using a composite cathode structure, containing the materials of both cathode and electrolyte. TPB is thereby extended beyond the cathode/electrolyte interface, into the cathode bulk, thus greatly enhancing cathode activity and performance [Østergard, 1995], and (b) optimizing cathodic structure, such as adjusting porosity [Tsai, 1997], particle size, spatial distribution of electrolyte materials and electrode materials (functional graded structure) [Hart, 2001] and the cathode thickness. It is found that, instead of an abrupt change in composition and microstructure between the electrochemically active layer and the current collecting layer, functional graded cathode has a graded interface at which the composition gradually changes from one layer to another, thus minimize the TEC mismatch and increase the cathodic performance.

Generally, strontium-doped lanthanum manganese perovskite is regarded as one of the most promising cathodes for SOFCs due to high electrical conductivity, adequate compatibility with YSZ electrolytes, and an acceptable thermal expansion coefficient compared to other cell components [Basu, 1997]. Thermal plasma processes that have a high suitability to make controlled graded layers are confronted with the problem that most perovskites are thermally sensitive, e.g., LSM can lose manganese or manganese oxide with the result that the perovskite decomposes losing its good conductivity and

electrochemical activity. In addition, at present, even if conditions can be found where perovskite decomposition can be avoided [Li, 1993], when it occurs a more or less important percentage of undesirable La_2O_3 is present in coatings thus diminishing their electrochemical performance as cathode material [Schiller, 1999]. To solve this problem, spraying is followed by a thermal treatment in a furnace under oxygen atmosphere in order to regenerate the chemical structure of perovskite [Mallener, 1992], however, this operation is energy and time consuming.

Vacuum plasma spray: The majority of research conducted thus far has focused on the use of vacuum plasma spraying (VPS) in the manufacture of cathodes, both single phase and composite. It has been demonstrated that SOFCs fabricated by VPS can achieve performance levels similar to those fabricated by traditional techniques [Barthel, 1998]. Moreover, Barthel et al. compared the two methods VPS and Flame Spraying (FS) for production of porous composite graded, non-graded and bilayered cathode coatings containing $(La_{0.8}Sr_{0.2})_{0.98}MnO_3$ (LSM) and ZrO_2/12% Y_2O_3 (YSZ). The electrochemical performance of the cathodes, evaluated by impedance spectroscopy, indicated significant improvements. Also flame spraying as a new processing tool seems to have a good potential for future applications, according to this paper [Barthel, 2000].

The influence of cathode structural features such as porosity, particle size and electrode thickness on the cathode performance was discussed by Rambert et al. [Rambert, 1999]. The cathode layers with different thickness deposited by three types of LSM-YSZ mixtures with different volume-ratio and grain size have been compared with conventional LSM cathodes made by VPS (Figure 3.27). The electrochemical

performance of the cathodes, evaluated by impedance spectroscopy (Figure 3.28), indicated the micro-mixed composite LSM cathode has the lowest polarization resistance due to its considerably lower pore size and higher specific surface.

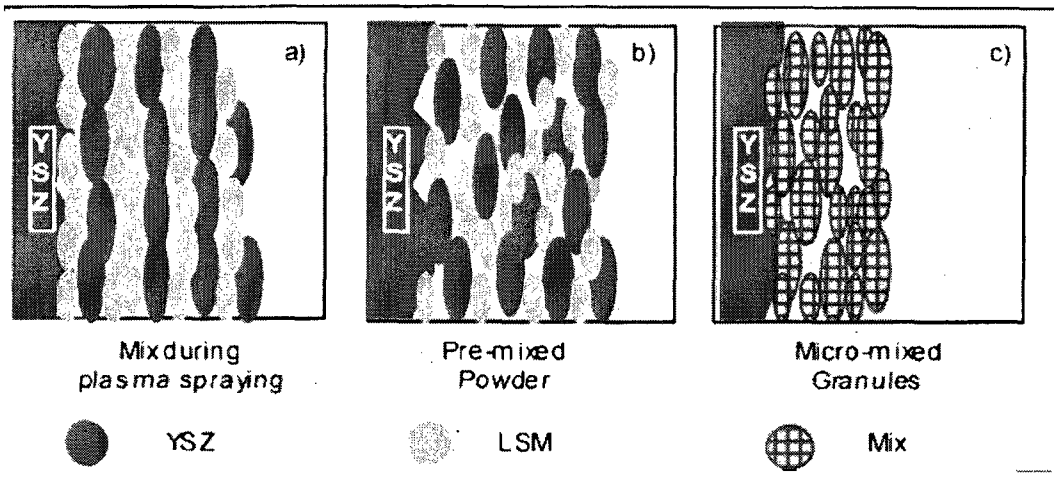

Figure 3.27 Deposited ccomposite cathodes using various processing routes [Rambert, 1999]

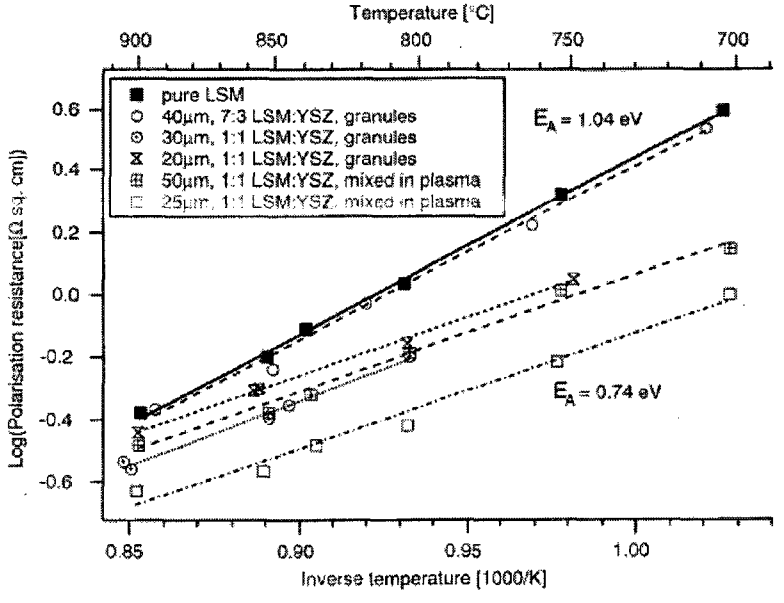

Figure 3.28 Polarisation resistances of standard LSM and composite LSM+YSZ cathode produced by VPS [Rambert, 1999].

Atmospheric plasma spray: There also have been attempts to fabricate SOFCs cathodes using APS, taking advantage of the relative simplicity and lower cost of the process. Kang et al. [Kang, 2001] developed a direct synthesis process of $La_{1-x}Sr_xMnO_3$ thin films using mixed raw materials (La_2O_3, $SrCO_3$, and MnO_3) in a reactive DC thermal plasma spray process. Cathode layers deposited from the mixture were compared to ones generated using a prereacted LSM powders prepared by a conventional solid-state reaction. The results showed that the reactive-spray formed coating layer was superior to the coating layer from the prereacted LSM powder.

More recently, White et al. [White, 2008] applied an APS system (Axial III Series 600, Northwest Mettech Corp., North Vancouver, BC, Canada) which contains three cathodes to axially inject pre-mixed LSM and YSZ powders to produce cathode layers. Argon and nitrogen were used as plasma generating gas to decrease processing costs and to avoid cathode material decomposition. In their experiments, the microstructures of LSM-YSZ composite cathodes produced using different combinations of APS parameter values were then examined using a factorial design experimental approach, and the conditions that produce the desired microstructures identified. It was found that coatings produced in moderate energy density plasmas at short standoff distances shows the significant improvement of cathode performance.

Suspension plasma spray: A very intricate interface between the porous perovskite and the dense electrolyte should be obtained with a large number of contact points to improve the SOFCs characteristics. It implies spraying of smaller particles to reduce splat dimensions. That is why, recently suspension plasma spraying has been developed to

spray finely structured cathode coatings by injecting a suspension of nano- or micro-sized particles in a DC plasma jet. Compared to the conventional APS process, SPS allows to create a much higher amount of triple-phase boundaries due to the much smaller particle size. Monterrubio-Badillo et al. [Monterrubio-Badillo, 2006] studied the optimization of composition of feedstock and plasma conditions achieve a minimum decomposition of the perovskite together with a sufficient particle melting in the plasma jet by SPS process. It had to be realized that the nature of plasma gas has a drastic influence on the obtained phases due to the sensitivity to the heat transfer of perovskites. The use of the Ar/H_2 plasma gas induced a complete destruction of the perovskite type powder. Pure argon is more suitable compare to other plasma gases. Eventually, with a stable suspension [Monterrubio-Badillo, 2003] containing a 20 mol% MnO_2 doped perovskite powder with 3 um particle size, the decomposition of pure perovskite in the cathode coating is only 5 wt.%. When using more sophisticated perovskites, for example, doped with the strontium, the decomposition can be totally eliminated. Such coatings are rather porous and when sprayed on YSZ electrolyte coatings, also obtained by suspension plasma spraying, they exhibited cohesive and very intricate interfaces with the thickness of 20 μm approximately (Figure 3.29).

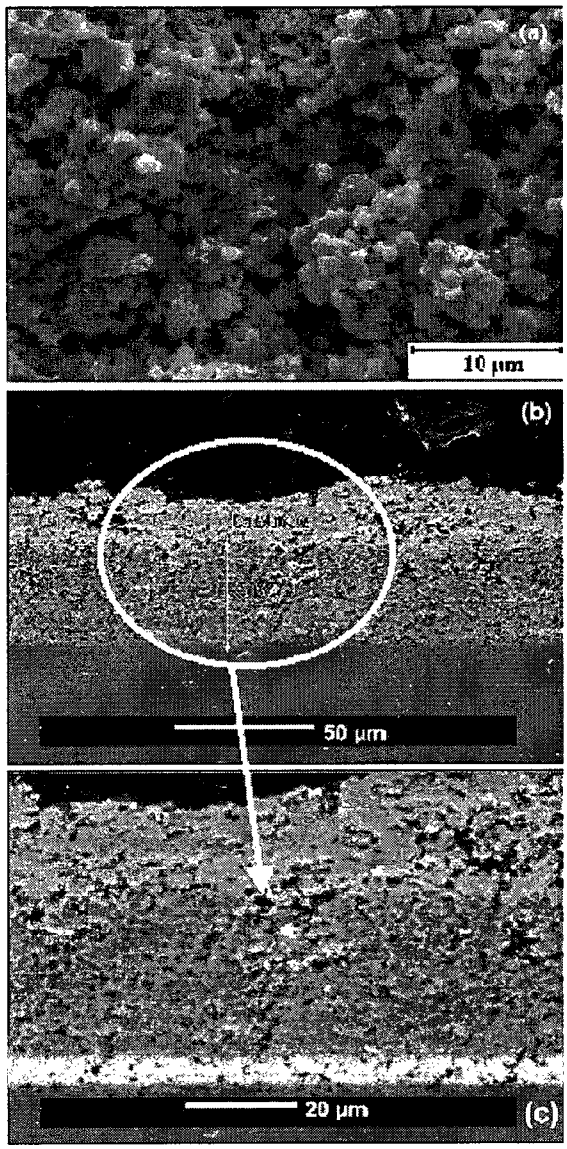

Figure 3.29 Cathode coatings obtained by suspension plasma spraying [Monterrubio-Badillo, 2003].

The SPS process is rather sensitive to change in the process parameters. The method of injecting the suspension is one of the most influencing parameter. In most cases, a single injection is used. Kassner et al. [Kassner, 2008] developed a new method of separate injection of two single-phase suspensions to produce LSM-YSZ cathode. Compared to

the single injection of a premixed suspension to form a mixed phase, there is no reaction between the two phases using two separate injection ports (Figure 3.31). The porosity of the coating is about 40%. The area-specific resistance of the cell is 1.3 Ωcm^2. At a cell voltage of 700 mV, a power density is about 120 mW/cm^2 is obtained. A further optimization with respect to homogeneity and grain size has to be made before an application is envisaged.

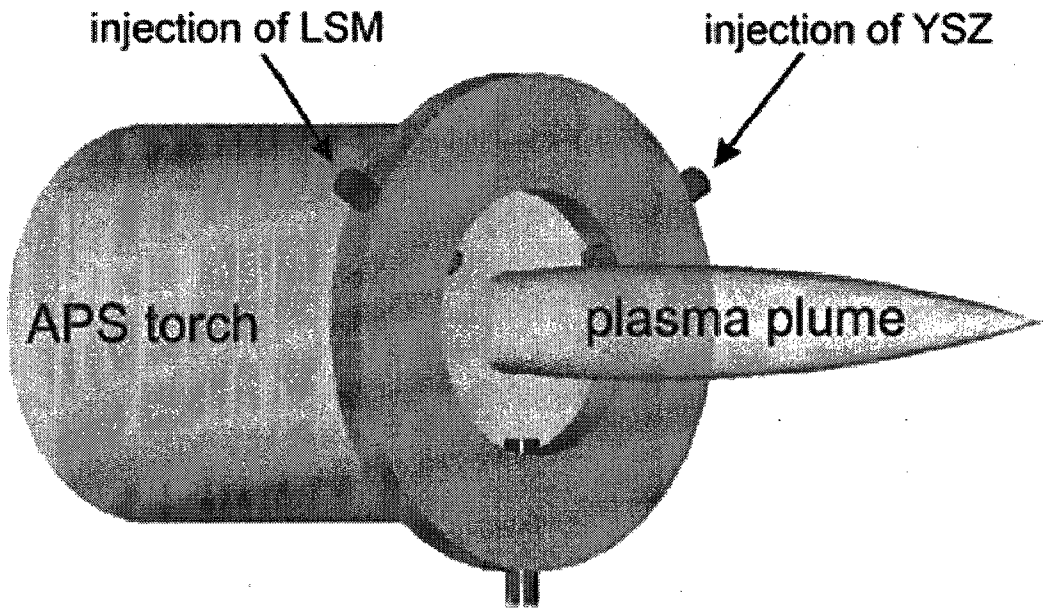

Figure 3.30 Injection of the two separate suspensions to produce cathode coatings by APS [Kassner, 2008]

Radio frequency induction plasma spray: Radio frequency induction plasma with its intrinsic properties, such as the ability to generate a slow-moving, large-volume plasma jet and the opportunity to inject the liquid precursor along the jet axis, offers a high potential for the development of SOFCs cathode. Schiller et al. [Schiller, 1999] prepared perovskite powders and coatings in the RF induction plasma using a precursor suspension

of MnO_2 powder in an ethanol solution of $LaCl_3$ with a 1 to 1 molar ratio of lanthanum and manganese. The experiments were performed using a vacuum reactor at DLR Stuttgart (Figure 3.31). As-sprayed coatings and collected powders showed perovskite contents of 70 to 90%. After a post-treatment with plasma that consisted of 80% oxygen, an almost pure $LaMnO_3$ deposit was achieved in the center of the incident plasma jet.

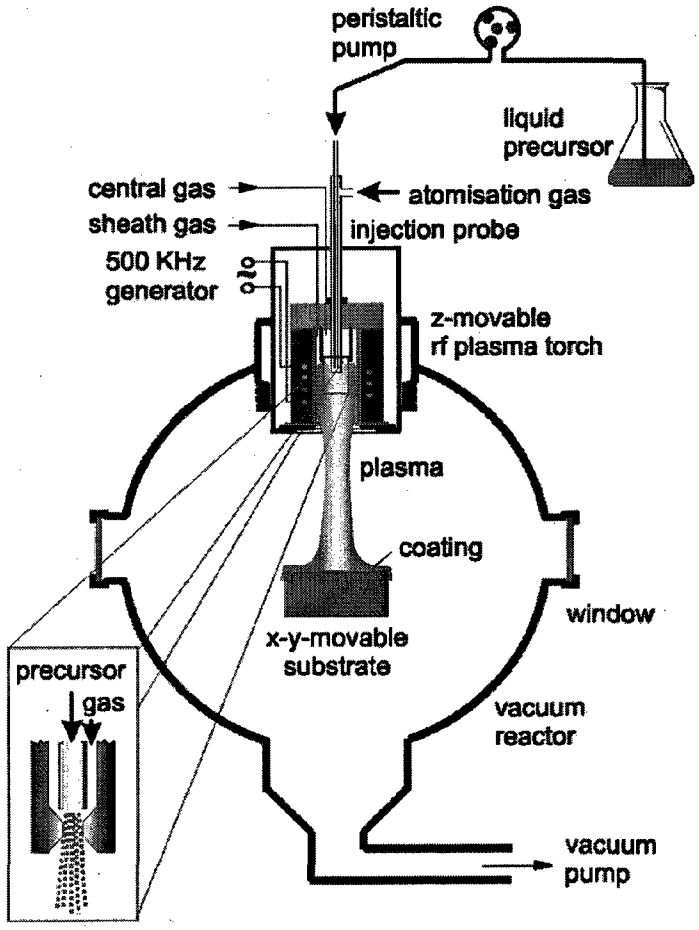

Figure 3.31 Set-up for RF inductively coupled thermal plasma for cathode deposition [Schiller, 1999]

A step further of research works have been continued by same group demonstrated the potential of thermal plasma chemical vapor deposition (TPCVD) method to deposit Sr-

doped La-(Mn, Fe, Co) perovskite (LSM, LSF, LSCF) cathodes from aqueous solutions [Müller, 2002] [Schiller, 2003]. With synthesis and in particular with the deposition of such complex oxides the thermal conditions have to be carefully controlled in order to avoid a decomposition which is particularly a problem with Mn-oxide containing species due to its high-vapor pressure. However, with adapted conditions attractive perovskite microstructures can be produced with TPCVD and heterogeneous nucleation. These structures promise due to the columnar crystals and the spaces between a highly extended surface for oxygen reduction and oxygen-ion entrance (Figure 3.32).

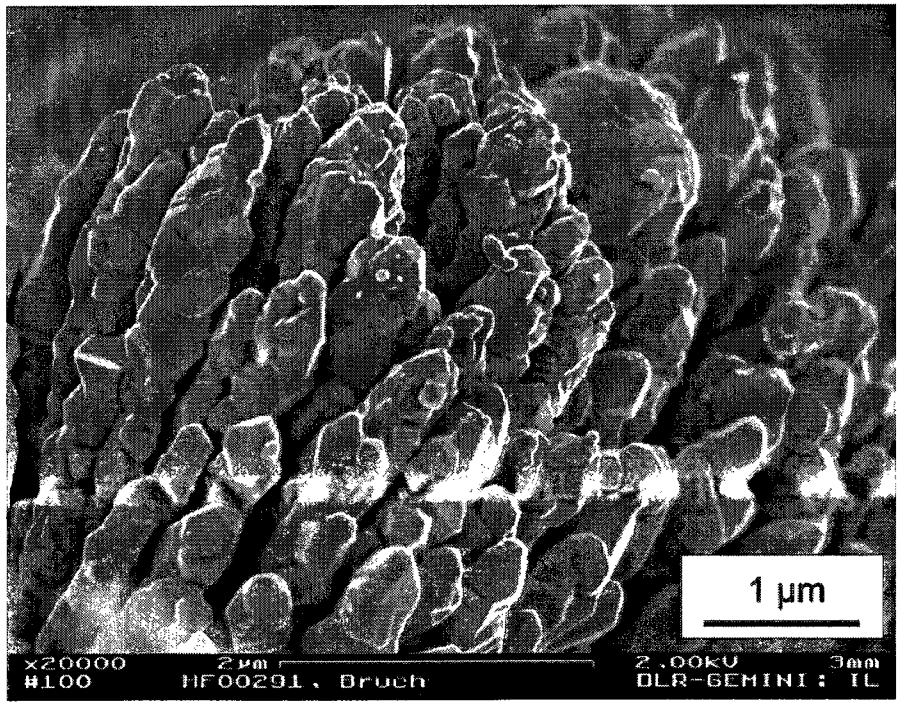

Figure 3.32 TPCVD LSCF cathode coating reveals a columnar microstructure [Müller, 2002]

It has been demonstrated that nano-structured cathodes with significantly higher surface area offer superior electrochemical properties, as long as a sufficiently large pore size and enough porosity are provided [Ivers-Tiffee, 2001]. Many works have been shown that

nano-structured cathodes dramatically reduce cathode/electrolyte interfacial polarization resistances and improve cell performance [Liu, 2004] [Princivalle, 2008] [Wang, 2008]. However, there is few work reported in the literature about the production of nano-structured cathode using thermal plasma spraying technology which need to be considered.

3.3.5 Nano-structured SOFCs' Components produced by thermal plasma spraying process

Thermal plasma spraying process has inherent advantages in the production of advanced materials in the form of coating of powders and nano-structured coatings. Plasma techniques offer a controllable and directional heat source. Plasma temperatures are much higher than achievable by using fossil fuel combustion, and are sufficiently high to melt aand/or dissociate any compounds fed into the plasma, to melt and/or vaporize virtually all elements, and to potentially allow the reactions between feedstock materials to take place in the gas phase. These high temperatures, along with the chemically reactive species formed in the plasma, may accelerate chemical reactions by several orders of magnitude. Residence time in the high-temperature zone is controllable. The ability to quench rapidly from very high temperatures produces very small spherical particles, typically a few tens of nanometers to a few hundred nanometers in diameter. By a suitable choice of plasma environments, reactions can take place in an inert atmosphere, or a suitable oxidizing, and reducing environment. Starting materials can be fed into the plasma reactors in gaseous, solution, suspension, and powder form.

Recently, two plasma spraying routes have been developing for the fabrication of nano-structured SOFCs' components: solution and suspension plasma spraying. The precursor solution used in SolPS comprises a metal precursor in the form of nitrates, sulfates, chlorides, or alkoxides dissolved in a suitable medium such as water. Upon injecting the precursor into the plasma flame, the products formed are directed toward the substrate by the carrier gas. Thus, SolPS enables the formation of metal oxides, multi-component composites coupling the process of material preparation and coating into a single step. In the SolPS process, the precursor is a solution that can enable the formation of nano-particles as coatings or powders. Since the report of preparation of alumina, zirconia, and yttria-stabilized zirconia nano-particles and deposits in 1997 [Karthikeyan, 1997], SolPS has been used to process many of the simple as well as complex oxides delivering a wide range of applications including thermal barrier coatings, fuel cells, and phosphor, magnetic, and biomedical coatings. SolPS process combines the simplicity and high through-put of the plasma spray process with versatility and economics of the spray pyrolysis process to produce the desired nano-structured materials and coatings.

US Nanocorp has produced nano-structured anode by SolPS process using a conventional air plasma spray system [Ma, 2005]. The SolPS-deposited LDC+NiO anode layer is highly porous, with porosity of 40–45 vol. %, and the thickness of the anode layer is 100–150 μm. The layer consists of a number of sub-micrometer sized particles that are partially melted and have a near-sphere shape. Porosity analysis indicated that the porosity distribution varies from 20 nm to 0.5 μm with a central value of 150 nm. By increasing the number of active sites at the TPB, the catalytic property of the anode, and hence, the efficiency of the SOFCs can be improved. Therefore, the nanometer and sub

micrometer porosity in the SolPS-formed LDC+NiO anode layer can be beneficial for increasing fuel gas permeability and anode catalytic property.

The SPS, recently developed to spray finely structured coatings by injecting, instead of micro sized powders, a suspension of nano-sized particles in a DC or RF plasma jet seems to be the most promising method to produce the nano-structured dense YSZ electrolyte coatings [Rampon, 2006] [Fauchais, 2005] [Delbos, 2003] [Berghaus, 2005] [Stöver, 2006] [Bonneau, 2000]. The coating microstructure is strongly depended on the initial powder size distribution in suspension and plasma spraying parameters.

In summary, many thermal spray technologies, especially thermal plasma spray processes, have been developed to produce the electrolyte and electrodes. Spray parameters controlling coating properties are all dependent and finally coating thermo-mechanical or service properties depend on about 50–60 spray parameters. The more advance understanding of the process we have, the more drastically improvement of the coating properties, reliability and reproducibility we could achieve. Therefore, (a) plasma formation and its interaction with its environment, (b) powder, suspension, or solution and its injections with the resulting particle parameters (temperature, diameter, velocity, number flux) at impact, (c) splat formation, splat layering and coating formation need to be studied.

3.4 Integrated SOFCs Production by Thermal Plasma Technology

In the above literature study, mainly single components of SOFCs made by thermal plasma spraying were described. Only a very few papers can be found in literature where the production of entire cells is treated. In most relevant papers either APS or VPS has

been applied. In some few cases different and differently adapted thermal plasma processes were combined [Henne, 2007].

According to literature study almost forty years ago, Tannenberger and Schmitt [Tannenberger, 1964] started with the use of thermal spraying to make complete cells. Then, Spacil and Tedmo [Spacil, 1969] were active by spraying the cell parts on an aluminum mandrel with a subsequent leaching of the mandrel with KOH followed by sintering of the resulting free standing product.

In the beginning of the 1990s several groups mainly in Europe and in Japan started with SOFCs R & D by thermal plasma spraying, mainly with VPS [Mallener, 1992]. The obtained power densities, at these times, were still below 100 mW/cm^2 at an operating temperature of about 1000 °C. The problem of thermal decomposition of perovskite material was already observed and parameters to suppress this effect were developed. For these experiments different types of substrates were used, e.g., porous sintered Ca-stabilized ZrO_2 on which the cathode was deposited or sintered porous ZrO_2-Ni parts serving simultaneously as anode.

Few years later a considerable progress could be obtained with Ni-felt as substrates. Gruner and Tannenberger [Gruner, 1990] reported a power density of about 160 mW/cm^2 at 0.7 V with VPS produced cells of 4.5 cm^2 at 910 °C fuelled with H_2 + 3% H_2O. They claimed the production of the entire cell in a consecutive spray process. Howver, concerning the use of Ni-felt as porous substrates—Ni has attractive electrochemical properties—it turned out that for larger cell sizes, the Coefficient of Thermal Expansion (CTE) of Ni is too high to be tolerable for the electrolyte. Cracks and also problems at

redox-cycles appeared. Therefore, later on porous ferrite substrates replaced the Ni-felts, having the better CTE-adaptation but, unfortunately a lower-electrochemical activity together with a higher-electrical resistance. Also the upper operating temperature limit is lower.

State of the art with VPS produced metallic substrate- supported thin film SOFC has been developed by DLR. This VPS technique has the potential to fabricate the entire membrane-electrode assembly (MEA) in a single consecutive fast spray process, avoiding any time-consuming sintering steps. High material deposition rates promise fast and cost-effective cell production, particularly where large active cell areas are required [Lang, 2001].

Completely vacuum plasma sprayed SOFCs consist of a NiO/YSZ anode, an YSZ electrolyte and a LSM/YSZ cathode, which were consecutively sprayed onto a porous Ni felt (Figure 3.33). The plasma sprayed YSZ electrolyte exhibits a dense lamellar microstructure, whereas the anode has a fine open porosity of 21 vol.% after the reduction of the NiO with H_2 to pure Ni. The overall porosity of the LSM/YSZ cathode reaches only about 10 vol.% with relatively coarse pores [Schiller, 2000].

Figure 3.34 shows the electrochemical performance of a plasma sprayed thin-film cell. At 900 °C, power densities in the range of 600 mW cm^{-2} are achieved at 0.7 V when operated with hydrogen and air. At reduced operating temperatures down to 750 °C the power densities decrease to approximately 200 mW cm^{-2}.

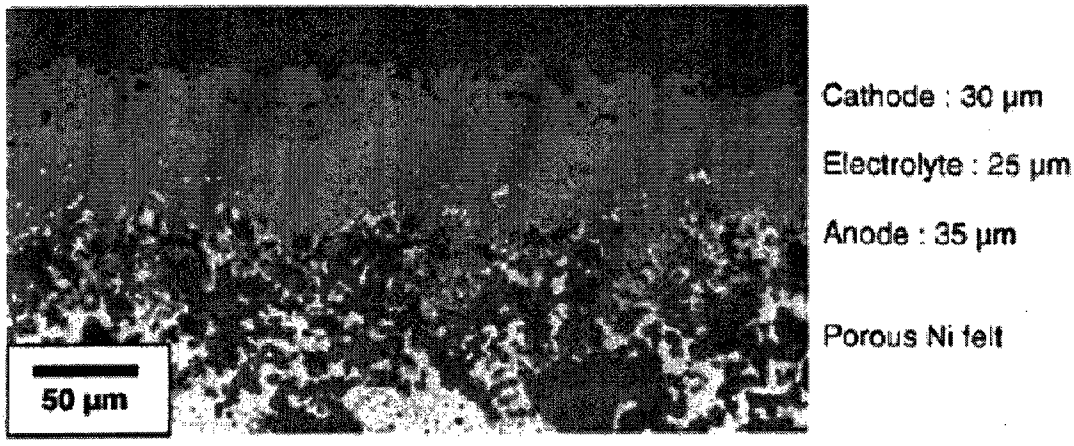

Figure 3.33 Vacuum plasma sprayed thin film SOFCs [Schiller, 2000]

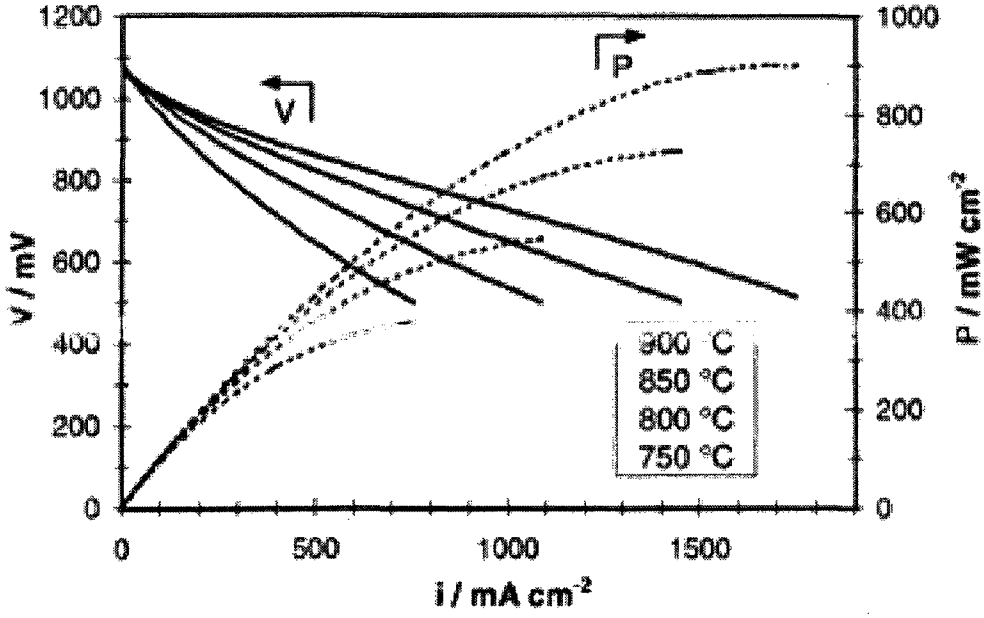

Figure 3.34 Electrochemical performance of a vacuum plasma sprayed thin film SOFCs [Schiller, 2000]

Moreover, Figure 3.33 shows the lack of such a "pore forming process" at the cathode side leads to a limited porosity of only 10-15%. It is believed that the highest contributor by far to the cell's polarization resistance from the cathode is its relatively low porosity. Therefore, much effort is needed to improve the cathode's pore structure. Recently, the radio frequency inductively coupled plasma (RF-ICP) is increasingly used at DLR for deposition of perovskite-type cathode layers to improve the cathode performance [Schiller, 2003].

For the cost reasons also APS was qualified in parallel to VPS for this task, and a considerable progress could be made in last few years [Takenoriri, 2000]. Ma et al. [Ma, 2005] has addressed to use inexpensive and universal APS system for integrated fabrication of dense electrolyte and porous electrode layers for a medium temperature SOFCs unit.

The APS sprayed single cell comprises a cathode LSM, electrolyte LSGM and anode Ni/YSZ, and its microstructure is shown in Figure 3.35, in which the thickness of the electrolyte layer is typically 50-80 μm. The microstructure observation verified that porous electrode and dense electrolyte layers have been obtained with APS process, and single cell could be fabricated in sequential plasma spray processing. The as-sprayed LSGM electrolyte mostly contained an amorphous phase; however, a high-level crystallized LSGM could be achieved by heat treatment at temperature above 700 °C.

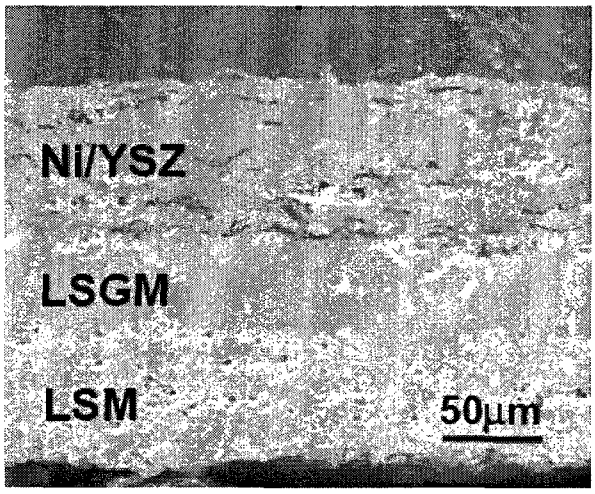

Figure 3.35 Atmospheric plasma spray sprayed SOFCs [Ma, 2005]

The cell electrical performance was evaluated by open circuit voltage (OCV) and voltage-current density at temperature 500-800 °C. Figure 3.36 presents the results of OCV, 0.95 V at 600 °C and 1.045 V at 700 °C. The OCV data indicates that the plasma sprayed electrolyte layer has a satisfactory gas tightness, and thus can isolated hydrogen and air effectively. The power density was measured as 80-150mW/cm^2 at the tested temperatures.

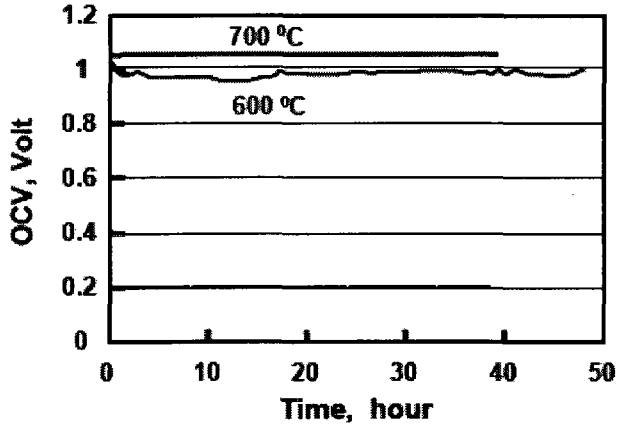

Figure 3.37 Open circuit voltage of an atmospheric plasma sprayed single cell [Ma, 2005]

Some activity is also around using RF with the intention to combine either the in-situ synthesis of materials or their deposition [Barthel, 2000] [Schiller, 1998], or also different plasma deposition methods into one consecutive process [Yoshida, 1991] [Gitzhofer, 2000] [Chen, 2000]. In this connection also the work with LPPS with its attractive properties has to be noticed [Refke, 2000].

In summary, thermal plasma technology, for example, APS, VPS, RFPS are the promising and cost-effective techniques for the manufacture of SOFCs units. Multiple SOFCs components, including the electrolyte and the electrodes, could be produced sequentially and directly on a metallic interconnect substrate or a reformer with a single deposition technique, thereby minimizing the number of processing steps and equipment required. In particular, the high temperature sintering steps required in many other layer deposition techniques could be eliminated. However, the electrochemical performance of the plasma sprayed SOFCs are still not fully satisfied. The processes should be optimized to implement the production of intermediate temperature SOFCs with the successful performance.

4. RESULTS AND DISCUSSIONS

This chapter comprises four papers which already be published, accepted or submitted for publication in peer-reviewed journals. The first paper "Induction Plasma Technology Applied to Materials Synthesis for Solid Oxide Fuel Cells" reports the contributions have been carried out or are currently explored on the field of SOFCs by University of Sherbrooke. The experiments of anode deposition and cathode deposition were done by Mr. Francois Hudon and Mr. Danik Bouchard, respectively. In the second paper "Induction Plasma Synthesis of Nano-structured SOFCs Electrolyte Using Solution and Suspension Plasma Spraying: A Comparative Study", two plasma spraying technologies: solution plasma spraying (SolPS) and suspension plasma spraying (SPS) were used to produce nano-structured Solid Oxide Fuel Cells (SOFCs) electrolytes. The comparison of two plasma spraying processes is based on electrolyte phase, microstructure, morphology, as well as on plasma deposition rate. The results showed that SPS process is more promised to produce the nano-structured thin and dense electrolytes than SolPS process. The third paper "Preparation of Nano-structural Electrolyte Thin Film for Solid Oxide Fuel Cells by Radio Frequency Suspension Plasma Spraying", the potential of RF suspension plasma spray process as a novel method for the production of thin, gas-tight and nano-structural SOFC electrolytes is explored. The laboratory-developed suspension feeding system enabling a separate injection of two single phase suspensions to form composite GDC electrolyte coatings, which provides the opportunity to produce the functional and/or graded SOFC composite components. The dynamic mask system has been developed to diminish the heating effects of a high-temperature deposition process.

It was demonstrated the electrolyte coatings deposit with mask exhibit lower porosity compares to electrolyte coatings deposit without mask. The last paper "Functionally Graded Anodes with Nanostructure for Intermediate-Temperature SOFCs" concerns the fabrication of functionally graded NiO-GDC anodes with nano-structure fabricated using solution plasma spraying. The plasma process parameters were optimized and the solution feeding system was developed. The gradient not only in chemical content but also in coating porosity was demonstrated in this anode coating.

The results obtained in these papers have demonstrated the feasibility of induction plasma spraying process applied to produce the porous nano-structured electrodes as well as dense electrolyte coatings. This represents an opportunity to fabricate the fully integrated nano-structured SOFC using solution and suspension plasma spraying process.

4.1 Induction Plasma Technology Applied to Materials Synthesis for Solid Oxide Fuel Cells

François Gitzhofer and Lu Jia

Energy, Plasma and Electrochemistry Research Centre (CREPE), Chemical and Biotechnical Engineering Department, Université de Sherbrooke, Québec, Canada, J1K 2R1, (819)-821-7171

ABSTRACT

Induction plasma technology has been successfully applied to the synthesis of nano-materials, for subsequent use in the screen printing of cathodes and the sintering of electrolytes. This plasma technology can also be directly used to synthesize anodes, electrolytes, and cathodes which were established on reformer-supported solid oxide fuel cells, in addition to the synthesis of the reformer component/structure. In this work, through the use of suspension and solution precursors, combined with supersonic or subsonic nozzles, induction plasma is shown to be a very versatile research tool, to vary the composition of the applied spray materials in flight and to control the resulting micro/nano-structure.

1. Introduction

Solid oxide fuel cells (SOFCs) have been intensively studied as an efficient and clean electric power generator for the future energy system [1]. There are three main issues in SOFC development which are identified as driving forces during recent years: cost reduction with respect to low-cost materials and simpler processing techniques, the improvement of power density, and durability in long-term operation. One strategy for addressing these challenges is to develop intermediate temperature SOFCs that operate at

reduced temperatures of 500–700°C. As related to SOFCs technology, lower operating temperature requires higher activity of electrodes, higher ionic conductivity of electrolytes, and the lower overall over-polarization. These requirements can be met through development of new electrode/electrolyte materials, new cell assembly concept, and particularly novel fabrication techniques [2-6].

Induction plasma with its intrinsic properties offers a high potential for the development of SOFCs. One of the primary reasons is that it is a very efficient high-temperature chemical reactor. Indeed, induction plasma is characterized by its relatively large plasma volume and low gas velocity in the plasma generation region [7]. Furthermore, because of the absence of electrodes, the technique offers a great flexibility with respect to the nature of the plasma gas used, such as neutral, reducing, or oxidizing atmospheres. The injection of the precursors is taking place axially. The injected precursors can be gaseous, solids, solutions, or suspensions. Induction plasma torches can also be fitted with a supersonic nozzle that allows for a substantial increase in the plasma and particle velocity before their impact on the substrate, after chemical reactions took place. The supersonic jet allows also with the associated cooling of the jet to freeze high-temperature phases as well as to favour nanostructures development [8].

Recent works have been devoted to the successful realization of SOFCs by thermal plasma spraying the whole stack [9]. Schiller and colleagues [10-12] have developed the vacuum plasma spray technique, as well as the induction plasma spray technique to consecutively deposit the entire membrane-electrode assembly onto a porous metallic substrate within a very short process time to produce the SOFCs. Specially adapted spray

powders were applied for the different layers during these depositions [10-11]. Other attempts tried to avoid the expensive powder preparation by application of liquid precursors [12].

The solution precursor plasma-spraying (SolPS) process was developed widely to produce SOFC materials and components [13-17]. This process consists in injecting liquid precursors containing the elements to be deposited. With induction plasma, the solid particles produced by the evaporation of the solution and the decomposition of precursors from agglomerates in the size of micrometers which are then remelted and sprayed.

An alternate process, suspension plasma-spraying (SPS) technique was invented and patented by Gitzhofer et al. [18] at Université de Sherbrooke in 1997. In SPS technology, a suspension of fine powder or precursor components is fed to an induction plasma torch and directly gas atomized into the plasma through an atomization probe. The whole in-flight process (atomization, drying, and melting associated with or without chemical reactions) occurs in approximately 10 ms. The powders are either collected for further application or directly deposited onto a substrate. This gives an opportunity to prepare the ceramic nano-powders for anode and electrolyte or perovskite nano-powders for cathodes as well as the nano-structured cell components [19-20].

The objective of this paper is to present a review of the different paths that have been used by the team working on SOFCs at Université de Sherbrooke. Innovative approaches had to be undertaken in order to be able to address the complexity of the materials selection, the process selection and the characterization of SOFCs. By using suspensions

and solutions precursors combined with supersonic or subsonic nozzles, induction plasma is shown to be a very versatile research tool, to vary the composition of the applied spray materials in flight and to adjust the resulting micro/nanostructure which has the potential to fabricate the fully integrated SOFC with nano-structured cell components.

2. Induction Plasma Process for the Synthesis of SOFCs Materials

2.1 Experimental setup and procedure

The induction plasma was generated using a PL-50 plasma torch (Tekna Plasma Systems, Sherbrooke, Canada), operating at a frequency of 3 MHz. The torch is equipped with subsonic nozzle (diameter = 45.0 mm) or supersonic nozzle (diameter = 24.2 mm), in order to control the particle velocity. Figure 1 shows the schematic illustration of an induction plasma system, which is used for the synthesis of SOFCs materials and the fabrication of SOFCs components.

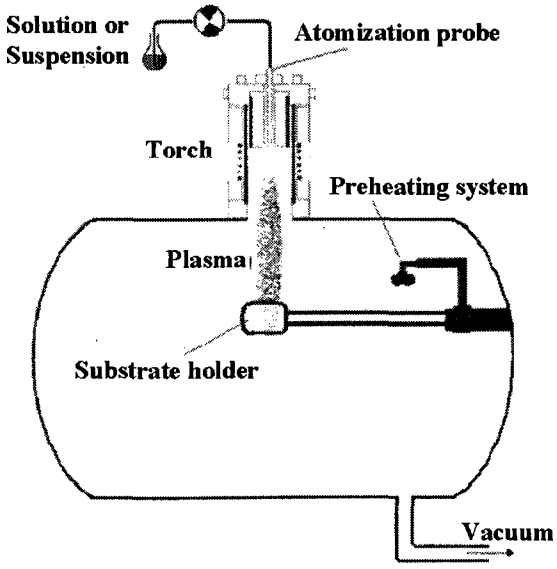

Fig. 1 Schematic illustration of induction plasma system

The precursors were fed at a rate between 4 and 10 mL/min by a peristaltic pump. The materials were directly injected into the hot plasma core by means of an atomization probe. Argon flow rate of 11.5 slpm was used to atomize the precursors. According to droplet size measurements which was performed by Malvern RTsizer (Malvern Instruments, Worcestershire, U.K.), the most frequent droplet size in our experimental range was about 11–12 μm (Figure 2). Detailed description of the induction plasma-spraying apparatus used for this study is available elsewhere [21]. Table I presents the fixed spraying parameters that were used for the synthesis of the electrolyte and electrodes materials.

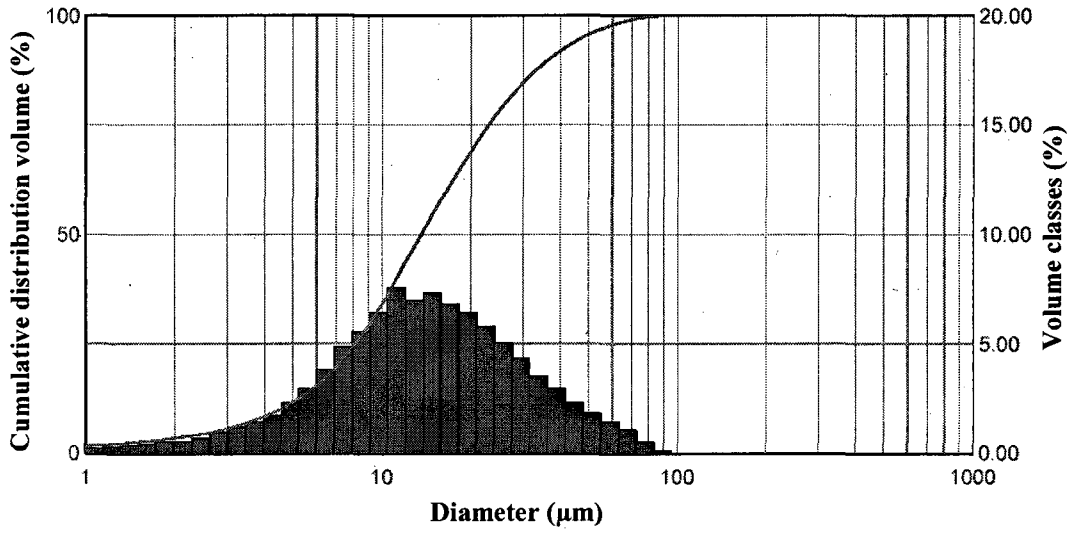

Fig. 2 Typical atomized droplets size distribution

The substrates of 10 mm diameter and 1.2 mm thickness, were produced by the sintering of pressed 44 wt% of green nickel oxide (Novamet type F), 48 wt% of filamentary nickel powder (Novamet 255) and 8 wt% of nickel powder (Novamet 210) for 1 h at 800 °C. In

order to reduce the thermal gradients during deposition, the substrates are heated before deposition using an electrical heating device.

Table I. Fixed induction plasma spraying parameters

Central Gas :	(Ar)	27	slpm
Sheath Gas :	(O_2)	80	slpm
Atomization Gas:	(Ar)	11.5	slpm
Probe Inner Gap :		0.4	mm
Probe Position :		+ 10	mm

2.2 Characterization and analysis

Different techniques are used to characterize the materials synthesized by the induction plasma process. Particle size distributions were determined using a Malvern Mastersizer 2000 particle analyzer. Phase analyses were conducted by X-ray diffraction (XRD) using a Philips X'Pert Pro MPD X-ray diffractometer (Eindhoven, The Netherlands). Morphologies and elemental analyses of deposited layers and powders were performed using a JEOL JSM 840A scanning electron microscope (SEM, Tokyo, Japan) and a Hitachi S4700 field emission SEM (FESEM, Tokyo, Japan). Coatings porosity was determined by image analysis two to five pictures which taken at different sample areas, according to the magnification used. A threshold method was used to determine the darker percentage of the picture that directly provided the porosity [22]. Transmission electron microscope imaging was performed with a Hitachi 7500 microscope. Gas permeability can be measured according to Darcy's law [23]:

$$k = Q\frac{\mu L}{A(\Delta P)}$$

where Q is the volumetric flow rate which passes through the sample, μ is the dynamic viscosity of the medium, L is the sample thickness, A is the cross-sectional area of the channel, and ΔP is the pressures difference across the sample. The system configuration is shown in Figure 3. The sample was placed in a cylindrical enclosure. One end of the enclosure is connected to a vacuum pump. The other opens to the atmosphere. The vacuum pump creates a pressure differential across the sample and drives the air through. A flow meter is placed after the enclosure to measure the air-flow rate.

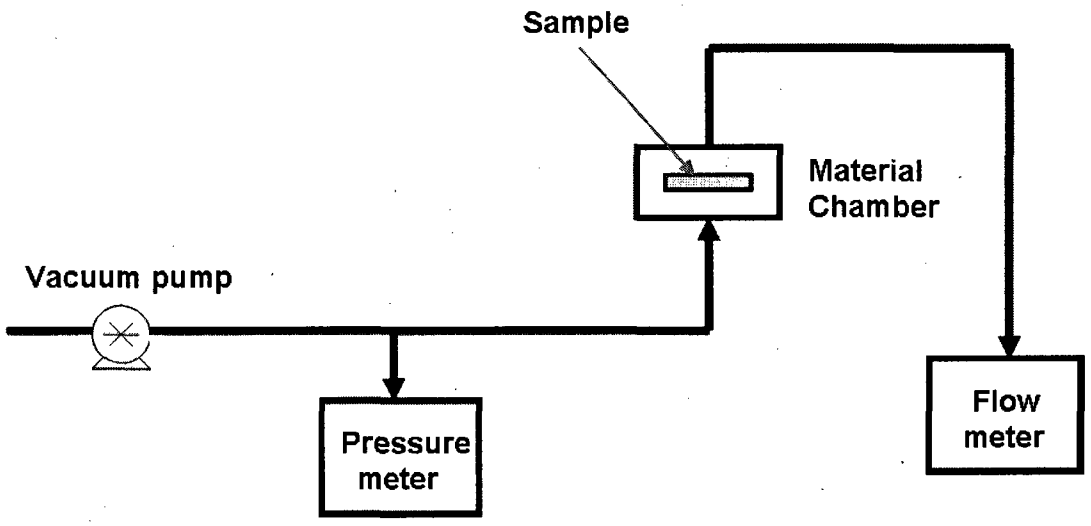

Fig. 3 A schematic of the permeability measurement system

2.3 Anode synthesis

Coating of NiO–GDC was produced from the corresponding nitrate solution using SolPS process. Nickel nitrate (Alfa Aesar, Ward Hill, MA; purity: 99.5%), cerium nitrate hexahydrate (Alfa Aesar, purity: 99.99%), and gadolinium nitrate hexahydrate (Alfa Aesar, purity: 99.9%) with required composition were dissolved into the water. The variable plasma-spraying parameters are given in Table II.

Table II. Anode specific induction plasma spraying parameters

Torch Nozzle Diameter :	45	mm
Reactor Pressure :	100	Torr
Plasma Power	33	kW
Stand-off Distance (for coating)	210	mm
Solution flow rate	5	mL/min
Deposition Loops (for coating)	5	

The microstructure of solution plasma sprayed NiO-GDC anode layer was examined by FESEM and is shown in Figure 4. The FEGSEM analysis of the deposits surface (Figure 4a) suggests that the anode layers deposited at the spraying distance of 210 mm and closer, predominantly consists of plasma-sprayed domains with developed surfaces where the desired nanostructure is well preserved (Figure 4b and 4c). Some in situ sintered domains were also found (Figure 4d). The micrographs also reveal that the anode is highly porous (coating porosity = 34.2%) and have very unique microstructure: each large agglomerate consists of smaller ones, which in turn contains even smaller particles (20 nm in diameter). This nano-structured anode has extremely high surface area and is expected to significantly extend the length of the triple-phase boundary. The XRD pattern of the anode shown in Figure 5a indicates that the anode consists of two highly crystallized phases: NiO and GDC. However, trace amounts of CeO_2 and Gd_2O_3, which were produced from the pyrolysis of cerium nitrate and gadolinium nitrate are also found.

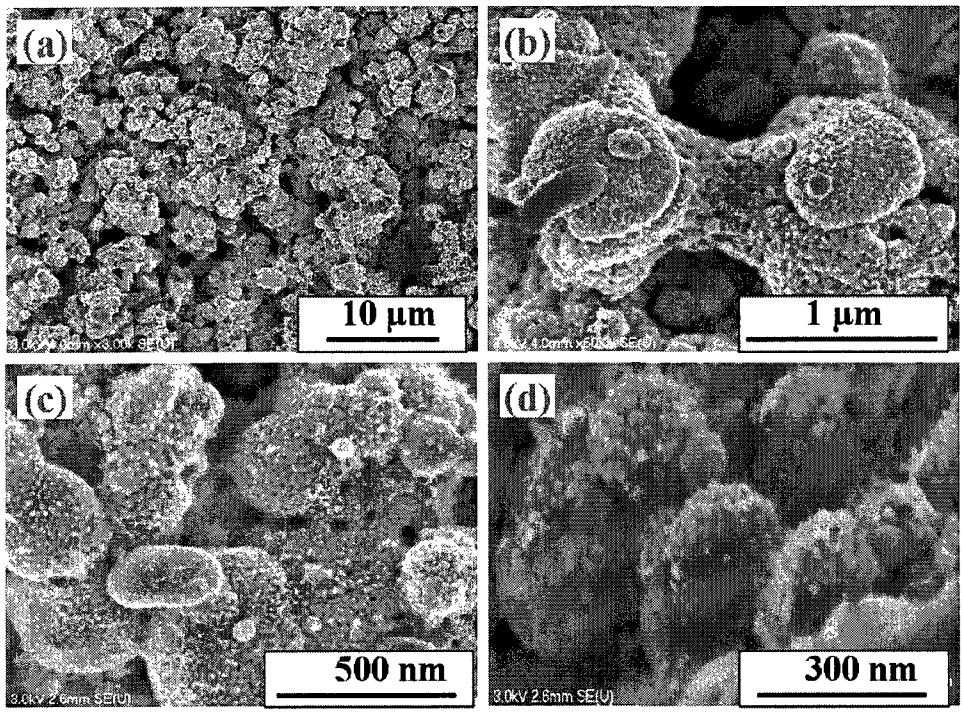

Fig. 4 FEGSEM image of (a) the anode surface, (b), (c) and (d) the magnified views of the same surface [24]

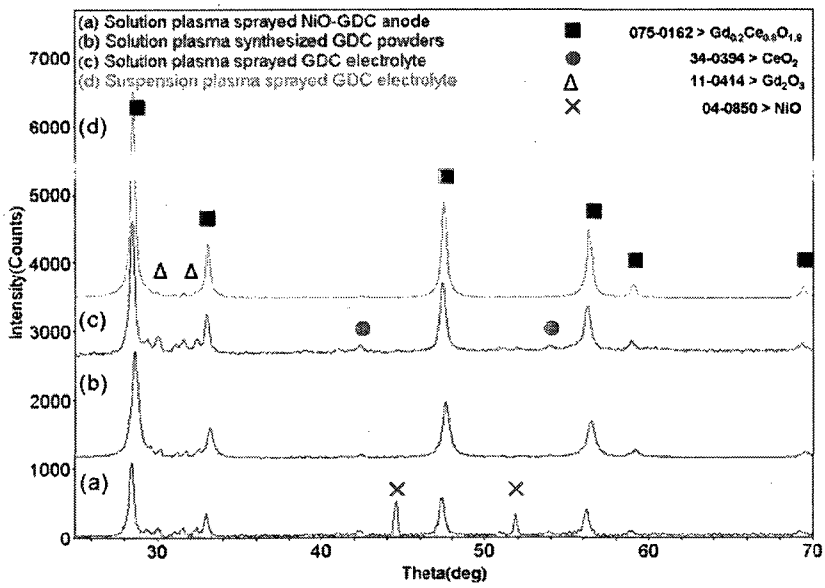

Fig. 5 X-ray analysis for (a) solution plasma sprayed anode, (b) solution plasma synthesized powders, (c) solution plasma sprayed electrolyte and (d) suspension plasma sprayed electrolyte

2.4 Electrolyte synthesis

The induction plasma synthesis process, based on the use of solution precursors as the process feedstock, has been used for the production of GDC nano-powders, which could be used for the depositions of fuel cell electrolyte on anodes by using SPS. Cerium nitrate hexahydrate (Alfa Aesar, purity: 99.99%) and gadolinium nitrate hexahydrate (Alfa Aesar, purity: 99.99%) with molar ratio 80/20 were dissolved into water to prepare a solution with a concentration of 0.6 g/mL. The variable plasma-spraying parameters are given in Table III for the electrolyte deposition layers.

Table III. Electrolyte specific induction plasma spraying parameters

Torch Nozzle Diameter :	24.2	mm
Reactor Pressure :	50-100	Torr
Plasma Power	33-50	kW
Stand-off Distance (for coating)	100	mm
Solution flow rate	4	mL/min
Deposition Loops (for coating)	10	

Figure 6 presents the micrographs of synthesized GDC nano-powders using SolPS technology. The nano-powders with a size of 20 ± 3% nm are created. The XRD pattern shown in Figure 5b indicates that the GDC powders also contains very small amount of CeO_2 and Gd_2O_3.

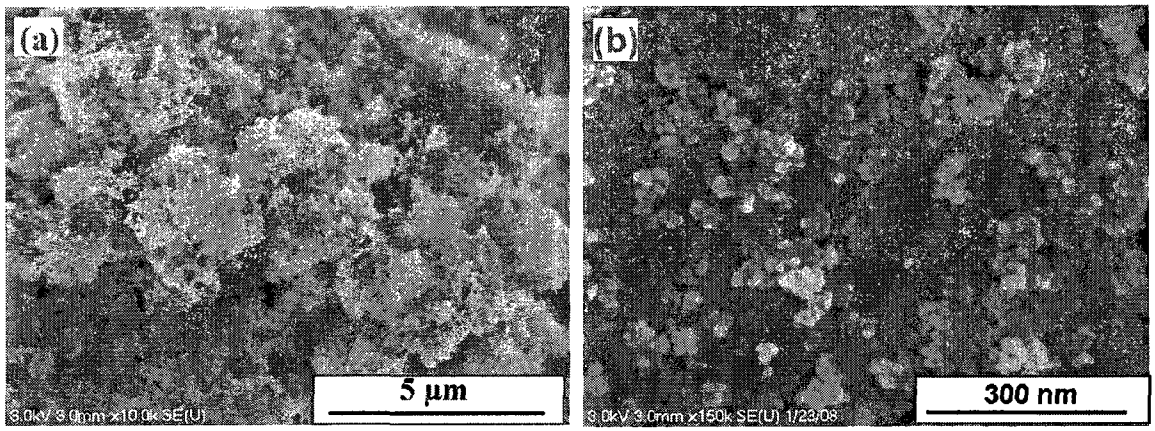

Fig. 6 Micrographs of synthesized GDC electrolyte nano-powders with different magnifications

The GDC electrolyte layers were solution and suspension plasma sprayed onto the anodes/reformer substrates, and their microstructures are exhibited in Figure 7. To prepare the GDC suspension, GDC nano-powders were directly dispersed in to the ethanol. The weight ratio of GDC to ethanol and GDC powder was kept at 7%. The suspension viscosity was adjusted by adding Darvan No. 7 (dispersing agent) into the suspension. The mass percentage of the dispersing agent selected for use is 2% of the GDC powder mass to obtain the lowest viscosity for adequate feeding. Before deposition, the suspension mixture was ultrasonically dispersed to break apart the large agglomerates. During deposition, a stirrer was used to prevent particles from settling down.

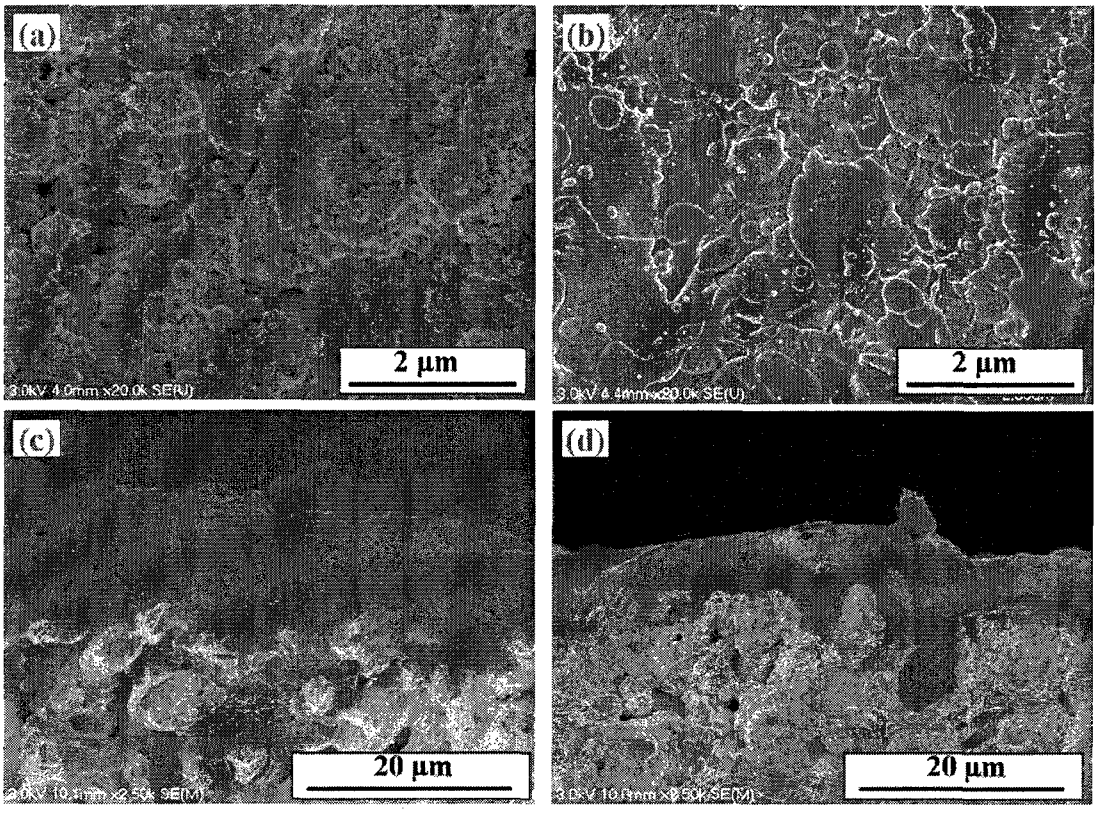

Fig. 7 The FESEM microstructure of as-sprayed electrolytes of surface morphologies (a) SolPS coating, and (b) SPS coating, fracture cross-section observations
(c) SolPS coating and (d) SPS coating

Two distinct morphologies of deposited electrolyte coatings were identified by FESEM: a combined splat-like and nodule-like (Figure 7a) and splat-like (Figure 7b). The splats were typically 0.5–3 μm, and the nodules <200 nm in diameter. The gas permeability of the GDC coating produced by SolPS is 6.60×10^{-15} m^2 (coating porosity=9.1%), which is more porous than that produced by SPS (gas permeability=0 and coating porosity=1.4%). This porosity difference is related to the amount of water present in the SolPS process with a high plasma energy fraction being used to evaporate it. The consequence is that the particles do not receive enough energy to be fully molten before depositing onto the substrate, and to form the porous coating. Figures 7c and 7d show the fracture cross

section of the SolPS and SPS-deposited electrolytes. It can be clearly seen that the SPS coating is much more homogeneous and shows better bonding and continuous contact with the Ni substrate compare with the SolPS coating. Normally, the electrolyte layer is 100–150 μm thick using conventional plasma-spraying process; however, the SPS process is capable of producing a thin layer of 5 μm while keeping the microstructure, continuity, uniformity and density of the deposit under the optimized plasma condition. The XRD patterns of the electrolytes shown in Figure 5c and 5d indicate that the electrolytes consist of the same composition as the plasma-synthesized powders; there is no major phase transformation during the SPS process.

2.5 Cathode synthesis

The metal nitrates $Sr(NO_3)_2$ (purity: 99.0%) used in this work were supplied by Aldrich Chemical (Sigma-Aldrich, St. Louis, MO), and $Fe(NO_3)_3 \cdot 9H_2O$ (purity: 98.0%) by Sigma (Sigma-Aldrich, St. Louis, MO). The $La(NO_3)_3 \cdot 6H_2O$ (purity: 99.9%) and $Co(NO_3)_2 \cdot 6H_2O$ (purity: 97.7%) were commercially obtained from Alfa Aesar.

Metal nitrate solutions of La, Sr, Mn (Fe or Co) were made up from their metal nitrate precursors. The desired molar ratios of La, Sr, Mn (Fe or Co), as nitrate salts, were mixed in water to provide 1 mol of the final perovskite. The stoichiometric-ratio metal nitrates of $La_{0.8}Sr_{0.2}MO_{3-\delta}$ (M=Mn, Fe, or Co) were dissolved to obtain a concentration of 1.1M solution. Glycine was added to the solution at a concentration of 1.45M.

Solution plasma-spraying synthesis technique was used to produce $La_{0.8}Sr_{0.2}MO_{3-\delta}$ powders. The variable plasma-spraying parameters are given in Table IV.

Table IV. Cathode specific induction plasma spraying parameters

Torch Nozzle Diameter :	45	mm
Reactor Pressure :	100	Torr
Plasma Power	33	kW
Stand-off Distance (for coating)	210	mm
Solution flow rate	10	mL/min
Deposition Loops (for coating)	2	

Figure 8a–8c, show high-resolution SEM micrographs of powders synthesized by the plasma process (in the order $La_{0.8}Sr_{0.2}MnO_{3-\delta}$, $La_{0.8}Sr_{0.2}FeO_{3-\delta}$ and $La_{0.8}Sr_{0.2}CoO_{3-\delta}$). All particles shapes are shown in these micrographs are almost globular. Figure 9a–9c shows the particle size and distribution of the plasma-synthesized $La_{0.8}Sr_{0.2}MnO_{3-\delta}$ (LSM), $La_{0.8}Sr_{0.2}FeO_{3-\delta}$ (LSF) and $La_{0.8}Sr_{0.2}CoO_{3-\delta}$ (LSC) powders, respectively. Particle size and distribution of these synthesized powders were not changed by exposure to 5 min to a 250 W ultrasonic treatment. Most of the particles of these plasma-synthesized powders have sizes around 63 nm with an average crystallite size of 20 ± 3% nm (Calculated by the Scherrer formula from the XRD data). Furthermore, when the plasma-synthesized powders are compared with the powders synthesized by Glycine Nitrate Combustion Process (GNP) or to the Pechini methods, induction plasma-synthesized powders have the smallest particle sizes and the largest BET specific surface area values [25].

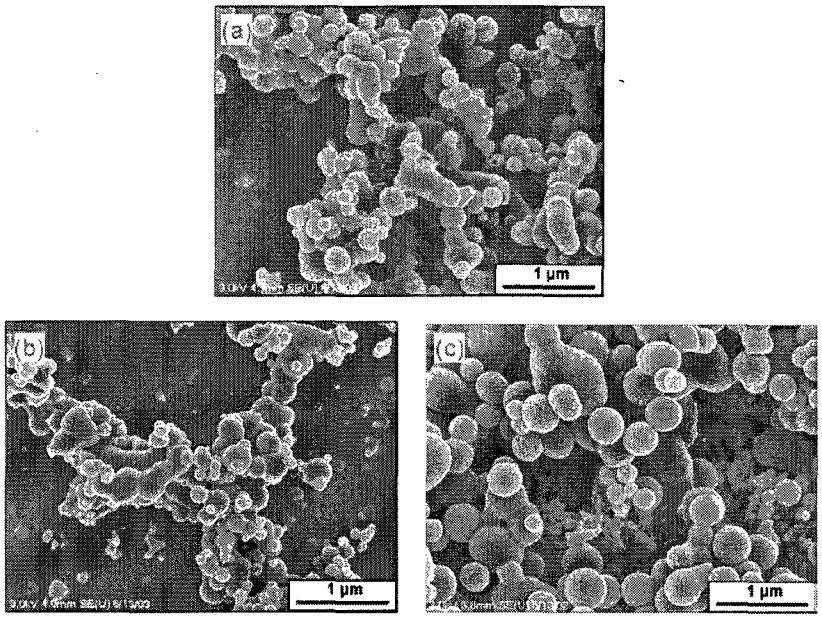

Fig. 8 Micrographs of synthesized (a) $La_{0.8}Sr_{0.2}MnO_{3-\delta}$; (b) $La_{0.8}Sr_{0.2}FeO3_{-\delta}$ and (c) $La_{0.8}Sr_{0.2}CoO_{3-\delta}$ cathode nano-powders

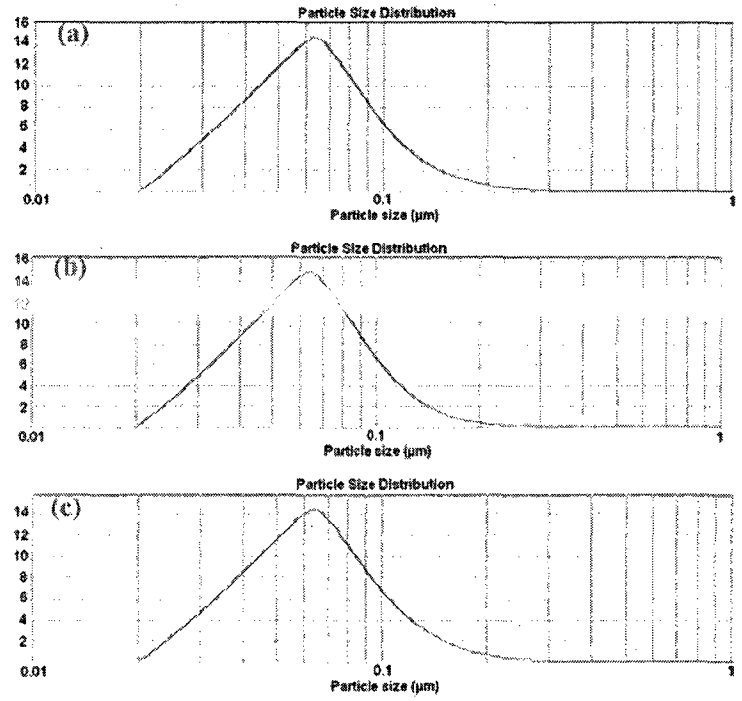

Fig. 9 Particle size and size distribution of (a) $La_{0.8}Sr_{0.2}MnO_{3-\delta}$; (b) $La_{0.8}Sr_{0.2}FeO3_{-\delta}$ and (c) $La_{0.8}Sr_{0.2}CoO_{3-\delta}$ powders produced by induction plasma process [25]

The phase composition for the solution plasma spraying synthesized cathode materials were analyzed by XRD. In Figure 10 [26], the XRD pattern shows the plasma synthesized of LSM powders have very small lanthanum oxide and lanthanum hydroxide peaks, indicating that very small amounts of lanthanum oxide and hydroxide were formed during the induction plasma synthesis. When Kang and Taylor [27] made porous LSM cathode thin film on mild steel, using a reactive DC plasma spray process, very small amounts of lanthanum oxide were also detected in the coating layer. During preparation of perovskite powders and coatings in a RF inductively coupled plasma, using precursor suspensions of MnO_2 powder in a $LaCl_3$/EtOH solution, the $LaMnO_3$ perovskite phase was formed as the primary phase along with a certain amount of additional phases, consisting mainly of lanthanum oxide [27]. In our case, the amount of lanthanum oxide in the plasma-sprayed powders is much lower than for the earlier reported results [27-28]. However, plasma-synthesized LSC powders are a pure perovskite phase, without detectable impurity, implying that it is possible to directly synthesize the pure perovskite cathode composition materials, in the form of nano-sized particles by the induction plasma-synthesis technique.

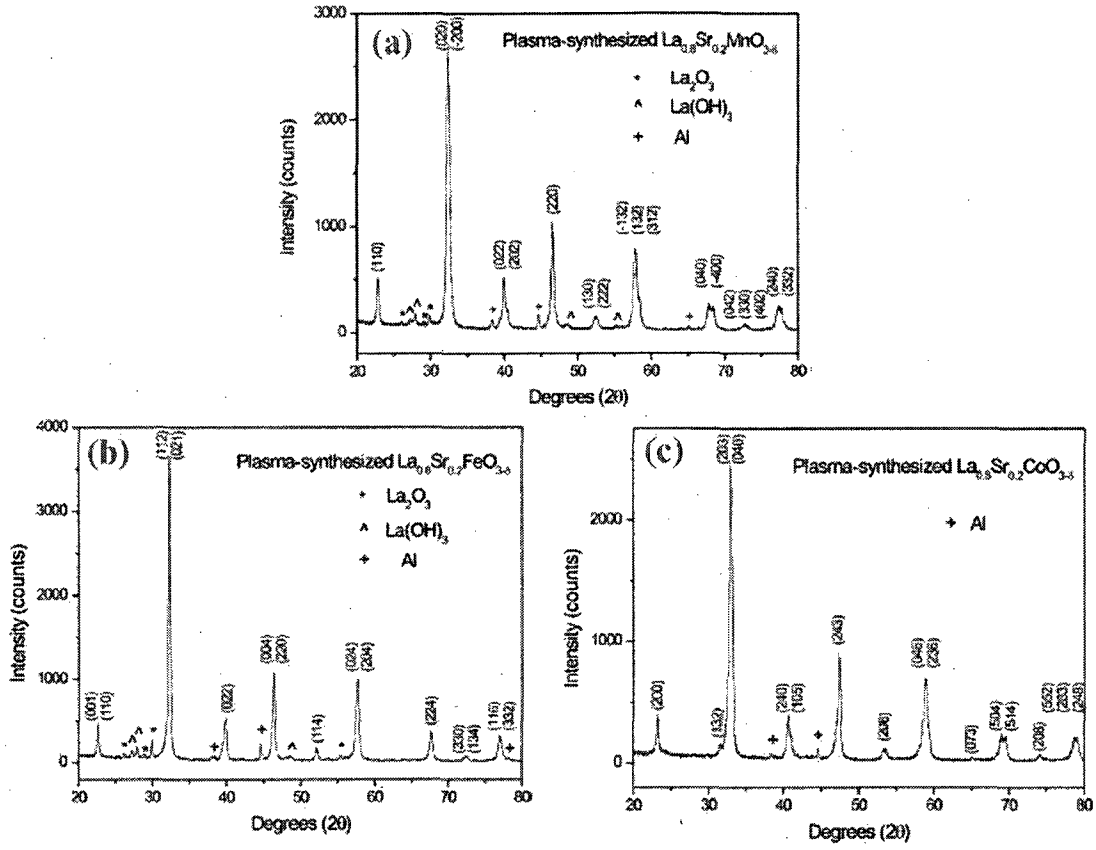

Fig. 10 X-ray analysis for as-synthesized (a) $La_{0.8}Sr_{0.2}MnO_{3-\delta}$; (b) $La_{0.8}Sr_{0.}2FeO3_{-\delta}$ and (c) $La_{0.8}Sr_{0.2}CoO_{3-\delta}$ cathode materials [26]

Shown in Figure 11a is a cross-sectional micrograph of the cathode layer fabricated by SolPS process. The deposited LSCF cathode is well adhered to the GDC electrolyte. Higher magnification FESEM micrographs shown in Figure 11b and 11c indicate that the larger particles (300–500 nm) consist of particles smaller than 20 nm in diameter. The resulting nanostructure offers extremely high surface area for oxygen reduction. Meanwhile, the large interconnected pore channels within the cathode layer facilitate oxygen mass transport.

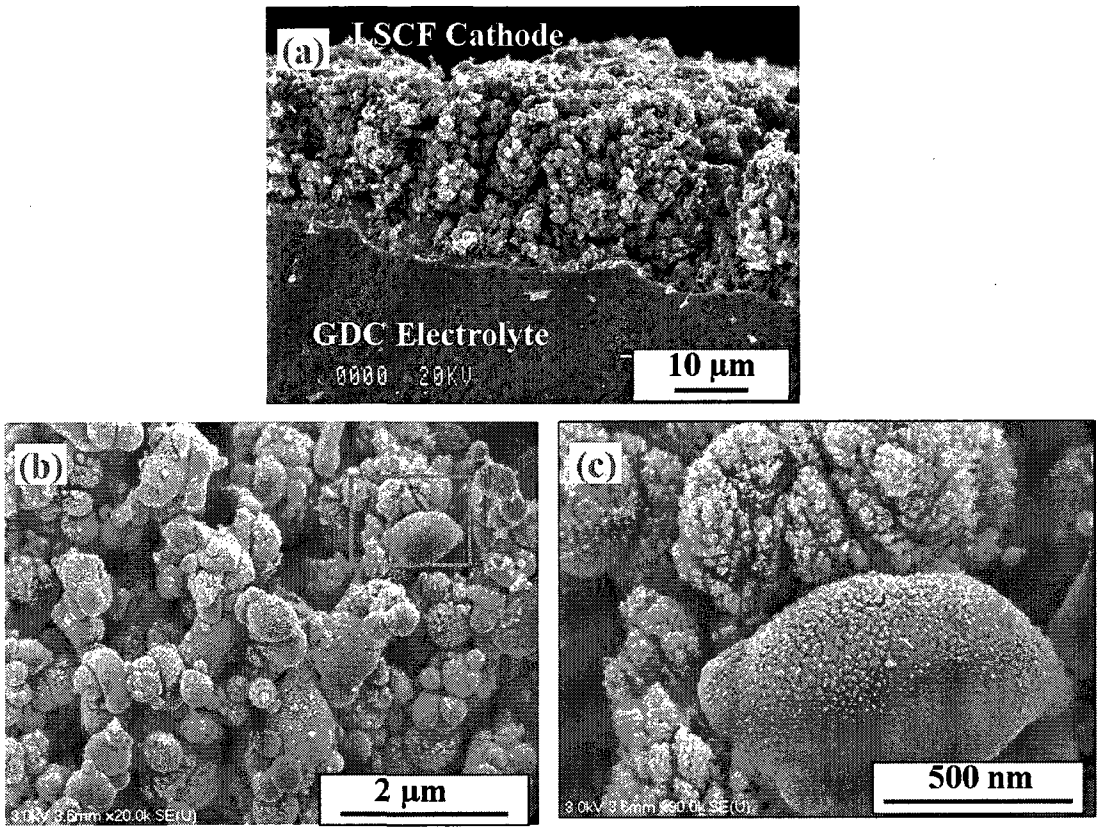

Fig. 11 (a) Cross-sectional view of cathode layer, (b) and (c) higher magnification FESEM micrographs of cathode [26]

Figures 12 and 13 show the polarization resistances of the cell with electrodes fabricated by the induction plasma-spraying process. Clearly, the fuel cell with solution plasma-sprayed cathode displayed much lower interfacial polarization resistances than those prepared by conventional methods: tape-casting [29], slurry printing [30] and spin-coating [31]. The activation energies (*Ea*) were extracted from the slopes and are identified for each curve on the graphic. Dusaste et al. [30] published some results about pure LSCF/GDC sintered at 500–700°C and the *Ea* was 1.54 eV. The fuel cell with solution plasma-sprayed cathode shows smaller *Ea*. This lower activation energy is probably due to the benefits of the fabrication technique which favors nano-structured features. As plasma-synthesized cells do not require any post processing such as

sintering, the performance of the cathodes can be maintained. Indeed, Murray et al. [31] in their paper about LSCF cathodes demonstrated that the sintering conditions affect the cathode performance. The activation energy for this pure LSCF cathode was 1.63 eV. It is believed that using solution plasma-spraying technology to produce the nano and submicron structured cathode and at the same time obtaining good adhesion is the key to achieve lower polarization resistances of cathodes.

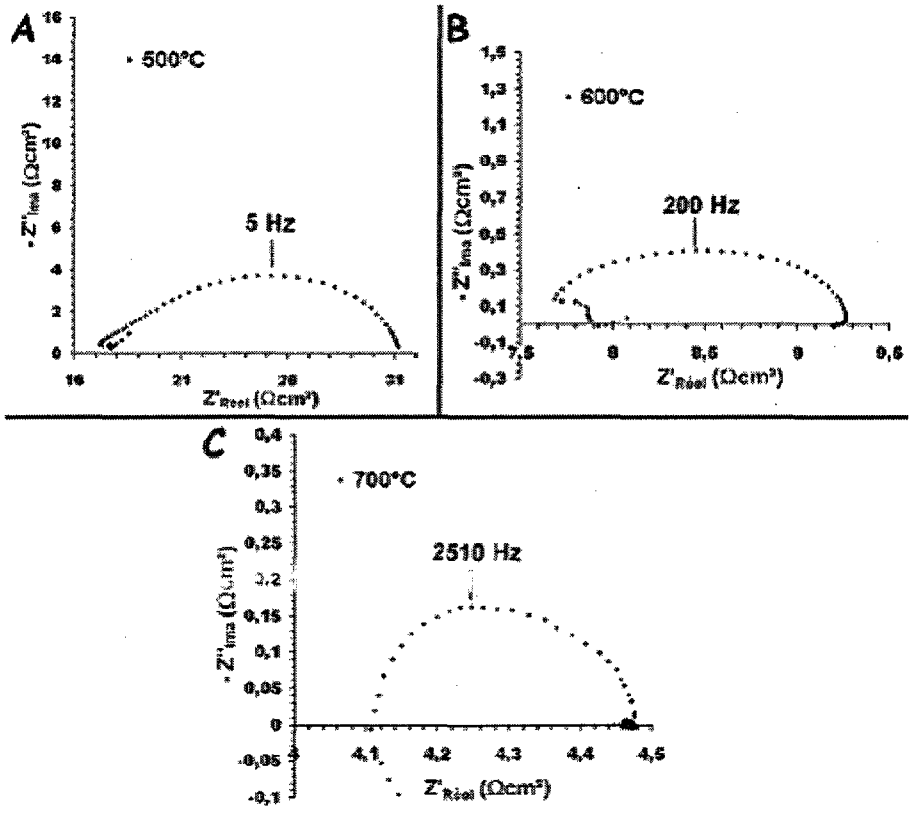

Fig. 12 Complex impedance spectra of LSCF pellets [25]

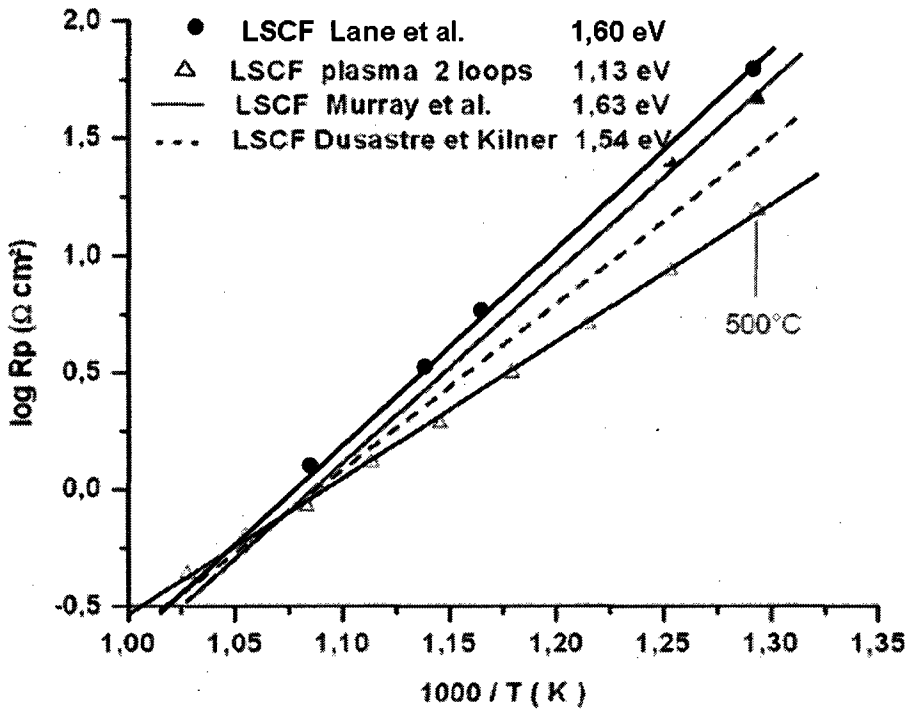

Fig. 13 Induction plasma sprayed cathode has lower cathodic polarization resistance compared to using other methods [25]

3. Conclusions and Future Works

Induction plasma technology has been successfully developed to synthesize the SOFC materials as well as the components. The nano-structured electrodes have very unique microstructures: each large agglomerate consists of smaller ones, which in turn contains even smaller particles. The resulting porous structures have large pores for rapid gas transport and extremely large surface area for fast electrochemical reactions. SOFCs with these electrodes have shown very low interfacial polarization resistances at intermediate temperature. Suspension plasma spraying process could produce much denser electrolyte compared to solution plasma spraying process. Preliminary results obtained at Université de Sherbrooke have demonstrated the feasibility of induction plasma spraying process

applied to produce the porous nano-structured electrodes as well as dense electrolyte coatings. This represents an opportunity to fabricate the fully integrated nano-structured SOFC using solution and suspension plasma spraying process.

Acknowledgement

The authors would like to acknowledge the support of Natural Sciences and Engineering Research Council of Canada (NSERC), Plasma Quebec and Nano Québec. Furthermore, the contributions of the highly qualified technicians of CREPE plasma laboratory, Mr. Francis Barrette, Mr. Patrice Poulin, are gratefully acknowledged.

References

[1] S. C. Singhal, "Advances in Solid Oxide Fuel Cell Technology," *Solid State Ionics*, 2000, **135**, 305-313.

[2] T. Yoshida, T. Okada, H. Hamatani, and H. Kumaoka, "Integrated Fabrication Process for Solid Oxide Fuel Cells Using Novel Plasma Spraying," *Plasma Sources Science Technology,* 1992, **1**, 195-201.

[3] X. Q. Ma, S. Hui, H. Zhang, J. Dai, J. Roth, T. D. Xiao, and D. E. Reisner, "Intermediate Temperature SOFC Based on Fully Integrated Plasma Sprayed Components," *Thermal Spray 2003: Advancing the Science & Applying the Technology, (Ed.). Moreau and B. Marple*, 163-168.

[4] B. Zhu, X. T. Yang, J. Xu, Z. G. Zhu, S. J. Ji, M. T. Sun, and J. C. Sun, "Innovative Low temperature SOFCs and Advanced Materials," *Journal of Power Sources*, 2003, **118**, 47-53.

[5] B. C. H. Steele, "Appraisal of $Ce_{1-y}Gd_yO_{2-y/2}$ Electrolytes for IT-SOFC Operation at 500°C," Solid State Ionics, 2000, **129** 95–110.

[6] S. W. Zha, W. Rauch, and M. L. Liu, "Ni-$Ce_{0.9}Gd_{0.1}O_{1.95}$ Anode for GDC Electrolyte-Based Low-Temperature SOFCs," *Solid State Ionics*, 2004, **166**, 241-250.

[7] M. I. Boulos, "RF Induction Plasma Spraying State-of-the Art," *Journal of Thermal Spray Technology*, 1992, **1,** 33-41.

[8] P. Fauchais, "Understanding Plasma Spraying," *Journal of Physics D: Applied Physics*, 2004, **37**, R86-R108.

[9] F. Gitzhofer, M. I. Boulos, J. Heberlein, R. Henne, T. Ishigaki, and T. Yoshida, "Integrated Fabrication Process for Solid-oxide Fuel Cells Using Thermal Plasma Spray Technology," *MRS Bulletin*, 2000, **25**, 38-42.

[10] M. Lang, R. Henne, S. Schaper, and G. Schiller, "Development and Characterization of Vacuum Plasma Sprayed Thin Film Solid Oxide Fuel Cells," J*ournal of Thermal Spray Technology,* 2001, **10**(4), 618-625.

[11] G. Schiller, R. H. Henne, M. Lang, R. Ruckdäschel, and S. Schaper, "Development of Vacuum Plasma Sprayed Thin-Film SOFC for Reduced Operating Temperature," *Fuel Cells Bulletin*, 2005, **21**, 7-12.

[12] G. Schiller, R. Henne, M. Lang, and M. Müller, "Development of Solid Oxide Fuel Cells by Applying DC and RF Plasma Deposition Technologies," *Fuel Cells*, 2004, **4**, 56-61.

[13] I. Castillo, and R. J. Munz, "Inductively Coupled Plasma Synthesis of CeO_2-based Powders from Liquid Solutions for SOFC Electrolytes," *Plasma Chemistry and Plasma Processing*, 2005, **25**(2), 87-107.

[14] M. Muller, E. Bouyer, M. v. Bradke, D. W. Branston, R. B. Heimann, R. Henne, G. Lins, and G. Schiller, "Thermal Induction Plasma Process for the Synthesis of SOFC Materials," *Mat.-Wiss. U. Werkstofftech*, 2002, **33**, 322-330.

[15] Z. Li, W. Mallener, L. Fuerst, D. Stoever, and F. D. Scherberich, "Plasma Sprayed Perovskite of the Composition Lanthanum Strontium Manganese Oxide ($La_{1-x}Sr_xMnO_{3-\delta}$): Phase Analysis and Electrical Conductivity," *Thermal Spray Coating Process: National Thermal Spray Conference, 5th*, 1993, 343-346.

[16] L. W. Tai, and P. A. Lessing, "Plasma Spraying of Porous Electrodes for a Planar Solid Oxide Fuel Cell," *Journal of the American Ceramic Society*, 1991, **74**(3), 501-504.

[17] K. Mailhot, F. Gitzhofer, and M. I. Boulos, "Supersonic Induction Plasma Spraying of Dense YSZ Electrolyte Membranes," *Thermal Spray: A United Forum for Scientific and Technological Advances, Ed. C.C. Berndt*, 1997, 21-25.

[18] F. Gitzhofer, E. Bouyer, and M. I. Boulos, "Suspension Plasma Spray Deposition," *U. S. Patent 5 609 921*, 1997.

[19] P. Fauchais, V. Ra, C. Delbos, J. F. Coudert, T. Chartier, and L. Bianchi, "Understanding of Suspension DC Plasma Spraying of Finely Structured Coatings for SOFC," *IEEE Transactions on Plasma Science*, 2005, **33**(2), 920-930.

[20] J. Oberste, Berghaus, J. G. Legoux, C. Moreau, R. Hui, and D. Ghosh, "Suspension Plasma Spaying of Intermediate Temperature SOFC Components Using an Axial Injection DC torch," Materials Science Forum, 2007, **539–543** [Part 2, THERMEC 2006] 1332–1337.

[21] L. Jia, C. Dossou-Yovo, C. Gahlert, and F. Gitzhofer, "Induction Plasma Spraying of Samaria Doped Ceria as Electrolyte for Solid Oxide Fuel Cells," *Proceedings of the International Thermal Spray Conference, Advances in Technology and Application*, 2004, 85-89.

[22] M. von Bradke, F. Gitzhofer, R. Henne, "Porosity Determination of Ceramic Materials by Digital Image Analysis--A Critical Evaluation," *Scanning*, 2005, **27**(3), 132-135.

[23] M. V. Chor and W. Li, "A Permeability Measurement System for Tissue Engineering Scaffolds," *Measurement Science and Technology*, 2007, **18,** 208–216.

[24] F. Hudon, "Fabrication Par Plasma Inductif d'Anodes et d'Électrolytes de Piles à Combustible à Électrolyte Solide (SOFC) à Basse Température," *Master Thesis*, Université de Sherbrooke, 2006, 24-34.

[25] D. Bouchard, L. Sun, F. Gitzhofer, and G. M. Brisard, "Synthesis and Characterization of $La_{0.8}Sr_{0.2}MO_{3-\delta}$ (M = Mn, Fe, or Co) Cathode Materials by Induction Plasma Technology," *Journal Thermal Spray Technology*, 2006, **15**(1), 37-45.

[26] D. Bouchard, "Développement d'une Interface Cathode/Électrolyte peu Résistive Projection Plasma pour Application aux Piles á Combustible á Électrolyte Solide (SOFC), " *Master Thesis*, 2005, Université de Sherbrooke.

[27] H. K. Kang and P. R. Taylor, "Direct Production of Porous Cathode Material ($La_{1-x}Sr_xMnO_3$) Using a Reactive DC Thermal Plasma Spray System," *Journal of Thermal Spray Technology,* 2001, **10**(3), 526-531.

[28] R. Henne, M. Muller, E. Pross, G. Schiller, F. Gitzhofer, and M. Boulos, "Near-Net-Shape Forming of Metallic Bipolar Plates for Planar Solid Oxide Fuel Cells by Induction Plasma Spraying," *Thermal Spray Technology*, 1999, **8**(1), 110-116.

[29] J. A. Lane, S. Adler, P. H. Middleton, and B. C. H. Steele, "Polarization Behavior of Mixed Conducting Perovskite Cathode Materials," *Proceedings of the Electrochemical Society*, 1995, **95**(1) [Solid Oxide Fuel Cells (SOFC-IV)], 584–596.

[30] V. Dusastre, and J. A. Kilner, "Optimisation of Composite Cathodes for Intermediate Temperature SOFC Applications," *Solid State Ionics*, 1999, **126**,163-174.

[31] E. Perry Murray, M. J. Sever, and S. A. Barnett, "Electrochemical Performance of $(La,Sr)(Co,Fe)O_3$–$(Ce,Gd)O_3$ Composite Cathodes," *Solid State Ionics*, 2002, **148,** 27–34.

4.2 *Induction Plasma Synthesis of Nano-structured SOFCs Electrolyte Using Solution and Suspension Plasma Spraying: A Comparative Study*

Lu Jia and François Gitzhofer, ing. PhD

Energy, Plasma and Electrochemistry Research Centre (CREPE), Chemical and Biotechnical Engineering Department, Université de Sherbrooke, Québec, Canada, J1K 2R1, (819)-821-7171

In this paper, two plasma spraying technologies: solution plasma spraying (SolPS) and suspension plasma spraying (SPS) were used to produce nano-structured Solid Oxide Fuel Cells (SOFCs) electrolytes. Both plasma spraying processes were optimized in order to achieve the thin gas tight electrolytes. The comparison of the two plasma spraying processes is based on electrolyte phase, microstructure, morphology, as well as on plasma deposition rate. The results showed that nano-structured thin electrolytes (~ 5μm thick) have been successfully SPS deposited on porous anodes with a high deposition rate. Compared to the electrolytes produced by SolPS, the SPS deposited electrolyte layer is much denser. During the SPS process, fine droplets of 0.5 to 1 μm in diameter impact on the surface of the coating and penetrate into the pores of the anode. As the stresses are reduced on the resulting 0.5 to 2 μm splats, there is no apparent micro-cracks network on the splats, this resulting in highly gas-tight coatings. It is demonstrated that the SPS process is beneficial for the improvement of the performance of the films to be used as SOFC electrolytes.

Keywords Solution plasma spray (SolPS), suspension plasma spray (SPS), solid oxide fuel cells (SOFCs), nano-structured electrolyte, thin film

1. Introduction

The successful introduction of solid oxide fuel cells (SOFCs) as an environmentally friendly energy converter into the highly competitive market for electric power generation depends on the development of technologies which will bring about reduction in production costs. Furthermore, development of intermediate temperature SOFCs (IT-SOFC) that operate at temperatures of 500-700°C is also added to the potential cost reduction [1-4]. In this perspective, the problems of ohmic loss [5] and the insufficient ionic conductivity of current yttria stabilized zirconia (YSZ) electrolytes [6] can be overcome by using alternative materials with higher ionic conductivity compared to YSZ, as well as by decreasing the electrolyte resistance by reducing its thickness to 10 to20 μm.

Cation-doped ceria with a fluorite structure is one of the most suitable electrolyte candidates for IT-SOFCs. Unfortunately, these cerium (CeO_2) based oxides are known to undergo reduction at low oxygen partial pressure, and become mixed conductors [7-15]. To overcome this problem and to improve the conductivity for IT-SOFCs, the influence of nano-structured features in the doped CeO_2 systems on the mixed conductivity should be taken into account [16-17]. A high density of defects in nano-structured materials provides a large number of active sites for ionic conduction and high diffusivity through nano-sized grain boundaries to promote fast kinetics and ion transportation [18]. On the other hand, a large fraction of grain boundaries also decreases the electronic conduction [19]. However, some other authors such as Chiang and co-workers [20] found strongly enhanced electronic conductivity for sintered 1.5 mol% gadolinium-doped cerium oxide having 10 nm average grain size compared to conventional samples. For higher mol% of gadolinium no change in ionic conductivity was measured as function of grain size. In

another work by Tuller et al. [21], conductivity of 5 μm and 10 nm grain sized CeO_2 were compared at 600°C. It was demonstrated that under low oxygen partial pressures ($-22 < \log PO_2 < -14$) as the conductivity was electronic, nanostrucutred CeO_2 showed 104 times higher conductivity. For high PO_2 ($2 < \log PO_2 < 6$) the conductivity of both materials converged. The nano-structured ceria-based thin films have demonstrated a number of great improvements, for example: higher surface area, better coherency and longer triple phase boundary length, compared with the bulk materials. They also provide new opportunity and feasibility for IT-SOFCs commercialization [22].

Thin layers of SOFCs electrolyte have been produced by a number of deposition techniques, including aerosol-assisted metal-organic chemical vapour deposition (MOCVD), polarized electrochemical vapour deposition (PEVD), RF magnetron sputtering, atomic layer deposition (ALD), screen printing, slurry coating, and the sol-gel process [23-29]. These techniques are generally expensive in both equipment and operation costs, and are of rather low efficiency, which makes them difficult to scale up for commercialization. Recently, the plasma spray processes, such as atmospheric plasma spraying (APS), vacuum plasma spraying (VPS), low pressure plasma spraying (LPPS), hybrid plasma spraying (HYPS) and high velocity oxy-fuel spraying (HVOF) have been developed and adapted to specific requirements of electrolyte deposition in a consecutive and cost-effective spray process [30-34]. However, they suffer from a relatively high coating thickness (50-100 μm), residual porosity/defects (consequently a post thermal treatment or an interlayer is needed to seal the anode), and thermal stresses which lack the capability to deposit comparable thin and dense homogenous SOFC electrolytes.

As a promising extension of conventional thermal spraying, the use of a liquid precursor permits feeding and spraying of either metal precursor solutions or a suspension of nano or submicro-sized particles to form thin coatings with more refined microstructure and grain size. The former is known as solution plasma spraying (SolPS) while the latter is known as suspension plasma spraying (SPS). The use of a solution precursor was first reported as a coating technology by Karthikeyan, et al [35-36]. In the SolPS process, solution feedstocks of desired resultant materials are injected into the plasma jet either by atomization or by a liquid stream. Rapid heating and evaporation of solution droplets result in the formation of the solid particles, which are heated and accelerated to the substrate to generate coatings [37]. The as-deposited coatings have the desired porosity. Its microstructure has nano and sub-micrometric features [38-44]. Suspension plasma spraying (SPS), the new method of preparing nano-structured coatings was invented in the mid-1990s by Université de Sherbrooke [45]. In this process, a suspension of micro or nano-powders is fed to an RF [46-47] or to a DC [48-51] plasma torch and axially or radially injected into the plasma flame [52-53]. The solid particles enclosed in each droplet are accelerated, evaporated (solvent), melted (solid particles), and then flattened onto a prepared substrate rapidly forming thin (5-10 μm) coatings with a more refined microstructure. Moreover, the composition of applied spray materials can be varied very easily.

In this contribution, the results of SolPS and SPS using inductively coupled thermal plasma for the deposition of dense and thin nano-structured gadolinia-doped ceria (GDC) electrolyte coatings (5-10 μm thick) are presented. The corresponding produced electrolyte layers were characterized and compared to illustrate the correlation between

deposition techniques and electrolyte microstructure. In the following sections, the experimental facilities will be presented first. The preparation of the electrolyte powder, of the solution and of the suspension will then be described, as well as the plasma spraying setup. In the third section, the characterization of the injection of the suspension/solution and the interactions of the plasma-particles will be discussed. Finally, the morphologies and microstructures of GDC coatings produced by SolPS and SPS will be compared.

2. Experimental

2.1 Powder preparation

Electrolyte powders of $Ce_{0.8}Gd_{0.2}O_{1.9}$ (GDC) were prepared by the glycine-nitrate process method (GNP) [54]. Stoichiometric amounts of $Ce(NO_3)_3 \cdot 6H_2O$ (Alfa Aesar, 99.99%) and $Gd(NO_3)_3 \cdot 6H_2O$ (Alfa Aesar, 99.99%) were dissolved in distilled water, to which 0.5 mol glycine per mole nitrate was added. Combustion of the metal nitrate-glycine solution was performed in a glass beaker on a hotplate, with about 20 ml of the solution (0.1 mol with respect to metal ions) burned at a time. The precursor solution turned to a brown-red gel as the solvent was evaporated and then spontaneous combustion occurred, leading to pale-yellow ash. The resultant ash was then collected and calcined in air at 600°C for 2

2.2 Solution precursor preparation

The solution precursor of GDC was prepared by dissolving separately cerium nitrate hexahydrate (Alfa Aesar, 99.99%) and gadolinium nitrate hexahydrate (Alfa Aesar, 99.99%) in distilled water according to stoichiometric compositions. The solution

concentration was 0.6 g/mL. A magnetic stirrer was used to fully mix the starting precursors.

2.3 Suspension precursor preparation

To prepare the GDC suspension, GNP-GDC powders were directly dispersed into ethanol. The weight ratio of GDC to ethanol was set to 10%. The suspension viscosity was adjusted by adding Darvan No. 7 (dispersing agent, R. T. Vanderbilt Company, Inc., Norwalk, USA) into the suspension. The mass percentage of the dispersing agent selected for use was 2% of the GDC powder mass to obtain the lowest viscosity for adequate feeding. Before deposition, the suspension mixture was ultrasonically dispersed to break apart the large agglomerates. During injection, a stirrer was used to prevent particles from settling.

2.4 Plasma spraying setup

The induction plasma spraying system consisted of a liquid precursor feeder system (Cole-Parmer Canada Inc., Montreal, Canada), an atomization probe (Tekna Plasma Systems Inc., Sherbrooke, Canada), a plasma torch and a plasma reactor. Figure 1 shows the schematic illustration of an induction plasma system. The induction plasma was generated using a PL-50 plasma torch (Tekna Plasma Systems Inc., Sherbrooke, Canada), operating at a frequency of 3 MHz. The torch is equipped with a supersonic nozzle (diameter = 24.2 mm), in order to increase the plasma velocity [55]. The liquid precursors such as solution or suspension were fed by a peristaltic pump and directly injected into the hot plasma core by means of an atomization probe, resulting in the formation of a coherent deposit. Detailed description of the induction plasma spraying apparatus used

for this study is available elsewhere [55]. Table I shows the spraying parameters that were used for the synthesis of the electrolytes. The RF power was varied in the range of 35 to 50 kW, the chamber pressure adjusted at 8 and 12 kPa, and spraying distance was varied from 100 to 220 mm. The atomization parameters were adjusted according to the droplet size measurements using the Malvern RTsizer (Malvern Instruments Limited, Worcestershire, UK) apparatus. The average droplet size (D_{50}) was about 12 μm as measured during water atomization testing.

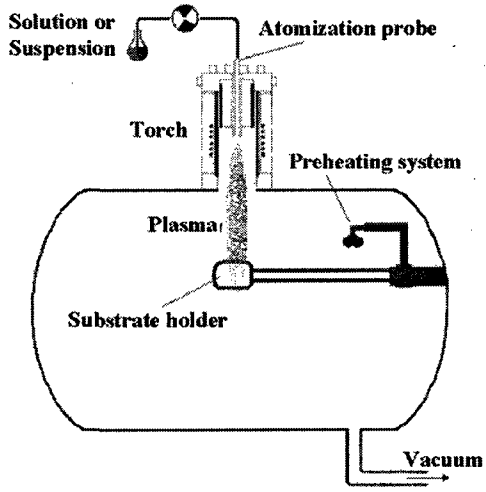

Fig. 1 Schematic illustration of induction plasma system

The substrates (10 mm diameter and 1.2 mm thick) were produced by the sintering of pressed 44% wt of green nickel oxide (Novamet type F), 48% wt of filamentary nickel powder (Novamet 255) and 8 %wt of nickel powder (Novamet 210) for 1 hour at 800°C. The substrates were fixed on a sample holder while the holder was scanned across the plasma flame by an electromotive arm. Multiple passes were used to build up the coatings. In order to reduce the thermal gradients during deposition and to obtain dense

coating [56], the substrates were heated up to 300°C prior to coating using an electric heating device.

Table.1. Induction Plasma Spraying Parameters

Plasma torch	Tekna PL - 50
Central plasma gas flow rate [slpm]	27 (Ar)
Sheath plasma gas flow rate [slpm]	80 (O_2)
Plasma power [kW]	35 - 50
Reactor pressure [kPa]	6 and 12
Atomization gas pressure [kPa]	345 (Ar)
Atomization gas flow rate [slpm]	21 (Ar)
Solution injection flow rate [mL/min]	10
Suspension injection flow rate [mL/min]	4
Spraying distance [mm]	100-220

2.5 Characterization

Different techniques were used to characterize the materials synthesized by the induction plasma process. Particle size distributions were measured using a Malvern Mastersizer 2000 particle analyzer (Malvern Instruments Ltd., Worcestershire, United Kingdom). Structural features analysis was conducted by X-ray diffraction (XRD) using an X'Pert Pro MPD X-ray diffractometer (Philips, Eindhoven, Netherlands). Morphologies and elemental analyses of electrolyte powders and as-deposited electrolyte layers were performed using a field emission scanning electron microscope (FESEM, model S-4700, Hitachi, Tokyo, Japan). Specific surface areas of the electrolyte powders were determined by the BET method, using an Autosorb-1 instrument (Quantachrome, Florida, USA). The as-sprayed coatings were cut using a Buehler ISOMET 2000 Precision Saw and then mounted (infiltrated with EPO-KWICK Buehler low viscosity resin using vacuum impregnation). The polishing was carried out on a Buehler ECOMET 3-VARIABLE SPEED GRINDER POLISHER using procedures outlined for thermal sprayed ceramic

coatings in Technical notes published by Buehler. These involve polishing on a 45 μm diamond grid followed by cloth polishing with 9 and 3 μm diamond suspensions and a final step of 0.05 μm alumina suspension. The semi-automatic procedures helped increase the reproducibility of polishing cross-sections [57]. Coatings porosity was determined by SigmaScan Pro 5, an image analysis software supplied by Systat Software Inc.. A sufficient number of pictures were taken at different sample areas, according to the magnification used. A threshold method was used to determine the darker percentage of the picture that directly provided the porosity [58]. Gas permeability was measured according to Darcy's law [59]. Detailed description of the gas permeability measurement apparatus used for this study is available elsewhere [60].

3. Results and Discussions

3.1 As-synthesized GNP-GDC powder characteristics

Figure 2 depicts the FESEM micrographs of as-synthesized GNP-GDC powders, indicating that the particle is highly porous with a foam-like microstructure. The XRD pattern (Figure 3(a)) of the GNP-GDC sample exhibits all peaks associated with the pure fluorite structure. The crystallite size of the GDC phase, calculated from XRD line-broadening analysis according to the Scherrer equation is 26.5 ± 3% nm. The specific surface of GDC powders determined by the BET method is 43.1 m^2/g.

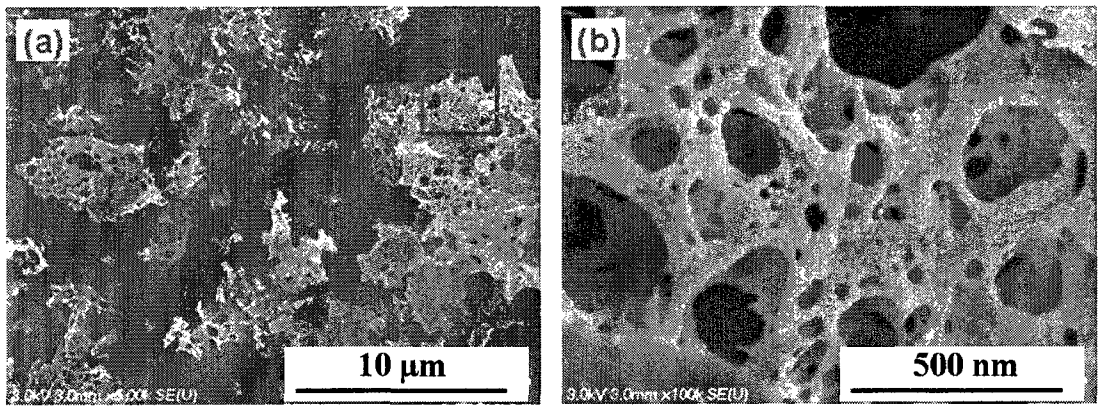

Fig. 2 SEM micrographs of GNP synthesized GDC nano-structured powders with different magnifications

Particle sizes distribution of GDC powders elaborated with the GNP technique are shown in Figure 4. An ultrasonic treatment of 5 minutes at 250 W power was applied before the particle size measurement. The particle sizes of the GDC powders were mostly about 0.6 μm in size with a narrow size distribution. However, before any ultrasonic treatment, the average particle size is 25.5 ± 3% μm. This is due to porous structures of the agglomerated GDC powders, whose agglomerates were easily broken by the ultrasound. These GDC powders are referred to as weakly agglomerates.

The quality of electrolyte coatings is highly dependent on the size and size distribution of the electrolyte powder particles during suspension preparation and droplet atomization. This is because fine droplets atomized with a narrow size distribution around 12 μm can be evenly plasma treated, resulting in coatings of high homogeneity, high density and a minimum of flaws.

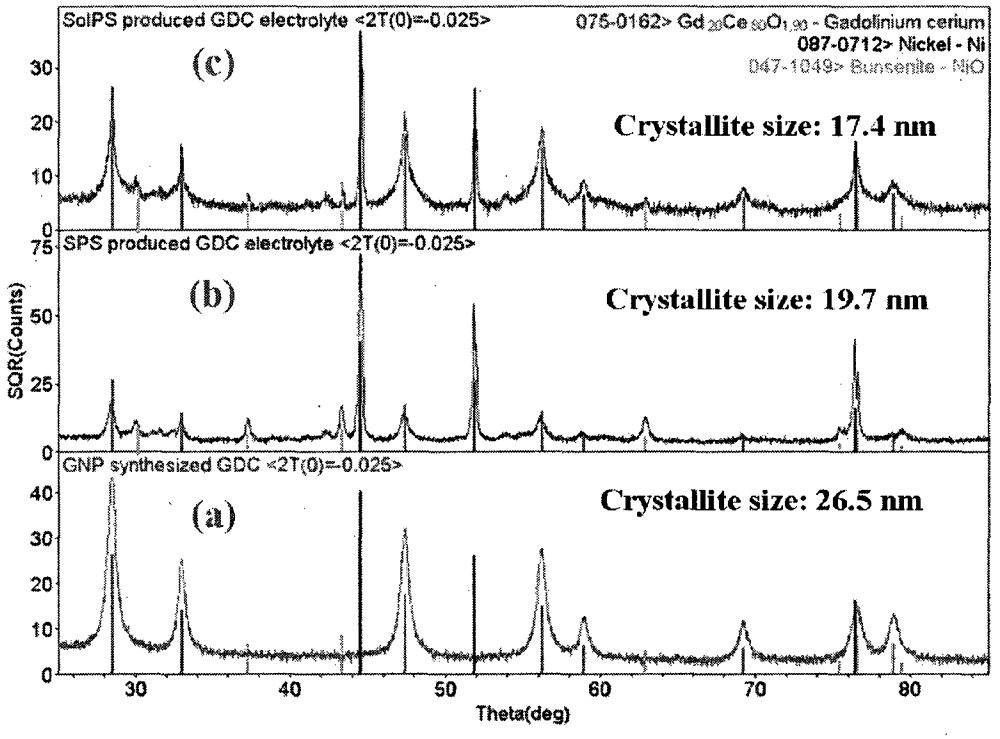

Fig. 3 X-ray analysis for (a) GNP synthesized GDC powders, (b) suspension and (c) solution plasma sprayed GDC electrolyte

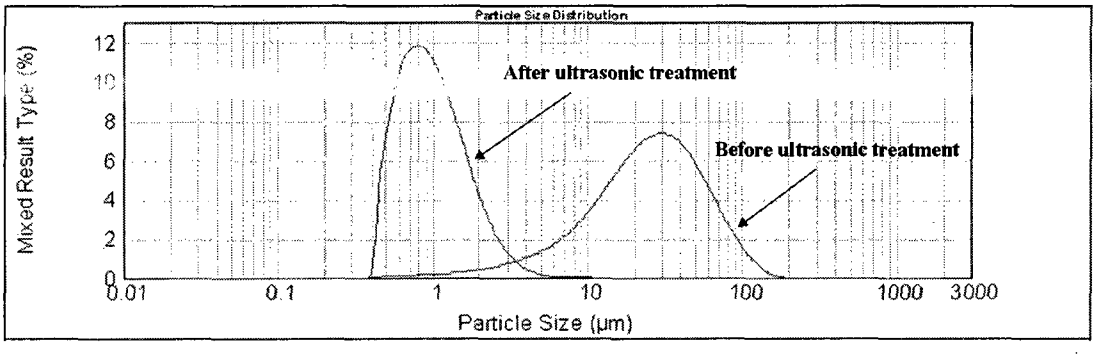

Fig. 4 GNP-GDC particle size distribution (after 5 min ultrasonic treatment)

3.2 Electrolytes phase analysis

The X-ray diffraction pattern of the electrolyte shown in Figure 3(c) indicates that the electrolyte produced by SolPS consists of one highly crystallized phase: GDC. The crystallite size of GDC was calculated from XRD line-broadening analysis according to the Scherrer equation. The crystallite size of GDC for the SolPS coating was estimated to be 17.4 ± 3% nm. It demonstrates the formation of nano-structured coating, which may enhance the electro-catalytic activity of SOFCs. In addition, traces of NiO and Ni can be identified on the XRD pattern. The NiO and Ni signals must be collected from the peripheral surface of the substrate. The concentration ratio of Ce and Gd in the precursor solution was chosen in such a way that the crystallite $Ce_{0.8}Gd_{0.2}O_{1.9}$ coatings were to be expected. This indicates the stoichiometric integration of Ce and Gd from the precursor into the coating. This successful synthesis was largely independent of any changes of the process conditions such as plasma power, reactor pressure, plasma gas composition, spraying distance and substrate temperature. The reason for this ideal stoichiometric behaviour might be due to the similar thermodynamic properties of the simple oxides of both elements: Gd_2O_3 and CeO_2 [14].

The XRD pattern of the electrolytes shown in Figure 3(b) also indicates that the GDC coatings deposited from suspensions had the same phase content as the initial GDC powders, which implies no major phase transformation during suspension plasma spraying. This is a consequence of the high thermodynamic stability of the solid solutions in the GDC system. The crystallite size of GDC for suspension coating was estimated around 19.7 ± 3% nm, which is slightly larger than the SolPS deposited GDC grain size. The difference in the coatings crystallites size can be related to the higher plasma

temperature associated with a lower fraction of liquid to evaporate for the SPS versus the SolPS, the result being a grain growth associated to a higher plasma heat flux to the substrate.

3.3 Coatings morphology

Two distinct morphologies of electrolyte coatings deposited by the SolPS process can be identified by FESEM. Figure 5 shows the micrographs of various magnifications of the coating top surface that was deposited by the SolPS process. The deposit consists of 20 nm size nodule-like particles (Figure 5(b)), which were agglomerated into powdery particles. There is an apparent lack of cohesion between different particles. The as-sprayed coatings have rather high porosity. No splats were observed in the SolPS-deposited coatings. The substrate bottom temperature was 400 °C during spraying.

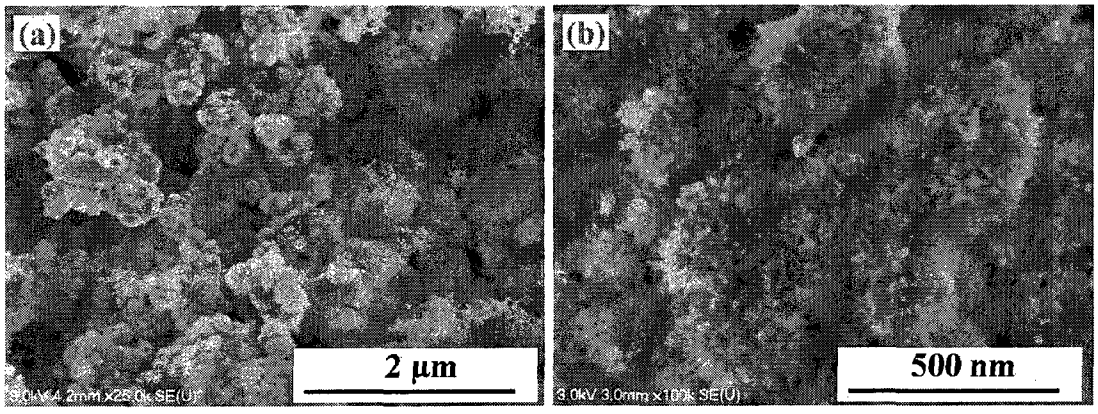

Fig. 5 FESEM micrographs of SolPS produced GDC electrolyte with different magnifications

Figure 6 shows FESEM micrographs of multiple splats obtained during SPS depositions. The substrate surface is uniformly covered by the splats. The splats diameter is typically from 0.2 to 2 μm, confirming that coatings obtained by suspension plasma spraying are nano-structured as a typical flattening ratio of 2.7 [61] results in a splat thickness of 8 to

80 nanometers nano-structured coatings. Figure 6(b) indicates that the second splat landed on a previously solidified splat and in spite of the perturbations caused by thickness variation and roughness, they maintained a relatively contiguous disk-shaped morphology. This suggests that the conventional plasma spray process phenomena [62] can be used to describe the SPS-deposition process.

Small spherical particles of GDC of about 20 nm were found on the splats (Figure 6(b). This could be due to the extremely high temperature of the induction plasma; the nano-powders in the suspension were vaporized and then condensed onto the coating surface. It was obvious that there was no crack network on the coating surface. This process provides an opportunity to obtain high density and high sealed electrolytes with thin coatings.

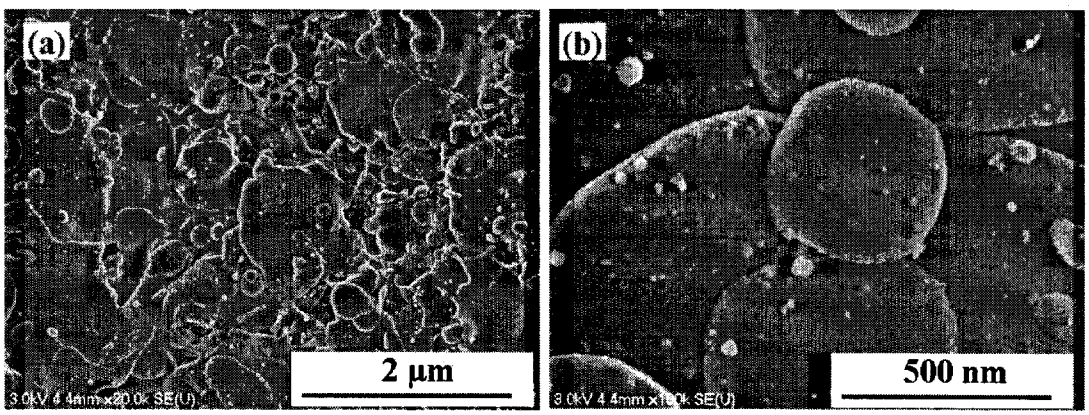

Fig. 6 FESEM micrographs of SPS produced GDC electrolyte with different magnifications

3.4 Coating Microstructure

Figure 7 is the FESEM micrographs of a cross-sectional fracture surface of the SolPS-deposited coatings. It is noted that all coatings deposited from the solution reveal a globular microstructure. The individual particles range in size from about 0.2 to 0.5 µm

which suggests that they were formed in flight by homogeneous nucleation from the supersaturated precursor vapours. These coatings seem to be constituted of stacking of small "particles", which increases the coating porosity to 7.3% (gas permeability = 3.70 × 10^{-15} m^2). Previous work demonstrated that a faster plasma jet can dramatically increase the particle impact velocity, which, in conjunction with high particle temperatures, leads to improved flattening of the splats and densification of the coating [30]. A short spraying distance (~100 mm) was found to be imperative to produce the dense electrolyte using induction plasma technology [47]. With a low spraying distance of 100 mm and a lower feed rate or a lower concentration, the porosity decreases to about 5.1% (gas permeability = 1.20 × 10^{-15} m^2), which is still not dense enough for SOFC application without post-treatment. The thickness of the coating measured on the cross section was approximately 5 μm. The higher magnification FESEM micrograph in Figure 7(b) shows that a good contact can be observed at the interface of sprayed GDC electrolyte and the substrate.

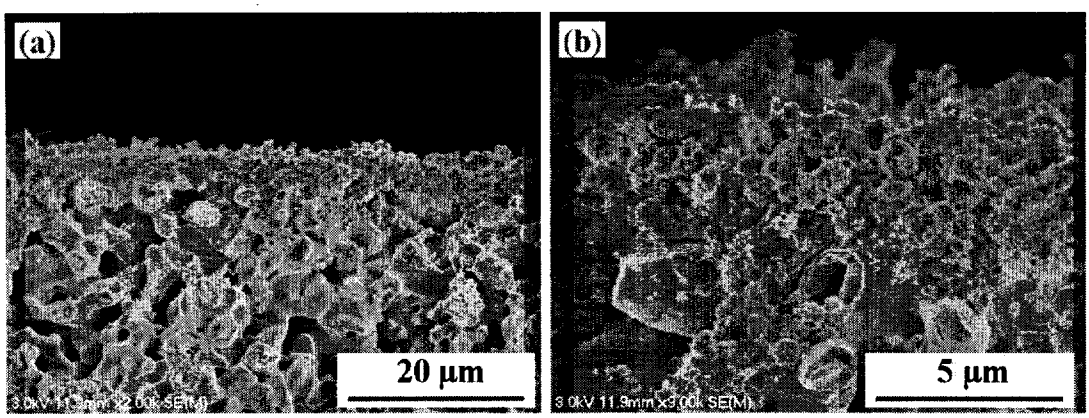

Fig. 7 FESEM micrographs of the fractured cross section of SolPS deposited electrolyte with different magnifications

Figure 8(a) and (b) show the fracture cross section of the SPS deposited electrolytes. It can be clearly seen that the SPS coating is much more homogeneous and shows better

bonding and continuous contact with the Ni substrate compared to the SolPS coating. Figure 8(b) (which is a magnified FESEM photograph of Figure 8(a)) illustrates that the GDC layer is very dense. The coating porosity is 1.4% (gas permeability = 0). The distinct interfacial boundary cannot be found between the GDC electrolyte and the substrate. The fine particles of well-dispersed GDC penetrate the pores and cracks of the support and certainly improve the smoothness to enable the formation of the dense GDC top layer. Due to this 3 dimensional penetration structure, the adhesion of the interface is improved; there is also an increase in the number of active reaction sites. It is beneficial for the ionic and electronic transfer; thus, it should improve the performance of the films to be used as SOFC electrolyte.

Normally, the electrolyte layer deposited by the conventional plasma spray process is 100-150 μm thick; however, the SPS process is suitable of producing a thin and dense layer of 5 μm in thickness while keeping continuity and uniformity of the coating under the optimized plasma condition. There is also no need of an intermediate layer between the anode and the thin electrolyte as described by Chen et al. [63].

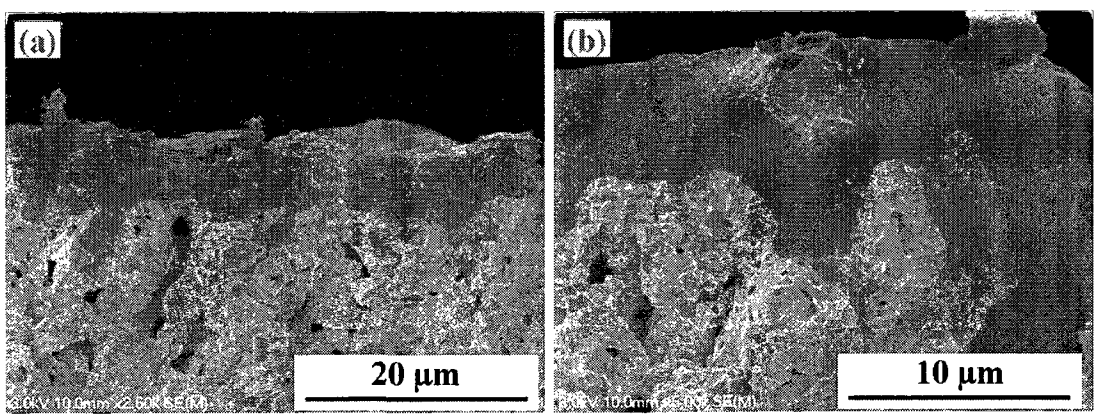

Fig. 8 FESEM micrographs of the fractured cross section of SPS deposited electrolytes

3.5 Deposition rates

The thickness of the coatings can be monitored very precisely with a relative easiness thanks to the precursor concentration and the number of deposition passes. Figure 9 presents the dependence of the thickness of GDC films as a function of the number of deposition passes. Considering the coating quality, the solution of 0.6 g/ml and suspension of 0.06 g/ml concentration were used. As it can be seen, the thickness is a linear function of the number of depositions and increases by 1 μm for each SPS pass and 2.5 μm for each SolPS pass, respectively. A small deviation from this relationship is observed for the first 2-3 passes, which is probably related to the establishment of a continuous film. Taking into account the mass concentration and injection flow rate differences of SolPS and SPS, SPS had an estimated deposition efficiency ten times larger than SolPS.

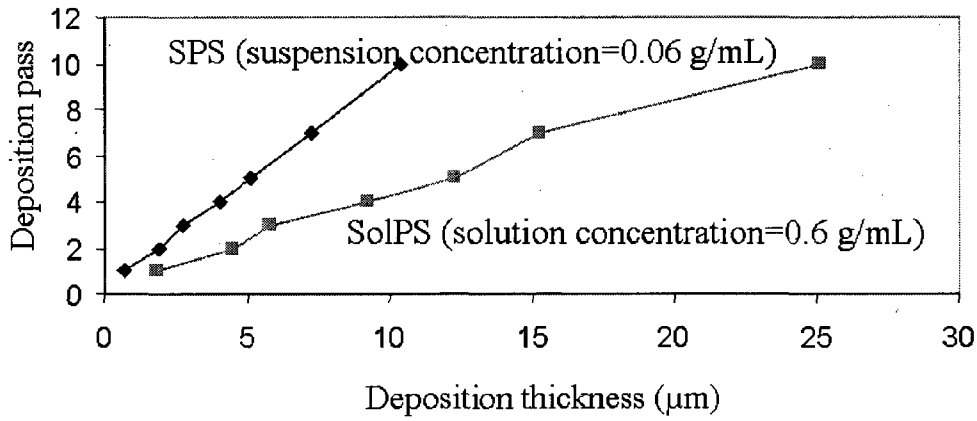

Fig. 9 SolPS/SPS deposition rates

4. Conclusions and Future Works

In the solution plasma spraying process, the solutions completely vaporized in the plasma, and then nano-structured GDC particles were synthesized in flight by homogeneous nucleation from the supersaturated precursor vapour, to subsequently build up a coating with high porosity. The formation of globular GDC coatings was observed over the entire experimental range of this study.

Suspension plasma spraying, a highly successful technology was adapted for dense electrolyte deposition. Nano-structured thin-film electrolyte (~ 5μm thick) could then be deposited on porous anodes with a high deposition rate. Compared to the electrolytes produced by SolPS, the GDC layer was impervious. These layers were deposited by layering splats. The size of the splats is from 0.2 to 2.0 μm. 3-D dimensional penetration structure eliminated the rough surface of the anode and made a much better cohesion between the electrolyte and anode, hence expects to create longer TPB lines, thus likely improving the electrochemical performance. These results have shown that SPS coating is a simple and potentially commercial technology for preparing the SOFCs electrolytes.

The open circuit voltage of the electrolytes will be measured in the near future, and the single cell will be fabricated and evaluated based on the result of the electrolyte electrochemical measurement. Moreover, in order to investigate the influence of electrolyte microstructure on the electrical conductivity of the electrolyte, single cell with nano-structured electrolyte will be compared to the one with coarse-grained electrolyte according to the electrochemical performance.

Acknowledgement

This project was funded by the Natural Sciences and Engineering Research Council of Canada (NSERC) through strategic grant # STPGP 350705-2007. Furthermore, the help of Doctoral Candidate Tony Rivard in the preparation of GNP-GDC powders is gratefully acknowledged.

References:

[1] D.T. Hooie, Status of SOFC Development in U. S. A., *Proceed. Electrochem. Soc.*, 1993, **93-94**, p 3-5

[2] S.C. Singhal, Science and Technology of Solid-Oxide Fuel Cells, *MRS Bull.*, 2000, **25**(3), p 16-21

[3] B.C.H. Steele, Materials for IT-SOFC Stacks 35 Years R&D: the Inevitability of Gradualness, *Solid State Ionics*, 2000, **134**(1, 2), p 3-20

[4] M.C. Williams, Status of Solid Oxide Fuel Cell Development and Commercialization in the U.S., *Proceed. Electrochem. Soc.*, 1999, **99-19**, p 3-9

[5] T. Tsai, E. Perry, and S. Barnett, Low-Temperature Solid-Oxide Fuel Cells Utilizing Thin Bilayer Electrolytes, *J. Electrochem. Soc.*, 1997, **144**(5), p 31-33

[6] S.R. Wang, T. Kobayashi, M. Dokiya, and T. Hashimoto, Electrical and Ionic Conductivity of Gd-Doped Ceria, *J. Electrochem. Soc.*, 2000, **147**(10), p 3606-3609

[7] B.C.H. Steele, Appraisal of $Ce_{1-y}Gd_yO_{2-y/2}$ Electrolytes for IT-SOFC operation at 500°C, *Solid State Ionics*, 2000, **129**, p 95-110

[8] M. Sahibzada, B.C.H. Steele, K. Zheng, R.A. Rudkin, and I.S. Metcalfe, Development of Solid Oxide Fuel Cells Based on a $Ce(Gd)O_{2-x}$ Electrolyte Film for Intermediate Temperature Operation, *Catal. Today*, 1997, **38**, p 459-466

[9] Y.P. Xiong, K. Yamaji, T. Horita, N. Sakai, and H. Yokokawa, Hole and Electron Conductivities of 20 mol%-$REO_{1.5}$ Doped CeO_2 (RE = Yb, Y, Gd, Sm, Nd, La), *J. Electrochem. Soc.*, 2004, **151**(3), p A407-A412

[10] K. Eguchi, T. Setoguchi, T. Inoue, and H. Arai, Electrical Properties of Ceria-Based Oxides and Their Application to Solid Oxide Fuel Cells, *Solid State Ionics*, 1992, **52**, p 165-172

[11] H. Inaba, and H. Tagawa, Ceria-based Solid Electrolytes, *Solid State Ionics*, 1996, **83**, p 1-16

[12] V.V. Kharton, F.M.B. Marques, and A. Atkinson, Transport Properties of Solid Oxide Electrolyte Ceramics: a Brief Review, *Solid State Ionics*, 2004, **174**, p 135-149

[13] N. Maffei, and A.K. Kuriakose, Solid Oxide Fuel Cells of Ceria Doped With Gadolinium and Praseodymium, *Solid State Ionics*, 1998, **107**, p 67-71

[14] M. Mogensen, N.M. Sammes, and G.A. Tompsett, Physical, Chemical and Electrochemical Properties of Pure and Doped Ceria, *Solid State Ionics*, 2000, **129**, p 63-94

[15] H.J. Park, and G.M. Choi, Oxygen Permeability of Gadolinium-Doped Ceria at High Temperature, *J. Eur. Ceram. Soc.*, 2004, **24**(6), p 1313-1317

[16] T. Mori, J. Drennan, Y.R. Wang, W.G. Mcphee, and J.G. Li, Nano Structural Features in Rare Earth Doped CeO_2 Electrolytes for Solid Oxide Fuel Cells Application, *Trans. Mater. Res. Soc. Japan*, 2004, **29**(5), p 1973-1976

[17] J. Maier, Nano-Sized Mixed Conductors (Aspects of Nano-Ionics. Part III), *Solid State Ionics*, 2002, **148**, p 367-374

[18] I. Kosacki, and H.U. Anderson, Microstructure-Property Relationships in Nanocrystalline Oxide Thin Films, *Ionics*, 2000, **6**, p 294-311

[19] B. Zhu, Fast Ionic Conducting Film Ceramic Membranes with Advanced Applications, *Solid State Ionics*, 1999, **119**, p 305-310

[20] Y.M. Chiang, E.B. Lavk, and D.A. Blom, Defect Thermodynamics and Electrical Properties of Nanocrystalline Oxides: Pure and Doped CeO_2, *Nanostruct. Mater.* 1997, **9**, p 633-642

[21] H.L. Tuller, Ionic Conduction in Nanocrystalline Materials, *Solid State Ionics*, 2000, **131**, p 143-157

[22] B. Zhu, Next Generation Fuel Cell R&D, *Int. J. Energy Res.*, 2006, **30**, p 895-903

[23] H.Z. Song, H.B. Wang, S.W. Zha, D.K. Peng, and G.Y. Meng, Aerosol-Assisted MOCVD Growth of Gd_2O_3-Doped CeO_2 Thin SOFC Electrolyte Film on Anode Substrate, *Solid State Ionics*, 2003, **156**(3-4), p 249-254

[24] M.A. Haldane, T.H. Etsell, Fabrication of Composite SOFC Anodes, *Mat. Sci. Eng. B, Solid-State Mater. Adv. Technol.*, 2005, **B121**(1-2), p 120-125

[25] Y. Yoo, Fabrication and Characterization of Thin Film Electrolytes Deposited by RF Magnetron Sputtering for Low Temperature Solid Oxide Fuel Cells, *J. Pow. Sour.*, 2006, **160**(1),p 202-206

[26] E. Gourba, A. Ringuede, M. Cassir, J. Paeivaesaari, J. Niinistoe, M. Putkonen, and L. Niinistoe, Microstructural and Electrical Properties of Gadolinium Doped Ceria Thin Films Prepared by Atomic Layer Deposition (ALD), *Proceed. Electrochem. Soc.*, 2003, **7**, p 267-274

[27] C Q. Xia, F.L. Chen, and M.L. Liu, Reduced-Temperature Solid Oxide Fuel Cells Fabricated by Screen Printing, *Electrochem. Solid-State Lett.*, 2001, **4**(5), p A52-A54

[28] R. Muccillo, E.N.S. Muccillo, F.C. Fonseca, Y.V. França, T.C. Porfirio, D.Z. de Florio, M.A.C. Berton, and C.M. Garcia, Development and Testing of Anode-Supported Solid Oxide Fuel Cells With Slurry-Coated Electrolyte and Cathode, *J. Pow. Sour.*, 2006, **156**(2), p 455-460

[29] B. Zhu, Fast Ionic Conducting Film Ceramic Membranes with Advanced Application, *Solid State Ionics*, 1999, **119**, p 305-310

[30] R. Vaβen, D. Hathiramani, J. Mertens, V.A.C. Haanappel, and I.C. Vinke, Manufacturing of High Performance Solid Oxide Fuel Cells (SOFCs) with Atmospheric Plasma Spraying (APS), *Surf. Coat. Technol.*, 2007, **202**, p 499-508

[31] G. Schiller, R. Henne, M. Lang, R. Ruckdäschel, and S. Schaper, Development of Vacuum Plasma Sprayed Thin-Film SOFC for Reduced Operating Temperature, *Fuel Cells Bull.*, 2005, **21**, p 7-12

[32] H.M. Hoehle, A. Refke, and M. Gindrat, New High Efficient Thermal Spray Solution for Perovskite Coatings and Dense Thin Electrolytes Using Triplex Pro-200 APS and LPPS-Thin Film Technology, *ECS Trans.-10th International Symposium on Solid Oxide Fuel Cells (SOFC-X)*, 2007, **7**(1), p 339-346

[33] T. Yoshida, T. Okada, H. Hamatani, and H. Kumaoka, Integrated Fabrication Process for Solid Oxide Fuel Cells Using Novel Plasma Spraying, *Plas. Sour. Sci. Technol.*, 1992, **1**(3), p 195-201

[34] J. O. Berghaus, J.G. Legoux, C. Moreau, R. Hui, C. Decès-Petit, W. Qu, S. Yick, Z. Wang, R. Maric, and D. Ghosh, Suspension HVOF Spraying of Reduced Temperature Solid Oxide Fuel Cell Electrolytes, *J. Therm. Spray Technol.*, 2008, **17**(5-6), p 700-707

[35] J. Karthikeyan, C.C. Berndt, J. Tikkanen, J.Y. Wang, A.H. King, and H. Herman, Preparation of Nanophase Materials by Thermal Spray Processing of Liquid Precursors, *Nanostruct. Mater.*, 1997, **9**, p 137-140

[36] J. Karthikeyan, C.C. Berndt, J. Tikkanen, S. Reddy, and H. Herman, Plasma Spray Synthesis of Nanomaterial Powders and Deposits, *Mater. Sci. Eng. A*, 1997, **238**, p 275-286

[37] J. Karthikeyan, C.C. Berndt, S. Reddy, J.Y. Wang, A.H. King, H. Herman, Nanomaterial Deposits Formed by DC Plasma Spraying of Liquid Feedstocks, *J. Amer. Ceram. Soc.*, 1998, **81**(1), p 121-128

[38] N.P. Padture, K.W. Schlichting, T. Bhatia, A. Ozturk, B. Cetegen, E.H. Jordan, M. Gell, S. Jiang, T.D. Xiao, P.R. Strutt, E. Garcia, P. Miranzo, and M.I. Osendi, Towards Durable Thermal Barrier Coatings with Novel Microstructures Deposited by Solution-Precursor Plasma Spray, *Acta Materi.*, 2001, **49**, p 2251-2257

[39] L. Xie, X. Ma, E.H. Jordan, N.P. Padture, D.T. Xiao, and M. Gell, Identification of Coating Deposition Mechanisms in the Solution-Precursor Plasma-Spray Process Using Model Spray Experiments, *Mater. Sci. Eng. A*, 2003, **362**, p 204-212

[40] L. Xie, X. Ma, A. Ozturk, E.H. Jordan, N.P. Padture, B.M. Cetegen, D.T. Xiao, and M. Gell, Processing Parameter Effects on Solution Precursor Plasma Spray Process Spray Patterns, *Surf. Coat. Technol.*, 2004, **183**, p 51-61

[41] X.Q. Ma, J.X. Dai, H. Zhang, J. Roth, T.D. Xiao, and D.E. Reisner, Solid Oxide Fuel Cell Development by Using Novel Plasma Spray Techniques, *J. Fuel Cell Sci. Technol.*, 2005, **2**(3), p 190-197

[42] F. Gitzhofer, M.E. Bonneau, and M.I. Boulos, Double Doped Ceria Electrolyte Synthesized by Solution Plasma Spraying with Induction Plasma Technology, *Therm. Spray 2001, New Surfaces for a New Millennium, C. C. Berndt, K. A. Khor, and E. F. Lugscheider, Eds.* Materials Park, OH: ASM, 2001, p 61-68

[43] R. Henne, Solid Oxide Fuel Cells: A Challenge for Plasma Deposition Processes, *J. Therm. Spray Technol.*, 2007, **16**(3), p 381-403

[44] Y. Wang, and T.W. Coyle, Solution Precursor Plasma Spray of Nickel-Yittia Stabilized Zirconia Anodes for Solid Oxide Fuel Cell Application, *J. Therm. Spray Technol.*, 2007, **16**(5-6), p 898-904

[45] F. Gitzhofer, E. Bouyer, and M.I. Boulos, Suspension Plasma Spray Deposition, *U. S. Patent 5 609 921,* 1997

[46] M. Bonneau, F. Gitzhofer, and M.I. Boulos, SOFC/CeO_2 Doped Electrolyte Deposition, Using Suspension Plasma Spraying, *Thermal Spray: Surface Engineering via Applied Research*, C.C. Berndt, Ed., May 8-11, 2000 (Montréal, Québec, Canada), ASM International, 2000, p 929-934

[47] F. Gitzhofer, and L. Jia, Induction Plasma Technology Applied to Materials Synthesis for Solid Oxide Fuel Cells, *Int. J. Appl. Ceram. Technol.*, 2008, **5**(6), p 537-547

[48] P. Fauchais, R. Etchart-Salas, C. Delbos, M. Tognonvi, V. Rat, J.F. Coudert , and T. Chartier, Suspension and Solution Plasma Spraying of Finely Structured Layer: Potential Application to SOFCs, *J. Phys. D: Appl. Phys.*, 2007, **40**, p 2394-2406

[49] P. Fauchais, V. Ra, C. Delbos, J.F. Coudert, T. Chartier, and L. Bianchi, Understanding of Suspension DC Plasma Spraying of Finely Structured Coatings for SOFC, *IEEE Trans. Plas. Sci.*, 2005, **33**(2), p 920-930

[50] P. Fauchais, Suspension and Solution Plasma or HVOF Spraying, *J. Therm. Spray Technol.*, 2008, **17**(1), p 1-3

[51] R. Rampon, C. Filiatre, and G. Bertrand, Suspension Plasma Spraying of YPSZ Coatings: Suspension Atomization and Injection, *J. Therm. Spray Technol.*, 2008, **17**(1), p 105-114

[52] J. Oberste Berghaus, J.G. Legoux, C. Moreau, R. Hui, and D. Ghosh, Suspension Plasma Spraying of Intermediate Temperature SOFC Components using an Axial Injection DC Torch, *Mater. Sci. For.*, 2007, **539-543**(2), p 1332-1337

[53] K. Wittmann, J. Fazilleau, J.F. Coudert, P. Fauchais, and F. Blein, A New Process to Deposit Thin Coatings by Injecting Nanoparticles Suspensions in a d.c. Plasma Jet, *International Thermal Spray Conference, ITSC 2002*, DVS-Verlag GmbH, Ed., March 4-6, (Essen, Germany), ASM International, 2002, p 519-522

[54] C.R. Xia, M.L. Liu, Microstructures Conductivities, and Electrochemical Properties of $Ce_{0.9}Gd_{0.1}O_2$ and GDC-Ni Anodes for Low-Temperature SOFCs, *Solid State Ionics*, 2002, **152-153**, p 423-430

[55] L. Jia, C. Dossou-Yovo, C. Gahlert, and F. Gitzhofer, Induction Plasma Spraying of Samaria Doped Ceria as Electrolyte for Solid Oxide Fuel Cells, *Thermal spray 2004: Advances in Technology and Application*, E. Lugscheider and C.C. Berndt, Eds. May 10-12, (Osaka, Japan), ASM International, 2004, p 85-89

[56] M. Suzuki, S. Sodeoka, and T. Inoue, Structure Control of Plasma Sprayed Zircon Coating by Substrate Preheating and Post Heat Treatment, *Mater. Trans.*, 2005, **46**(3), p 669-674

[57] S. Deshpande, A. Kulkarni, S. Sampath and H. Herman, Application of Image Analysis for Characterization of Porosity in Thermal Spray Coatings and Correlation with Small Angle Neutron Scattering, *Surf. Coatings Technol.*, 2004, **187**(1), p 6-16

[58] M. von Bradke, F. Gitzhofer, R. Henne, Porosity Determination of Ceramic Materials by Digital Image Analysis--A Critical Evaluation, *Scanning*, 2005, **27**(3), p 132-135

[59] M.V. Chor, and W. Li, A Permeability Measurement System for Tissue Engineering Scaffolds, *Meas. Sci. Technol.*, 2007, **18,** p 208–216

[60] L. Jia, and F. Gitzhofer, Induction Plasma Technology Applied to Materials Synthesis for Solid Oxide Fuel Cells, *Int. J. Appl. Ceram. Technol.*, 2008, **5**(6), p 537-547

[61] J. Madejski, Solidification of Droplets on a Cold Surface, *Int. J. Heat Mass Transfer*, 1976, **19** (12), p 1351-1356

[62] L. Pawlowski, The Science and Engineering of Thermal Spray Coatings, *Wiley*, New York, 1995

[63] H.C., Chen, J., Heberlein, and T. Yoshida, Preparation of Films for Solid Oxide Fuel Cells by Center-Injection Low Pressure Plasma Spraying, *Thermal Spray: Meeting the*

Challenges of the 21st Century, C. Coddet Ed., May 25-29, (Nice, France), ASM International, 1998, **2**, p 1309-1314

4.3 *Preparation of Nano-structural Electrolyte Thin Film for Solid Oxide Fuel Cells by Radio Frequency Suspension Plasma Spraying*

L. Jia, and F. Gitzhofer, ing. PhD

Energy, Plasma and Electrochemistry Research Centre (CREPE), Chemical and Biotechnical Engineering Department, Université de Sherbrooke, Québec, Canada, J1K 2R1, (819)-821-7171

The emerging technology of radio frequency inductively coupled thermal plasma (RF-ICTP) suspension spraying was explored to produce thin and gas tight nano-structured solid oxide fuel cells (SOFCs) electrolytes, which is an effort to develop a cost-effective and scalable fabrication technique for high performance SOFCs. Glycine-nitrate process (GNP) produced cerium oxide (CeO_2) and gadolinium oxide (Gd_2O_3) nano-powders were used to prepare suspensions and then separately injected to form composite $Gd_{0.2}Ce_{0.8}O_{1.9}$ (GDC) electrolyte coatings. A dynamic mask system has been developed to diminish the heating effects of a high-temperature plasma deposition process. The experimental results of the nano-structured SOFCs GDC electrolytes produced using induction suspension thermal plasma spraying process with the newly proposed mask were compared to the ones without mask. The potential of this deposition technique to improve the electrolyte coating uniformity and to diminish the coating porosity, as well as the nano-splats formation which enhance metastable phases in the coating was demonstrated.

Keywords: induction plasma spraying, suspension plasma spraying (SPS), solid oxide fuel cells (SOFCs), nano-structured electrolyte thin film, dynamic mask system

1. Introduction

Increase of power density, lifetime, and reduction of fabrication costs, are common objectives of all development work presently carried out on solid oxide fuel cells (SOFCs) [1]. Therefore, recent development focuses on possibilities allowing for reduction of operating temperature [2-3], and on more cost-effective processes for the production of relevant materials and of cell components [4-5]. In order to decrease the working temperature, applications of alternative electrolyte materials such as cation doped ceria with inherently higher ionic conductivity than traditional yttria stabilized zirconia (YSZ) [6-11], and/or preparation of thin electrolyte coatings with thickness only a few micros has been recommended [12-14].

Induction plasma spraying process is a promising and cost effective technique for the development of SOFCs [15-20]. Multiple SOFC components, including the electrodes and the electrolyte, could be produced sequentially and directly on a reformer with a single deposition technique, thereby minimizing the number of processing steps and equipment required [21]. In particular, the high temperature sintering steps required in many other layer deposition techniques could be eliminated. A thin, fully dense and nano-structural electrolyte is essential to reduce internal resistant loss, and consequently to achieve a high performance of intermediate temperature SOFCs [22-29]. It implies spraying of smaller particles to reduce splat dimensions. However, it is not possible to inject too small particles (less than 5 μm) without drastically perturbing the plasma jet by the high carrier gas flow rate necessary to give them a sufficiently high momentum.

This is why, recently a new technology has been developed to deposit finely structured coatings by injecting a suspension of nano or submicron-size particles into an induction thermal plasma jet [20, 30-31]. The suspension plasma spraying (SPS) process was initially invented by Université de Sherbrooke in 1994 and a patent was awarded in 1997 [32]. In this process, a suspension of micro or nano-powders is fed to an induction plasma torch and is directly gas atomized into the plasma through an atomization probe. The solid particles enclosed in each droplet were accelerated, evaporated, melted, and then flattened onto a prepared substrate rapidly forming thin (5-10 μm) coatings with a refined microstructure [33], and smooth surface finishes are created [34-35]. Moreover, the composition of applied spray materials can be varied very easily in this process [36]. Recently, the suspension plasma spraying process has been developed to be one of the most promising coating processes for intermediate temperature SOFCs.

In the present paper, nano-structured SOFCs electrolyte coatings with a 5μm thickness were produced by suspension plasma spraying. The possibility to in flight vary the composition of the sprayed materials using a suspension feeding system is discussed. The impact of a mask system on the coating microstructure is as well demonstrated.

2. Experimental Setup and Procedures

2.1 General setup

Fig.1a shows the general setup of the suspension plasma spraying system. The plasma is generated using a PL-50 induction plasma torch (Tekna Plasma Systems Inc., Sherbrooke, Canada), operating at a frequency of 3 MHz. The torch is equipped with a supersonic nozzle (throat diameter = 24.2 mm) in order to increase the plasma velocity [36]. The suspension is fed by a laboratory developed suspension feeding system to the

atomisation probe which is designed as an airblast atomizer. Once in the high temperature plasma, the liquid phase boils, the resulting agglomerated powders sinter and melt and then impact by piling splats on the nickel substrate. The porous Ni substrates are held stationary by a sample holder, while the holder is scanned across the plasma flame by the electromotive sting; multiple passes are used to build up the coatings. In order to reduce the thermal gradients during deposition and to obtain dense coatings, the substrates are heated prior to coating using an electrical heating device [37]. A detailed description of the plasma system was given in [19]. Spraying conditions and injection parameters evaluated in the current study are presented in Table 1.

Table.1. Induction Plasma Spraying Parameters

Plasma torch	Tekna PL - 50
Central plasma gas flow rate [slpm]	27 (Ar)
Sheath plasma gas flow rate [slpm]	80 (O_2)
Plasma power [kW]	45 - 55
Reactor pressure [kPa]	6 and 12
Atomization gas pressure [kPa]	345 (Ar)
Atomization gas flow rate [slpm]	21 (Ar)
Suspension injection flow rate [mL/min]	4-10
Spraying distance [mm]	100

2.2 Mask system

A dynamic mask system (Fig.1b) has been developed to diminish the heating effects from the high-temperature deposition process, as well as to improve the quality of the sprayed films. The mask system includes a heat resistant surface and a removable ring with a gas diffuser which can be exchanged according to the experimental needs. The mask surface is protected from the high temperature plasma by using high pressure thin film cooling water under a stainless steel plate. The diameter of the gas diffuser is 20 mm; it has eight

holes with 15° upward angle. The mask installation position and the sheath flow rate are varied in the present investigation.

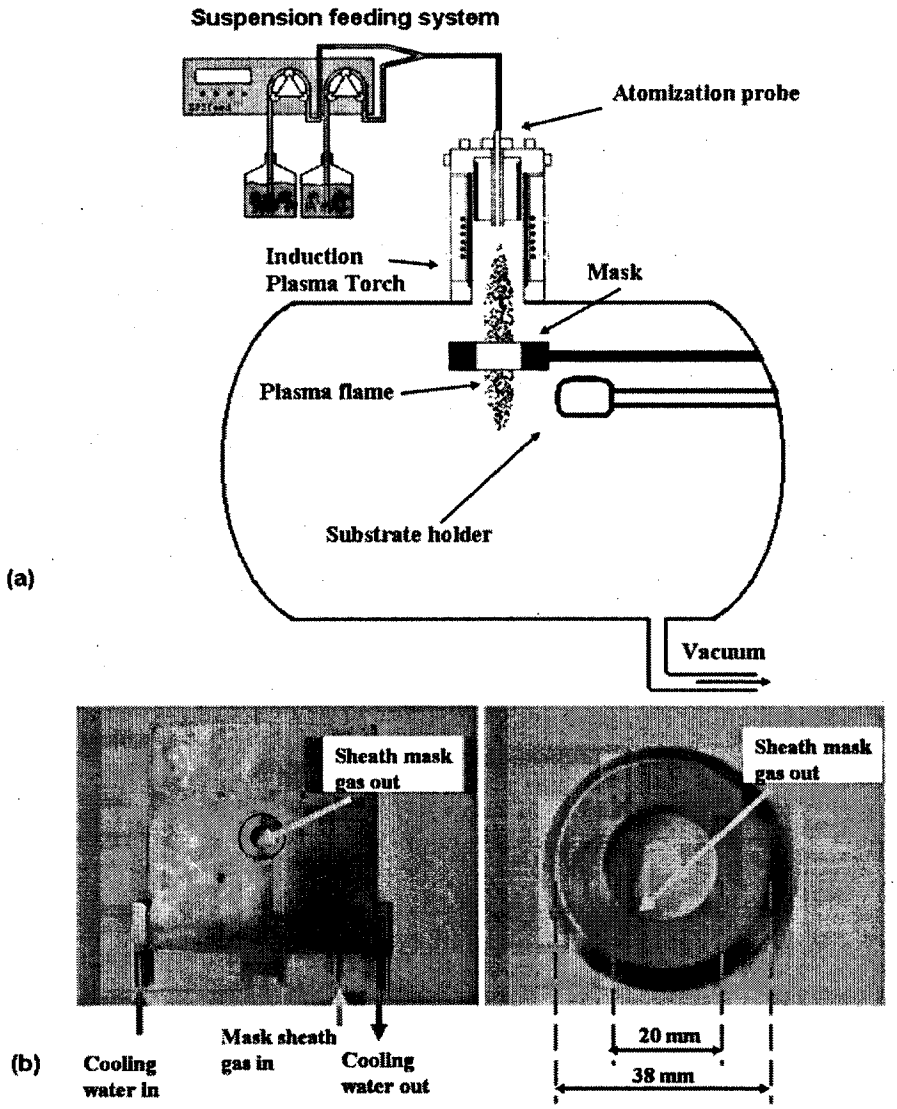

Fig. 3: Schematic illustration of induction plasma system (a) and a view of the mask system (b)

2.3 Suspension feeding system

Fig.1a also shows the schematic of a suspension feeding system based on DIGI-STALTIC Modular Dispensing Pumps (Cole-Parmer Canada Inc., Montreal, Canada).

This system is microprocessor controlled and programmable. It offers a virtually pulse-free feeding unit with up to four fluids. The flow rate variation enables a delivery of the liquid ranging from 0.5 to 60 ml/min. A single injection of a mixed suspension or a separate injection of two single phase suspensions to form various coating composition could be performed by this suspension feeding system. This suspension feeding system provides the opportunity to vary the composition of the injection feedstock easily, which is necessary for the production of functional and/or graded SOFCs composite components.

2.4 Suspension precursors preparation

Electrolyte powders of cerium oxide (CeO_2) and gadolinium oxide (Gd_2O_3) were prepared by the glycine-nitrate process method (GNP) as described elsewhere [38]. To prepare the suspensions, GNP-CeO_2 and Gd_2O_3 powders were directly dispersed into the ethanol. The ethanol was chosen as a solvent for suspensions due to the lower vaporisation enthalpy of ethanol (0.8×10^6 J kg^{-1}) compared to that of water (2.3×10^6 J kg^{-1}) and the heat emission during the ethanol combustion reaction. The solid loading of CeO_2 and Gd_2O_3 suspensions were kept at 7 wt.% and 14.4 wt.%, and the suspension feed rates of CeO_2 and Gd_2O_3 were set in all experiments to be 8 and 2 ml/min, respectively, to produce the desired stoichiometric compositions. The suspensions must have a low viscosity and a good stability to be compatible with the process. A suitable dispersant which adsorbs on the particle surface allows an effective dispersion of the powders in the solvent. The dispersion used here is Darvan 7 (R. T. Vanderbilt Company, Norwalk, USA). The mass percentage of the dispersing agent selected for use is 2% of the powders mass to obtain the lowest viscosity for adequate feeding. Before deposition,

the suspensions were ultrasonically dispersed to break apart the large agglomerates. During deposition, the stirrers were used to prevent particles from settling.

2.5 Characterization and analysis

Different techniques are used to characterize the coatings produced by the SPS process. Particle size distributions were determined using a Malvern Mastersizer 2000 particle analyzer (Malvern Instruments Ltd., Worcestershire, United Kingdom). In-flight particle states were measured with the DPV2000 system (Tecnar, Saint-Bruno, Quebec, Canada). Morphologies and elemental analyses of electrolyte powders and as-deposited electrolyte layers were performed by scanning electron microscopy (SEM) (JSM-610, JEOL, Tokyo, Japan) and field-emission scanning electron microscopy (FESEM) (S4700, Hitachi, Tokyo, Japan). Porosity was assessed on the cross-section by FESEM, using image analysis [39]. Phase analysis was conducted by X-ray diffraction (XRD) using an X'Pert Pro MPD X-ray diffractometer (Philips, Eindhoven, Netherlands). The crystallite size was approximated from the Scherrer equation at the principal diffraction lines.

3. Results and Discussions

3.1 As-synthesized GNP-CeO_2 and Gd_2O_3 powders characteristics

Shown in Fig. 2 are the FESEM micrographs of as-synthesized GNP-CeO_2 and Gd_2O_3 powders, indicating that both particles are highly porous with a foam-like microstructure. The XRD patterns (Fig. 3) of CeO_2 and Gd_2O_3 samples exhibit all peaks associated with that of a pure fluorite structure. The crystallite size of CeO_2 and Gd_2O_3 phases, calculated from XRD line-broadening analysis according to the Scherrer equation are $14.9 \pm 3\%$ nm and $23.0 \pm 3\%$ nm, respectively.

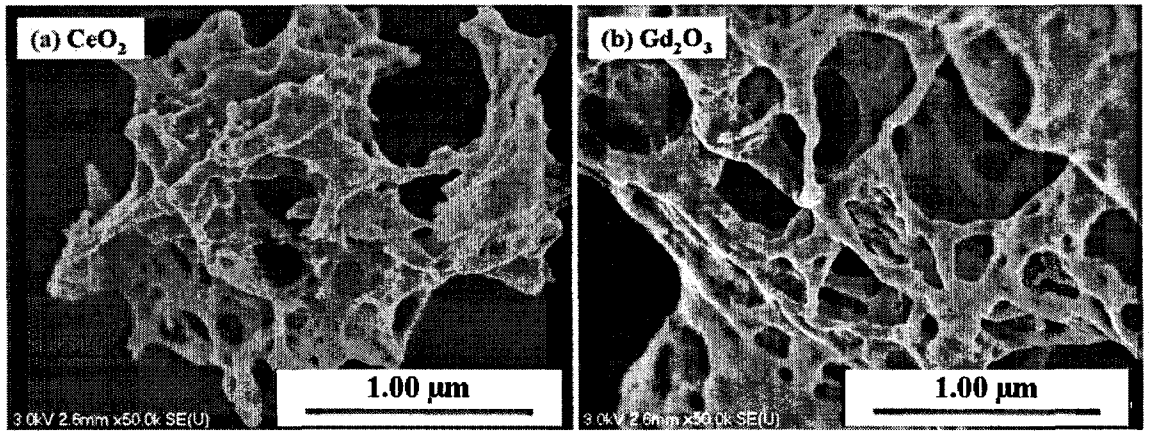

Fig. 4: SEM micrographs of GNP synthesized CeO_2 (a) and Gd_2O_3 (b) nano-crystalline powders used in suspensions

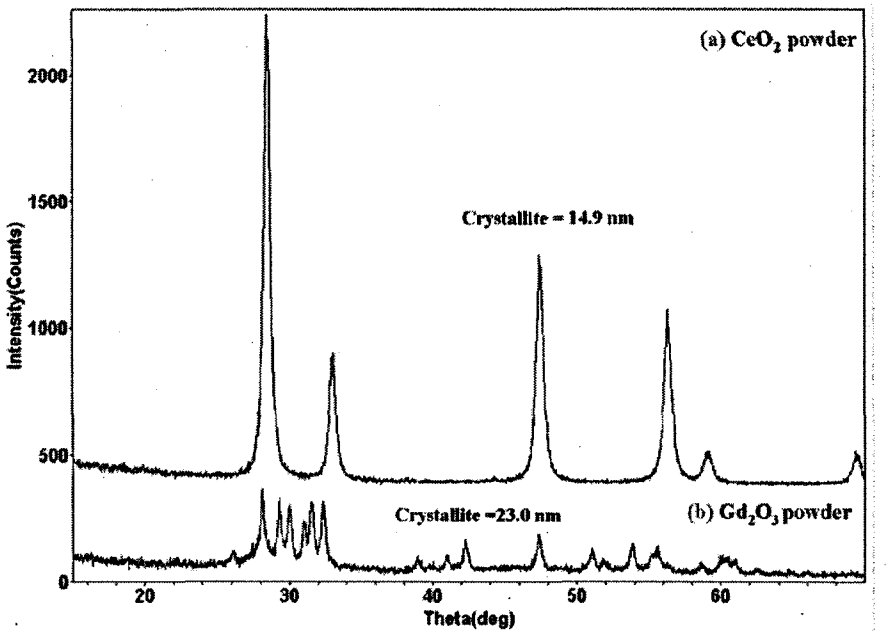

Fig. 5: XRD analysis of CeO_2 (a) and Gd_2O_3 (b) nanocrystalline powders used in suspensions

An ultrasonic treatment of 5 minutes at 250 W power was applied to both powders before the particles size distribution measurements. The powders were characterized by a weak agglomeration due to porous structures of the agglomerated powders which could be

broken during the ultrasonic treatment. The average size of CeO_2 and Gd_2O_3 particles was 1.8 μm and 2.3 μm (Fig.4), with a specific surface area of 25.5 m^2/g and 21.3 m^2/g, respectively. The narrow size distribution of CeO_2 and Gd_2O_3 is the critical factor to evenly treat solid particles within the plasma and therefore result in a homogeneous thermal treatment of solid particles. It might be expected that the narrow size distribution would help in maximizing homogeneity and minimizing defects.

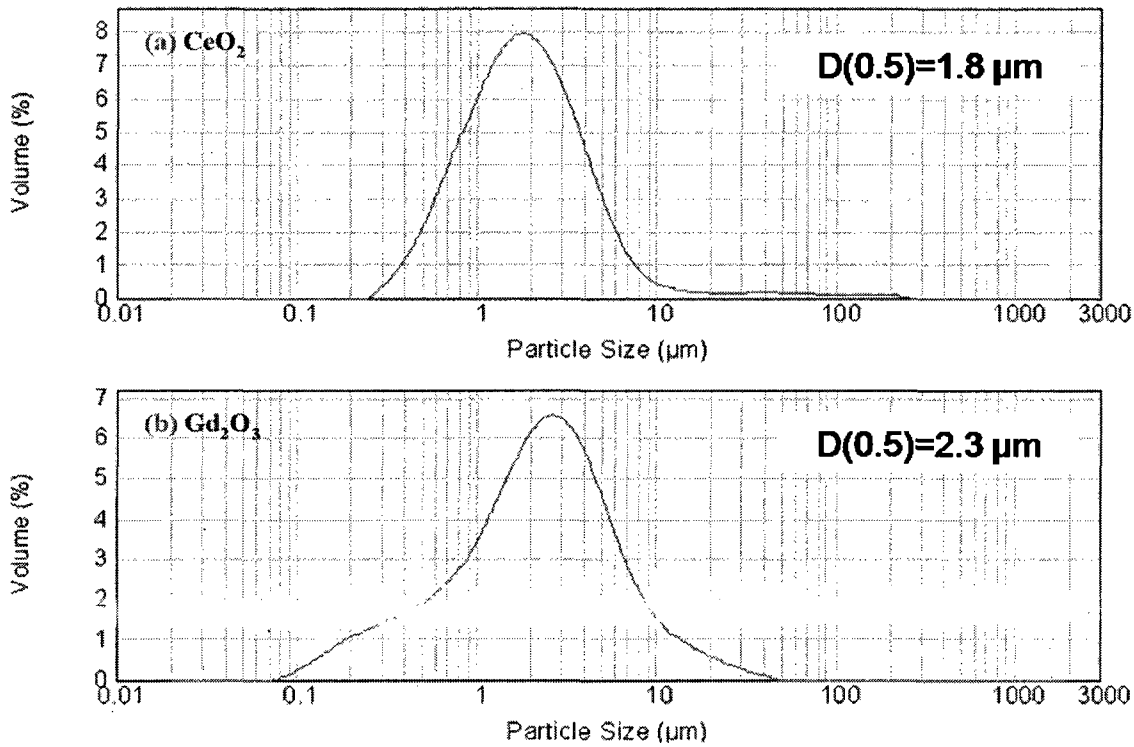

Fig. 6: The size distributions of CeO_2 (a) and Gd_2O_3 (b) nano-crystalline powders used in suspensions

3.2 Electrolytes phase analysis

Two single-phase suspensions were used for the separate injection. In contrast to the result of previous work which was using GNP synthesized $Gd_{0.2}Ce_{0.8}O_{1.9}$ (GDC) in a

single injection to produce the electrolyte coating [40], the XRD pattern (Fig. 5) of the electrolyte deposited by separate injection of the suspensions of CeO_2 and Gd_2O_3 shows that GDC is not the only product, some phases of CeO_2 and Gd_2O_3 which come from non-reacted materials are also identified. It might be because of the partial mixture of CeO_2 and Gd_2O_3 suspensions in the injection tubing and also from in flight atomised droplets explosions. In the future development of suspension feeding systems, the use of a static mixer or of an external energy source such as ultrasounds should be considered.

The phase GDC indicates the stoichiometric integration of Ce and Gd from the suspensions into the coating. In addition, it also demonstrates the proper weight ratios of CeO_2 and Gd_2O_3 in the primary suspension as well as the proper injection flow rates. The crystallite size of GDC is estimated to be about 17 ± 3% nm according to the Scherrer equation. This reveals that an as-deposited coating by nano-structured CeO_2 and Gd_2O_3 suspensions exhibits nano-grain crystalline structures which can enhance the electro-catalytic activity.

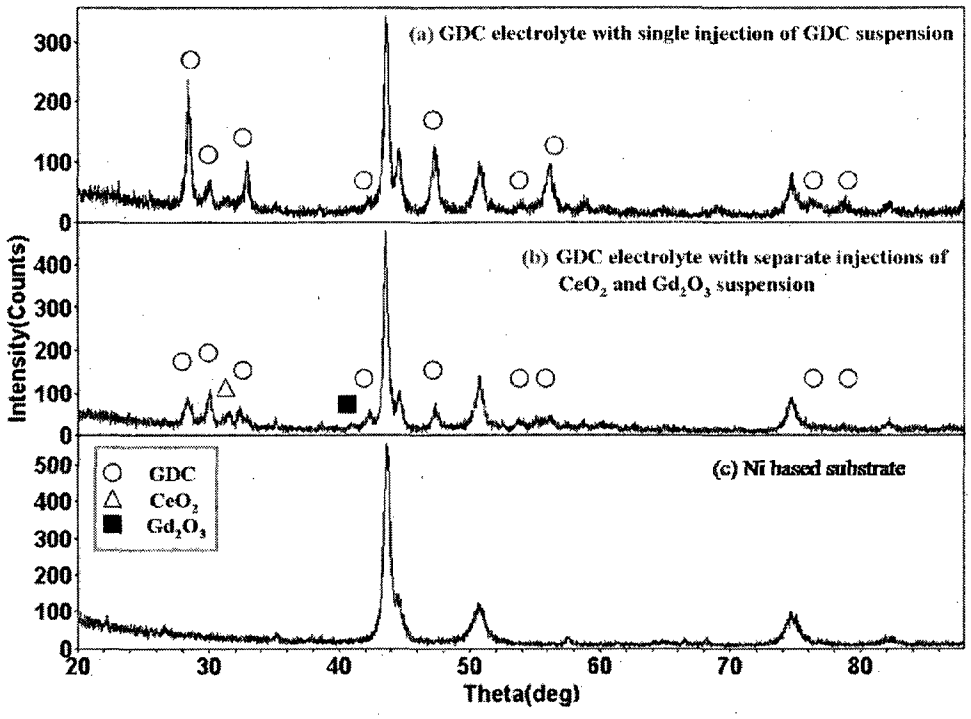

Fig. 7 : XRD patterns for the sprayed GDC electrolyte layer by single injection of GDC suspension (a) and separate injections of CeO_2, Gd_2O_3 suspensions (b) and substrate (c)

3.3 Determination of the mask sheath gas flow rate

The sheath gas introduced into the mask system is used to quench the droplets as well as to protect the mask. Helium (He) is applied as the sheath gas due to its higher thermal conductivity compared to that of other inert gases (7.5 and 5 times greater than argon and nitrogen, respectively). In order to determine the sheath gas flow rate, a set of experiments were carried out using different sheath gas flow rate from 0 to 43 slpm (Ultrasonic treatment was not applied when the suspensions were prepared). Fig 6 shows clearly that higher sheath gas flow rates (43, 36 and 29 slpm) result in cutting and even a deflection of plasma jet. Slowly reduces the sheath gas flow rate to 15 slpm, the plasma gas begin to pass through the mask. In-flight particle states (the particle velocity and

temperature measurement point is 10 mm below the mask) as a function of mask installation location are exemplified in Fig 7. Obviously, when the mask installation location is closed to the torch nozzle (75 mm), the particle temperatures (2450 and 2470 °C, respectively) have a very slight change compare to the case that the mask is not applied (2480 °C), no matter the quench gas flow rate is 15 or 8 slpm. However, the particle velocity is reduced sharply when the quench gas flow rate is 15 slpm (from 320 m/s drop to 250 m/s) compares to the quench gas flow rate is 8 slpm (from 320 m/s drop to 305 m/s). As mentioned above, the particle velocity and temperature are the critical parameters to achieve dense and homogeneous deposition. In our application, the mask installation distance of 75 mm and the quench gas flow rate of 8 slpm are fixed as the optimum parameters in the experimental tests.

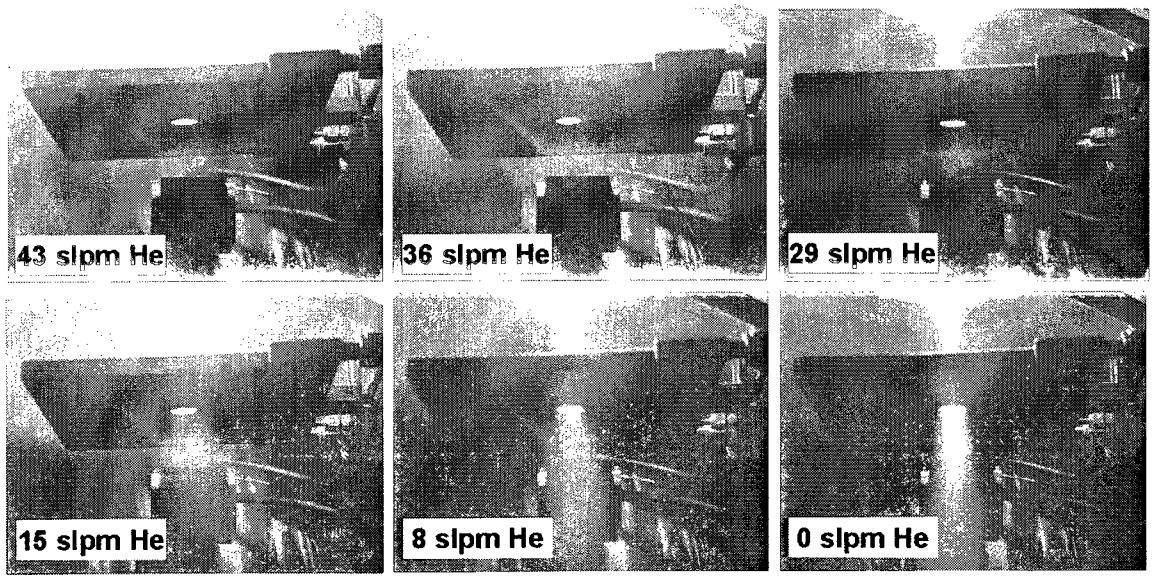

Fig. 8 : Influence of the sheath gas flow rate on the plasma plume

3.4 Morphology of electrolyte coatings

Generally, in suspension plasma spraying, suspensions injected into a plasma jet are melted and propelled onto a substrate, where they spread upon impact and rapidly solidify. The flattened and solidified particles represent the building blocks of the coating. The dynamics of the splat formation involves flattening of a molten droplet driven by the droplet kinetic energy, surface tension, heat transfer and rapid solidification processes [41]. The diameter of the splats is generally in the range of 1 to 5μm due to the smaller size of particles in suspensions.

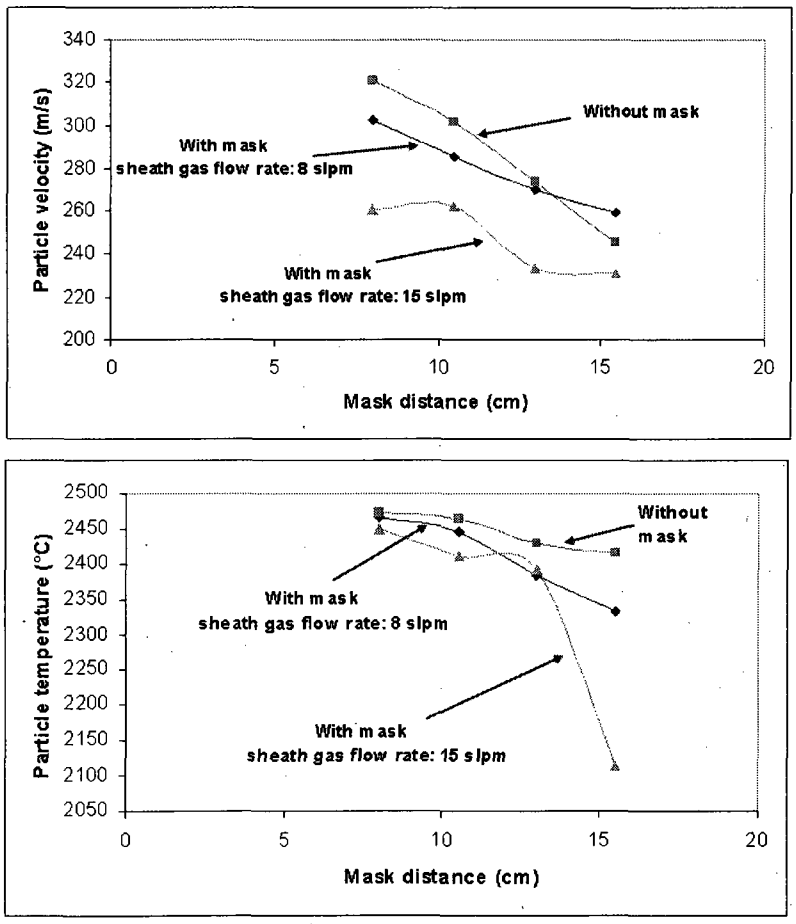

Fig. 9 : Influence of mask installation location on the particle velocity (a) and temperature (b)

Fig. 8a shows that, without the mask, the surface of the deposited electrolyte coating is rather rough. The coating surface is composed of either spheres bellow 20 nm, highlighting that these ultra-fine particles have been molten, vaporized and condensed, or solidified droplets, together with some underlying splats. Some unmolten agglomerates of primary particles deposited on the surface can also be observed. The porosity estimated by image analysis is 5.8%. Previous researcher [15] has reported that the plasma plume is characterized by a certain temperature distribution in both radial and axial directions. The temperature of the plasma plume fringes is much lower and the droplets in this plasma region are rapidly solidified before reaching the substrate. As a consequence, because of the multiple passes of the coating under the flame, the sprayed coating will be a sandwich of porous and dense layers. Moreover, a close-up FESEM micrograph of a splat in Fig. 8b shows the presence of micro-cracks on the coating surface. The coating surface is overheated due to the high heat flux at this unusually short (at least for induction plasma spraying) spraying distance (100 mm). This results in an increase of the overall stress distribution of the coating which when cooling down surpasses its cohesive strength.

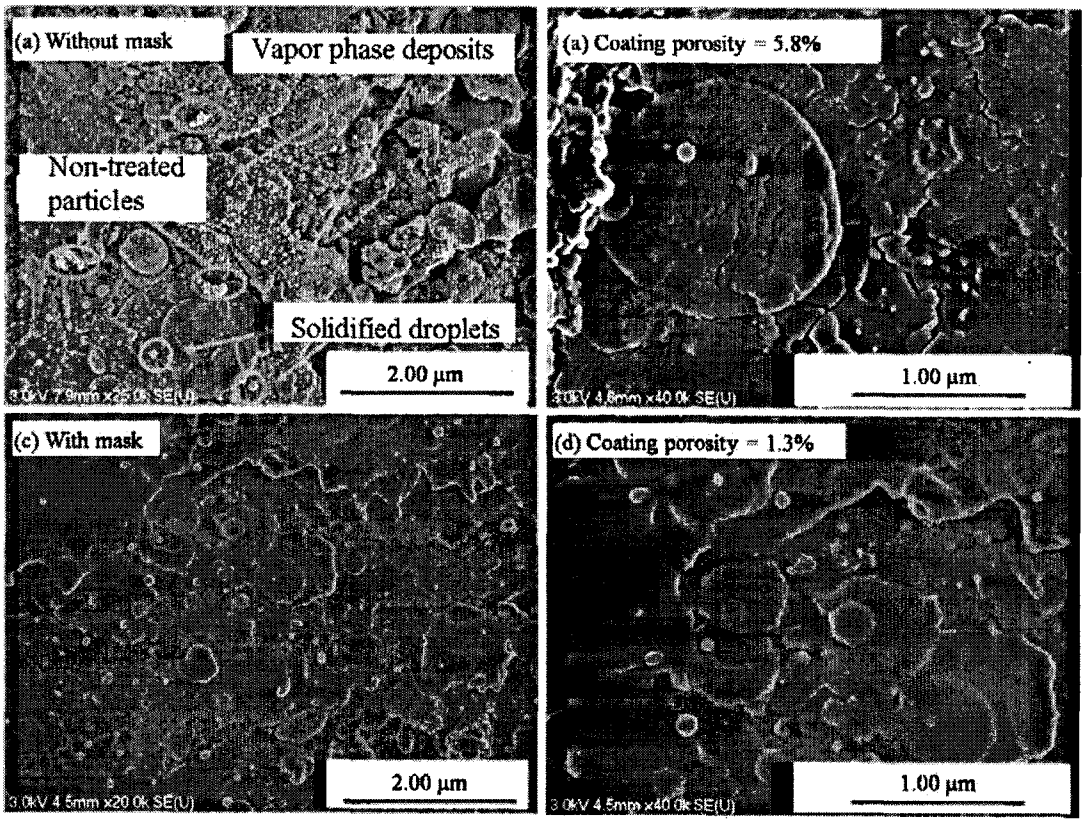

Fig. 10 : FESEM of suspension plasma sprayed coating surfaces without mask (a, b) and with mask (c, d) at different magnifications

Fig. 8c and 8d show FESEM micrographs of multiple splats obtained during SPS depositions using the mask. The substrate surface was uniformly covered by the splats. The presence of the other features presented in Fig. 8a could not be observed. So the mask prevents solidified, condensed, and primary particles from being imbedded into the coating, thus increasing its homogeneity. No micro-cracks were observed on the coating surface as the mask prevents the coating from overheating. The porosity estimated by image analysis is 1.3%. Furthermore, the morphology of powders collected from the top surface of the mask in Fig. 9 confirms that the mask prevents partially molten particles (Fig. 9b) and the powdery particles (Fig. 9c) to be incorporated in the coating. The splats

were typically 0.2 to 2 μm in diameter, thus assuming a flattening ratio of 2.7 [42], the overall splat thickness would be in the range of 8 to 80 nm. The coating can then be called nano-structured (by definition at least one dimension of a nano-object should be smaller than 100 nm). With such a small splat thickness, the cooling rate of the splats could be one or two orders of magnitude higher than the one measured by McDonald [43] (2.0×10^8 K/s), on 2 μm thick zirconia splats flattened with the same 2.7 flattening ratio. Such high cooling rate can give access to high temperature metastable phases which could be different than the one obtained with conventional thermal plasma sprayed 2 μm thick splats. A tentative metastable phase diagram for plasma sprayed alumina was presented by McPherson [44] as a function of the cooling time and of the splat thickness. The extrapolation of this diagram with the 40 nm estimated thick splats obtained in this study suggests that those thin splats could remain 100% gamma alumina. This shows the relevance of nano-range splat thickness for metaltable phase's synthesis. It was noted in Fig. 8c and d that some of the splats are so thin that they are transparent to the electrons. By using the Kanaya-Okayama Transmission Electron Range R_{KO} [45], it is possible to calculate the electron transparency of GDC as a function of the thickness. By applying a 0.3 coefficient to the calculated electron range, it is possible to estimate the depth of backscattered electron information [46] which could contribute to provide a signal from the underlying information.

$$R_{KO} = 27.6\ A\ E_o^{1.67} / (Z^{0.889}\ \rho)\ \text{nm}$$

Where E_o, the acceleration voltage of the SEM used is given in keV, A in g/mol, ρ in g/cm^3 and Z is the atomic number of the material. In Fig. 10, there is the evidence that

electron transparency can be observed through a splat. By using GDC properties (A=174.7 g/mol, ρ = 7.13 g/cm^3 and Z= 57.2) and Z = 3keV, R_{KO} = 116 nm and 0.3*R_{KO} is 35 nm which represents the max splat thickness shown by an arrow, with a 500nm diameter splat. Assuming a 35 nm splat thickness, the flattening ratio is 2.1 and with a 25 nm splat thickness, the flattening ratio becomes 2.4, close to the assumed 2.5 value which was derived from Madejski [42].

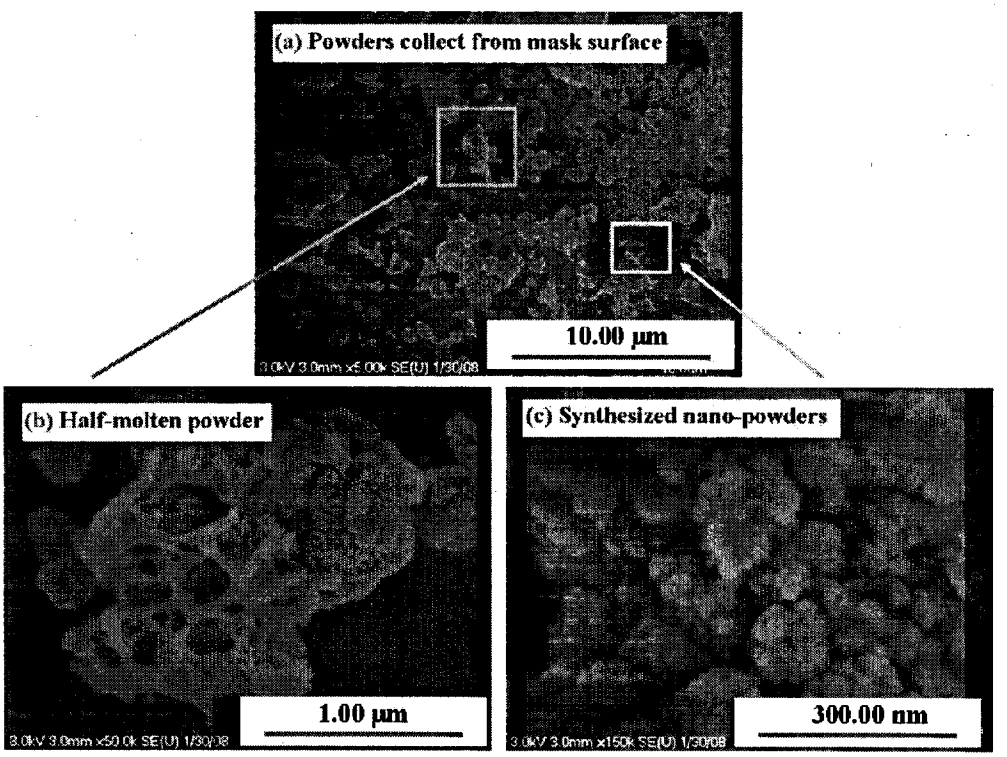

Fig. 11 : FESEM of powders collected from mask surface (a) contain half-molten powders (b) and synthesized nano-powders

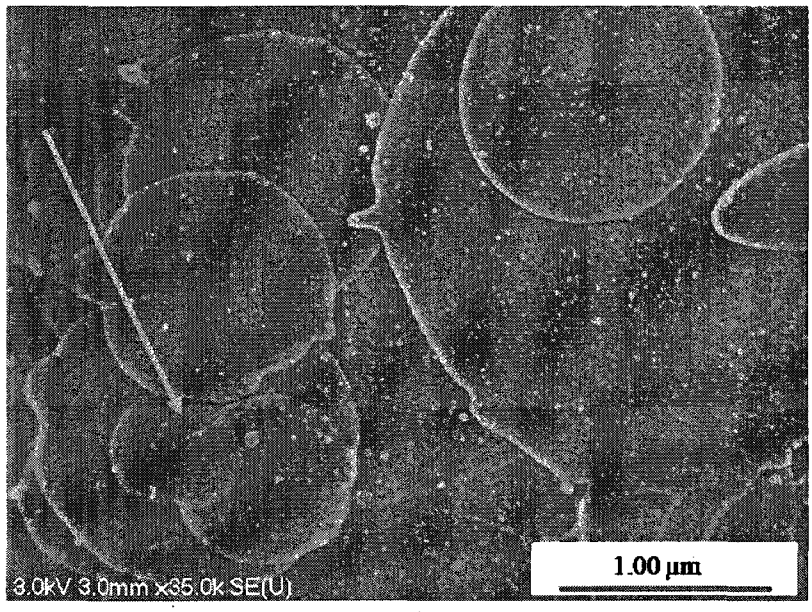

Fig. 10: Example of electron transparency evidence for one splat

3.5 Microstructure of electrolyte coatings

The micrographs of the fractured coatings are presented in Fig. 11. Fig. 11a shows the coating produced without the mask and Fig. 11b with the mask. Considerable micron-size pores are apparent in certain regions of Fig. 11a which could be related to the presence of non melted and or cooled down particles, thereby creating some porosity in the coating microstructures. The lamellar structure, which is a common characteristic in conventional plasma sprayed coatings, cannot be seen in the present SPS coating at the 5000 magnification.

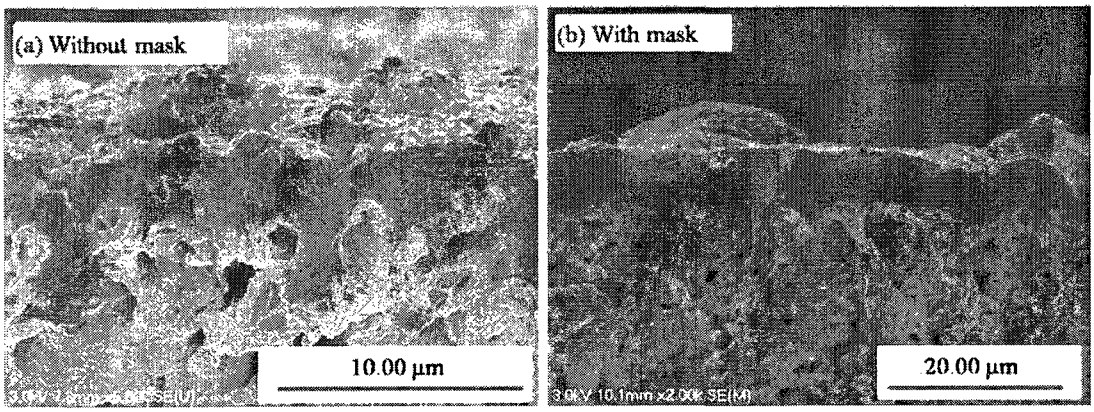

Fig. 121: FESEM of suspension plasma sprayed coating fractured cross-section without mask (a) and with mask (b)

Figure 11(b) shows the fracture cross section of the SPS deposited electrolytes with mask. It can be clearly seen that the SPS coating is much more homogeneous and showing better bonding and continuous contact with the nickel substrate compared to electrolyte coating without mask. Obviously, the Ni substrate surface is quite rough. With the large pores on the surface of the substrate, a transition layer has been commonly considered to apply to improve the connection between anode and electrolyte [47]. However, the electrolyte coatings deposited by SPS with the mask system is well filling in and bridging the large surface pores and perfectly following the roughness of the substrate surface. There are no obvious splat boundaries observed on the fracture surface. Moreover, the GDC layer is virtually free of cracks or pinholes. Indeed, no delamination or spallation was observed when the GDC coated specimen was broken during bending. Furthermore, the distinct interfacial boundary can not be found between the GDC electrolyte and the substrate. The GDC deposits penetrate the pores of the support and certainly improve the smoothness to enable the formation of the dense GDC top layer (with the porosity level estimated to be 1.2%). Due to this 3-D dimensional penetration

structure, the adhesion of the interface is improved, as well as the possibility to increase the number of active reaction sites. It will be beneficial for the ionic and electronic transfer; thus, it should improve the performance of the films to be used as SOFC electrolyte.

4. Conclusion

The potential of induction thermal suspension plasma spraying as a novel method for the production of thin, gas-tight and nano-structural SOFC electrolytes is explored. The high plasma temperature, the nano-splat sizes, and the possible control of the coating microstructure make this technique a promising candidate. The developed suspension feeding system enabling a separate injection of two single phase suspensions to form a composite GDC electrolyte coating provides the opportunity to produce functional and/or graded SOFC composite components. The dynamic mask system has been developed to diminish the heating effects of a high-temperature deposition process. It was demonstrated that the electrolyte coating deposit with mask exhibits a lower porosity compares to electrolyte coatings deposited without mask. A nano-structured electrolyte produced with 80 nm and below thin splats obtained by using the SPS technology applied to induction thermal plasma spraying has the potential to exhibit metastable phases because of the high quench rate of these nano-splats. Future studies will be devoted to the evaluation of the electrochemical properties of GDC electrolyte coatings and to the fabrication of whole single cell using the induction solution/suspension thermal plasma spraying process.

Acknowledgement

This project was funded by the Natural Sciences and Engineering Research Council of Canada (NSERC) through strategic grant # SG30685. Furthermore, contribution of the CCM for FESEM analysis is gratefully acknowledged.

References

[1] E. Ivers-Tiffée, A. Weber, and D. Herbstritt, Materials and Technologies of SOFC-Components, *J. Euro. Ceram. Soc.*, 2001, 21, p 1805-1811

[2] S.M. Haile, Fuel Cell Materials and Components, *Acta Metall.*, 2003, **51**, p 5981-6000

[3] S.C. Singhal, Advances in Solid Oxide Fuel Cell Technology, *Solid State Ionics*, 2000, **135**, p 305–313

[4] R. Henne, Solid Oxide Fuel Cells: A Challenge for Plasma Deposition Processes, *J. Therm. Spray Technol.*, 2007, **16**(3), p 381-402

[5] R. Hui, Z. Wang, O. Kessler, L. Rose, J. Jankovic, S. Yick, R. Maric, and D. Ghost, Thermal Plasma Spraying for SOFCs: Applications, Potential Advantage, and Challenges, *J. Power Sourc.*, 2007, **170**, p 308-323

[6] H. Inaba, and H. Tagawa, Ceria-Based Solid Electrolytes, *Solid State Ionics*, 1996, **83**, p 1-16

[7] A. Ambabu, S. Ghost, and H. Jeda, Novel Wet-Chemical Synthesis and Characterization of Nanocrystalline CeO_2 and $Ce_{0.8}Gd_{0.2}O_{1.9}$ as Solid Electrolyte for

Intermediate Temperature Solid Oxide Fuel Cell (IT-SOFC) Applications, *J. Mater. Sci.*, 2006, **41**(22), p 7530-7536

[8] B.C.H. Steele, Appraisal of Ce_{1-y} Gd_y $O_{2-y/2}$ Electrolytes for IT-SOFC Operation at 500°C, *Solid State Ionics*, 2000, **129**, p 95-110

[9] M. Mogensen, N.M. Sammes, and G.A. Tompsett, Physical, Chemical and Electrochemical Properties of Pure and Doped Ceria, *Solid State Ionics*, 2000, **129**, p 63-94

[10] V.V. Kharton, F.M.B. Marques, and A. Atkinson, Transport Properties of Solid Oxide Electrolyte Ceramics: a Brief Review, *Solid State Ionics*, 2004, **174**, p 135-149

[11] N. Maffei, and A.K. Kuriakose, Solid Oxide Fuel Cells of Ceria Doped With Gadolinium and Praseodymium, *Solid State Ionics*, 1998, **107**, p 67-71

[12] J. Will, A. Mitterdorfer, C. Kleinlogel, D. Perednis and L.J. Gauckler, Fabrication of Thin Electrolytes for Second-Generation Solid Oxide Fuel Cells, *Solid State Ionics*, 2000, **131**, p 79–96

[13] O. Yamamoto, Solid Oxide Fuel Cells: Fundamental Aspects and Prospects, *Electrochim. Acta*, 2000, **45**, p 2423-2435

[14] A. Weber, E. Ivers-Tiffée, Materials and Concepts for Solid Oxide Fuel Cells (SOFCs) in Stationary and Mobile Applications, *J. Power Sourc.*, 2004, **127**, p 273–283

[15] M.I. Boulos, RF Induction Plasma Spraying State-of-the-Art Review, *J. Therm. Spray Technol.*, 1992, **1**, p 33-41

[16] F. Gitzhofer, M.I. Boulos, J. Heberlein, R. Henne, T. Ishigaki, and T. Yoshida, Integrated Fabrication Processes for Solid Oxide Fuel Cells Using Thermal Plasma Spray Technology, *MRS Bulletin*, 2000, **25**(7), p 38-42

[17] R. Henne, G. Schiller, V. Borck, M. Müller, M. Lang, and R. Ruckdaschel, SOFC Components Production - An Interesting Challenge for DC- and RF-Plasma Spraying, *Thermal Spray: Meeting the Challenges of the 21st Century*, C. Coddet Ed., May 25-29, (Nice, France), ASM ***International***, 1998, p 933-938

[18] M. Müller, E. Bouyer, M.v. Bradke, D.W. Branston, R.B. Heimann, R. Henne, G. Lins, and G. Schiller, Thermal Induction Plasma Process for the Synthesis of SOFC Materials, *Mat.-Wiss. U. Werkstofftech*, 2002, **33**, p 322-330

[19] L. Jia, C. Dossou-Yovo, C. Gahlert, and F. Gitzhofer, Induction Plasma Spraying of Samaria Doped Ceria as Electrolyte for Solid Oxide Fuel Cells, *Thermal spray 2004: Advances in Technology and Application*, E. Lugscheider and C.C. Berndt, Eds. May 10-12, (Osaka, Japan), ASM International, 2004, p 85-89

[20] F. Gitzhofer, and L. Jia, Induction Plasma Technology Applied to Materials Synthesis for Solid Oxide Fuel Cells, *Int. J. Appl. Ceram. Technol.*, 2008, **5**(6), p 537-547

[21] G. Schiller, R. Henne, M. Lang, and M. Müller, Development of Solid Oxide Fuel Cells by Applying DC and RF Plasma Deposition Technologies, *Fuel Cells*, 2004, **4**(1-2), p 56-61

[22] L.R. Pederson, P. Singh, and X.D. Zhou, Application of Vacuum Deposition Methods to Solid Oxide Fuel Cells, *Vacuum*, 2006, **80**, p 1066–1083

[23] G. Schiller, R.H. Henne, M. Lang, R. Ruckdäschel, and S. Schaper, Development of Vacuum Plasma Sprayed Thin-Film SOFC for Reduced Operating Temperature, *Fuel Cells Bulletin.*, 2000, **3**(21), p 7-12

[24] M. Lang, R. Henne, S. Schaper, and G. Schiller, Development and Characterization of Vacuum Plasma Sprayed Thin Film Solid Oxide Fuel Cells, *J. Therm. Spray Technol.*, 2001, **10** (4), p 618–625

[25] M. Lang, R. Henne, S.E. Pohl, G. Schiller, and E. Hubig, Vacuum Plasma Spraying of Thin-Film Planar Solid Oxide Fuel Cells (SOFC)—Development and Investigation of the YSZ Electrolyte Layer, *International Thermal Spray Conference, ITSC 2002*, DVS-Verlag GmbH, Ed., March 4-6, (Essen, Germany), ASM International, 2002, p 807-812

[26] X.Q. Ma, F. Borit, V. Guipont, and M. Jeandin, Vacuum Plasma Sprayed YSZ Electrolyte for Solid Oxide Fuel Cell Application, *International Thermal Spray Conference, ITSC 2002*, DVS-Verlag GmbH, Ed., March 4-6, (Essen, Germany), ASM International, 2002, p 116-121

[27] B. Zhu, Next Generation Fuel Cell R&D, *Int. J. Energy Res.*, 2006, **30**, p 895-903

[28] T. Mori, J. Drennan, Y.R. Wang, W.G. Mcphee, and J.G. Li, Nano Structural Features in Rare Earth Doped CeO_2 Electrolytes for Solid Oxide Fuel Cells Application, *Trans. Mater. Res. Soc. Jpn*, 2004, **29**(5), p 1973-1976

[29] I. Kosacki, and H.U. Anderson, Microstructure-Property Relationships in Nanocrystalline Oxide Thin Films, *Ionics*, 2000, **6**, p 294-311

[30] M. Bonneau, F. Gitzhofer, and M.I. Boulos, SOFC/CeO_2 Doped Electrolyte Deposition, Using Suspension Plasma Spraying, *Thermal Spray: Surface Engineering via Applied Research*, C.C. Berndt, Ed., May 8-11, 2000 (Montréal, Québec, Canada), ASM International, 2000, p 929-934

[31] G. Schiller, M. Müller, and F. Gitzhofer, Preparation of Perovskite Powders and Coatings by Radio Frequency Suspension Plasma Spraying, *J. Therm. Spray Technol.*, 1999, **8**(3), p 389-392

[32] F. Gitzhofer, E. Bouyer, and M.I. Boulos, Suspension Plasma Spray Deposition, *U. S. Patent 5 609 921,* 1997

[33] J. Oberste Berghaus, S. Bouaricha, J.G. Legoux, and C. Moreau, Suspension Plasma Spraying of Nanoceramic Using an Axial Injection Torch, *Thermal Spray Connects: Explore Its Surfacing Potential*, E. Lugscheider and C. C. Berndt, Ed., May 2-4, 2005 (Basel, Switzerland), ASM International

[34] P. Fauchais, R. Etchart-Salas, C. Delbos, M. Tognonvi, V. Rat, J.F. Coudert , and T. Chartier, Suspension and Solution Plasma Spraying of Finely Structured Layer: Potential Application to SOFCs, *J. Phys. D: Appl. Phys.*, 2007, **40**, p 2394-2406

[35] P. Fauchais, V. Ra, C. Delbos, J.F. Coudert, T. Chartier, and L. Bianchi, Understanding of Suspension DC Plasma Spraying of Finely Structured Coatings for SOFC, *IEEE Trans. Plas. Sci.*, 2005, **33**(2), p 920-930

[36] P. Fauchais, Understanding Plasma Spraying, *J. Phys. D: Appl. Phys.*, 2004, **37**, R86-R108

[37] D. Bouchard, L. Sun, F. Gitzhofer, and G. Brisard, Comparison of Cathode/Electrolyte Interfaces Prepared by Plasma Spray and Screen Printing Forit-sofc *Solid Oxide Fuel Cells IX, SOFC IX: Materials - Proceedings of the International Symposium*, 2005, p 1684-1694

[38] C.R. Xia, and M.L. Liu, Microstructures, Conductivities, and Electrochemical Properties of $Ce_{0.9}Gd_{0.1}O_2$ and GDC-Ni Anodes for Low-Temperature SOFCs, *Solid State Ionics*, 2002, **152-153**, p 423-430

[39] M. von Bradke, F. Gitzhofer, and R. Henne, Porosity Determination of Ceramic Materials by Digital Image Analysis--A Critical Evaluation, *Scanning*, 2005, **27**(3), p 132-135

[40] L. Jia, and F. Gitzhofer, Induction Plasma Synthesis of Nano-structured SOFCs Electrolyte Using Solution and Suspension Plasma Spraying: A Comparative Study, *J. Therm. Spray Technol.*, 2010

[41] A. Vardelle, C. Moreau, and P. Fauchais, The Dynamics of Deposit Formation in Thermal-Spray Processes, *MRS Bull.*, 2000, **25**(7), p 32-37

[42] J. Madejski, Solidification of Droplets on a Cold Surface, *Int. J. Heat Mass Trans.*, 1976, **19**(12), p 1351-1356

[43] A. McDonald, C. Moreau, and C. Chandra, Thermal Contact Resistance between Plasma-Sprayed Particles and Flat Surfaces, *Int. J. Heat Mass Transfer,* 2007, **50**(9-10), p 1737-1749

[44] R. McPherson, On the Formation of Thermally Sprayed Alumina Coatings, *J. Mater. Sci.*, 1980, **15**, p 3141—3149

[45] K. Kanaya, and S. Okayama, Penetration and Energy-Loss Theory of Electrons in Solid Targets, *J. Phys. D. Appl. Phys.*, 1972, **5**, p 43—58

[46] J. Goldstein, D.E. Newbury, D.C. Joy, C.E. Lyman, P. Echlin, E. Lifshin, L.C. Sawyer, and J.R. Michael, Scanning Electron Microscopy and X-ray Microanalysis, 3rd ed., 2003, ed. Springer

[47] R.Q. Yan, D. Ding, B. Lin, M.F. Liu, G.Y. Meng, and X.Q. Liu, Thin Yttria-Stabilized Zirconia Electrolyte and Transition Layers Fabricated by Particle Suspension Spray, *J. Power Source*, 2007, **164**, p 567-571

4.4 Functionally Graded Anodes with Nanostructure for Intermediate-Temperature SOFCs

Lu Jia, Yan Shen, and François Gitzhofer, ing. Ph.D

Energy, Plasma and Electrochemistry Research Centre (CREPE), Chemical and Biotechnical Engineering Department, Université de Sherbrooke, Québec, Canada, J1K 2R1, (819)-821-7841

Cermet based SOFCs anodes require long triple phase boundary (TPB) and appropriate gas diffusion pass for the fast transport of both fuel and exhaust gases, but the area where gas diffusion passes are especially required would be different from the area suitable for electrochemical reaction in the anodes. Functionally graded anodes in both composition and porosity have been proposed to fulfill the anodic functions in adequate anodic areas. On the basis of the optimized spraying conditions and the laboratory developed solution feeding system, NiO-GDC functionally graded anodes were prepared using solution plasma spraying (SolPS) process. Then the microstructure and material composition of the anodes were analyzed. A graded distribution in contents of both nickel and GDC was found in the coating. Field emission scanning electron microscopy (FESEM) observation exhibited a continuous variation in porosity from 35% to 9% along the direction across the coating thickness. It is expected that the functionally graded anodes deposited by SolPS process minimize the thermal expansion mismatch between SOFC components and increase the length of triple phase boundary, which should lead to the improvement of the anodic performances.

Keywords: solution plasma spraying (SolPS), solid oxide fuel cells (SOFCs), functionally graded anode, microstructure, porosity

1. Introduction

Solid oxide fuel cells (SOFCs) continue to garner interest for use in stationary power system due to their low SO_x, NO_x emissions and high efficiencies [1]. To make the SOFCs a competitive energy conversion technology its operating temperature needs to be reduced from typically 1000 to below 700 °C. This would allow more cost-effective materials to be used [2]. However, as the operating temperature is reduced, some critical issues arise, such as the losses from diffusion polarization in anode drastically increase due to the effect of slower kinetics [3]. The anode performance has been an important factor to influence the properties improvement of SOFCs.

Recently, functionally graded anodes have been applied to SOFCs and have provided the possibility of enhancing the cell performance [4-12]. Grading can be classified in three ways: (1) composition grading, (2) particle size grading, and (3) porosity grading. The aim of grading is to optimize the electronic/ionic conductivity, to increase the electrochemical reactivity of the anode, and to minimize the mass transport resistance of gas mixtures inside anode. Ideally, the best structure of anodes should be with both compositional gradient and porosity gradient, consisting of fine grains (and high surface area) close to anode/electrolyte surface, and large grains (and thus large pore size) at hydrogen side [13].

The functionally graded anode is schematically illustrated in Fig.1. The anode has a gradient in porosity from the substrate/electrode interface to the surface. The region close to the electrolyte consists of small pores in order to provide long triple phase boundary. The porosity gradually increase toward the substrate in order to promote rapid transport

of fuel and exhaust gases, and thus both electrochemical reaction and gas distribution are expected to be very effective over the entire surface. This can lead to significant drop in concentration activation polarization, and yield remarkable improvement in electrical efficiency [8]. It is believed that, instead of an abrupt change in composition and microstructure between the substrate and electrolyte, functional graded anodes have a graded interface at which the composition gradually changes from substrate side to electrolyte side, thus minimize the thermal expansion coefficient mismatch and increase the anodic performances [10].

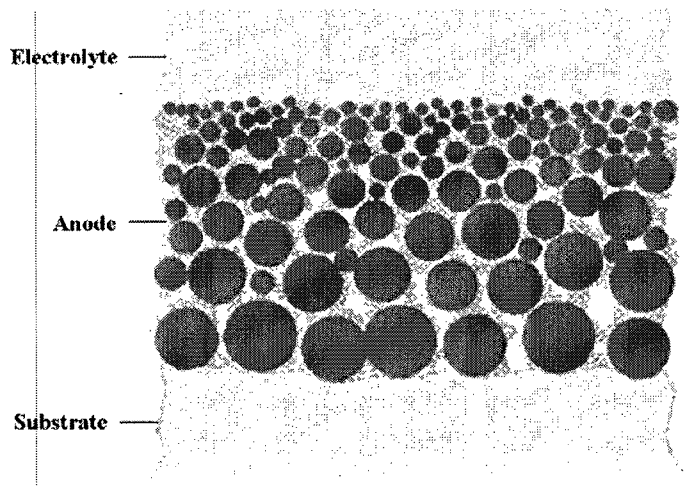

Fig. 1 Principle of a functionally graded SOFCs anode

It has been demonstrated that nano-structured electrodes with significantly high surface area offer superior electrochemical properties as long as sufficiently large pore size and enough porosity are provided [14-17]. Previous researchers have reported that nano-structured electrodes dramatically reduce electrode/electrolyte interfacial polarization resistances and improve cell performance [18-19].

Different technologies have been investigated to fabricate SOFCs anodes in the past, including chemical capor deposition (CVD) [20], physical vapour deposition (PVD) [21], electrochemical vapour deposition (EVD) [22], sol-gel method [23], tape-casting [24], screen-printing [25], and thermal spray routes [26]. Especially thermal spray process has the potential of low cost production, easy operation, high deposition efficiency, wide selection of materials, and the ability to coat large surfaces [27]. It has thus appeared as a promising canadiate and attracted much attention for the industrial production of SOFCs [28]. Atmospheric plasma spray (APS) process has been successfully developed by numerous researchers to prepare the anode using powders [30], suspensions [31], or solutions [32-34]. Lang et al. from German Aerospace Center (DLR) produced the thin (30-40 μm) and porous (20-25 vol. %) Ni-YSZ anodes using vacuum plasma spray (VPS) process [35]. Refke et al. used the low pressure plasma spray (LPPS) equipment for processing of mixtures of Ni(C) with YSZ and reached the desired layer porosity of about 30% with a deposition efficiency of 40-50% [36]. Plasma sprayed graded morphologies and/or compositions coatings can be fabricated by hybrid spraying technologies (two or more plasma guns) [37] or by only one plasma gun feeding with gradually changing compositions of powders. During the thermal plasma spray process, functionally graded and consecutively adjusted microstructures can be easily deposited, which are difficult to realize by using wet ceramic processing [38]. The control of composition, porosity, and microstructure within sprayed coatings only requires variation of the spraying parameters. Xia et al. [39] prepared the functionally graded layers using APS process. The prepared SOFCs with the graded layers showed larger electronic conductivity and lower interface resistance compare to without graded layers. It was domenstrated that thermal spray

technologies have been used for manufacturing SOFC components including anodes and that these technologies are versatile enough for depositing anodes with graded morphologies and/or compositions.

In this paper, the relationship between the anode properties to be graded and the plasma processing parameters was established in order to design a graded property profile. The work on fabrication of anode coatings with a gradient nanostructure using solution plasma spraying (SolPS) was reported. The as-sprayed anode coating shows a gradient in chemical content, porosity, and particle size along the cross-section of the coating. These functional gradients can be achieved during deposition by varying the plasma spray and solution injection parameters while building the layers.

2. Experimental set-up and procedure

2.1 Solution precursor preparation

The solution precursor of nickel was prepared by dissolving nickel nitrate hexahydrate (Alfa Aesar, purity: 99.99%) in distilled water, and the solution of $Ce_{0.8}Gd_{0.2}O_{1.9}$ (GDC) was prepared also by dissolving cerium nitrate hexahydrate (Alfa Aesar, purity: 99.99%) and gadolinium nitrate hexahydrate (Alfa Aesar, purity: 99.99%) in distilled water according to stoichiometric compositions, separately. A magnetic stirrer has been used to fully mix the starting precursors.

2.2 Plasma spraying setup

The induction solution plasma spraying setup consists of a laboratory -developed solution precursor feeding system, an atomization probe, a plasma torch and a plasma reactor. The induction plasma was generated using a PL-50 plasma torch (Tekna Plasma Systems inc.,

Quebec, Canada), operating at a frequency of 3 MHz. The torch is equipped with a convergent nozzle with a dimension of 45 mm. The liquid precursors of nickel and GDC were fed separately by laboratory developed solution feeding system (Fig.2 [40]) and directly injected into the hot plasma core by means of the atomization probe. The atomization parameters have been adjusted according to the droplet size measurements performed using the Malvern RTsizer apparatus. The average droplet size (D_{50}) in our experimental range was about 12 μm as measured during water atomization. The porous nickel substrate of 10 mm diameter and 1.2 mm thick produced by sintering method is held stationary by a sample holder, while the holder is scanned across the plasma flame by the electromotive arm. Multiple passes are used to build up the coatings. In order to reduce the thermal gradients during deposition, the substrates are heated up to 300 °C prior to coating using an electrical heating device. Detailed description of the induction plasma spraying apparatus used for this study is available elsewhere [41].

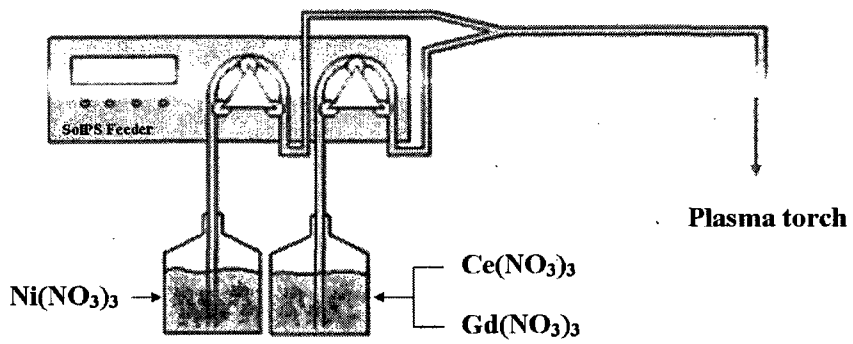

Fig. 2 Schematic illustration of laboratary developed solution injection system [19]

In generation of graded property profile requires an in-depth understanding of the relationship that prevails between plasma spraying process parameters and the properties

that need to control and vary. According to the extensive preliminary work [42], some major plasma spraying parameters, such as plasma power, reactor pressure, substrate temperature, spraying distance, liquid injection flow rate, etc., significantly influence the coating thickness, porosity, morphology and microstructure. It in turn determines the catalytic activity of SOFCs anode. These parameters also influence the uniformity of the temperature and stress distribution during the coating deposition. These already established connections between the processing parameters and the properties were adopted in the following experimental tests. Table 1 presents the plasma spraying parameters that were used for the production of functionally graded anode coating.

Table.1 Induction Solution Plasma Spraying Parameters

Plasma Torch	Tekna PL-50
Torch Nozzle Diameter (mm)	45
Atomization Probe Inner Gap (mm)	0.4
Atomization Probe Position (mm)	+ 10
Central plasma gas flow rate (slpm)	27 (Ar)
Sheath plasma gas flow rate (slpm)	63 (O_2)
Atomization gas flow rate (slpm)	10.6 (Ar)
Reactor Pressure (torr)	100-200
Plasma Power (kW)	33-40

2.3 Characterization and analysis

After coating deposition, the phase composition of the coatings was conducted by Philips X'Pert Pro MPD X-ray diffractometer (XRD) with parallel Cu Kα (Philips, Eindhoven, Netherlands). The microscopic features of the as-deposited anodes were characterized using a Hitachi S4700 field emission SEM (FESEM) with an energy dispersive spectroscopy (EDS) attachment (Hitachi, Tokyo, Japan). Particle size distributions were measured using a Malvern Mastersizer 2000 particle analyzer (Malvern Instruments Ltd., Worcestershire, United Kingdom). Coatings porosity was determined by image analysis

two to five pictures taken at different sample areas, according to the magnification used. A threshold method was used to determine the darker percentage of the picture that directly provided the porosity [43].

3. Results and Discussions

3.1 Preliminary test-Determination of spraying distance

According to the previous study [42], spraying distance was the one of the most critical parameters to control the coating porosity and microstructure. A series of preliminary tests were carried out to determine the injection model by continuously changing the spraying distance from 210 mm to 160 mm during the interval of deposition passes. The substrate bottom temperature was changed from 310 °C to 370 °C when the spraying distance was varied from 210 mm to 160 mm. Two distinct morphologies of as-deposited NiO-GDC coatings were identified by FESEM: on the surface of deposited coating under the condition of long spraying distance, the cauliflower-like (Fig. 3a) particles are uniformly distributed and connected and large numbers of pores channels with size of 5-10 um are uniformly built, which is desirable for rapid transport of fuel and exhaust gases. In short spraying distance deposited coating, the nodule-like particles (Fig.4a) have smaller grain size with more homogenous microstructure, and numbers of pores with the sub-micro size are uniformly dispersed. This homogeneous microstructure lead to good connections between NiO-NiO, GDC-GDC and NiO-GDC grains, which is important in fabricating a high performance Ni-GDC anode because of improving TPB.

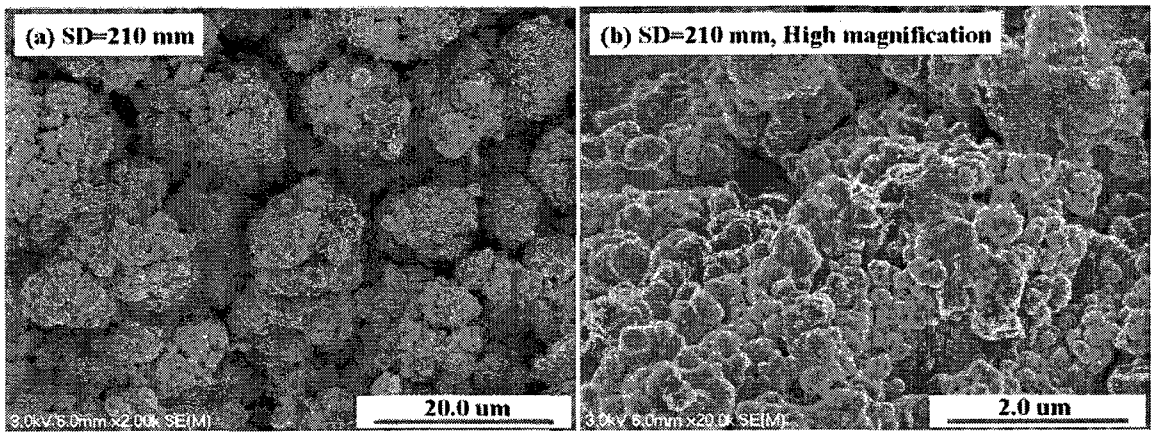

Fig. 3 FESEM top view of SolPS produced anode coating deposited under the condition of long spraying distance with different magnifications

The NiO-GDC coating was formed from a pyrolysis reaction of the nitrate solution precursor in SolPS process. After injected into plasma, the atomized droplets experienced sequential steps of evaporation, pyrolysis, homogeneous nucleation, (partially or/and fully melting) cluster condense and growth. At last, if the droplet keeps traveling in the plasma plume, flattening, solidification, and even sintering are occurred while this combination impinged on the substrate. Consequently, the SolPS coating morphology was dominated by the thermal history of liquid droplets in the plasma [44]. High magnification FESEM micrographs shown in Fig.3b and Fig.4b indicate that the large cauliflower-like particles (10 um) consist of particles around 0.2 um in diameter, and the nodule-like particles (2 um) consist of particles smaller than 10 nm. It seems that long spraying distance promoted the formation of large-size particles in the coating which associated with long residence time for clusters condense and grow in the plasma plume.

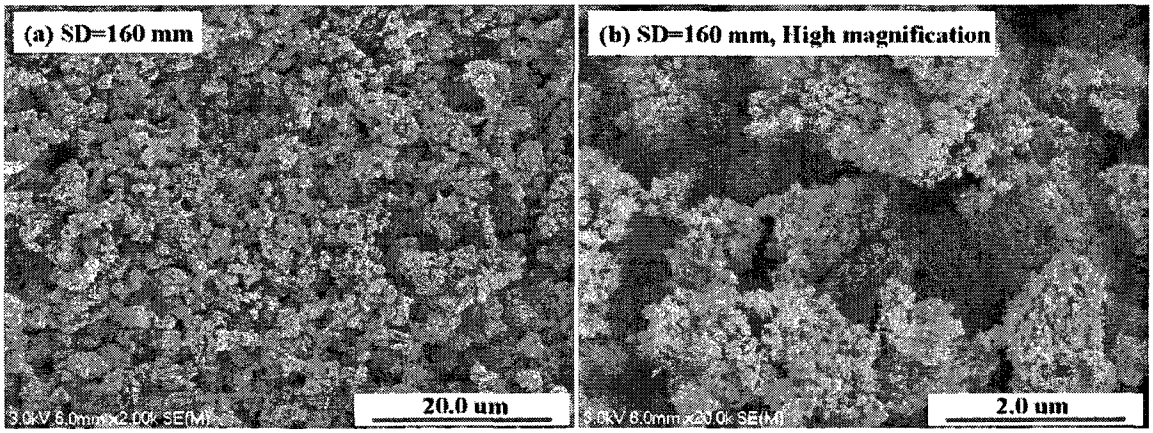

Fig. 4 FESEM top view of SolPS produced anode coating deposited under the condition of short spraying distance with different magnifications

Fig.5a, b show cross-sectional FESEM views corresponding to interface of substrate/anode deposited at different spraying distance. In both cases, the NiO-GDC layers are strongly attached to the Ni substrate and showed a well-defined interface. This fact confirms the correct selection of NiO-GDC weight ratio on the Ni/NiO-GDC interface. The coating prepared from long spraying distance reveals a columnar microstructure which promises a highly extended surface for hydrogen oxidation. The coating porosity estimates by image analysis is 32.2%. However, the coating prepared from short spraying distance results a globular microstructure. The coating porosity is 9.3%. This nano-structured coating is contributable to the increasing of TPB length in the NiO-GDC anode.

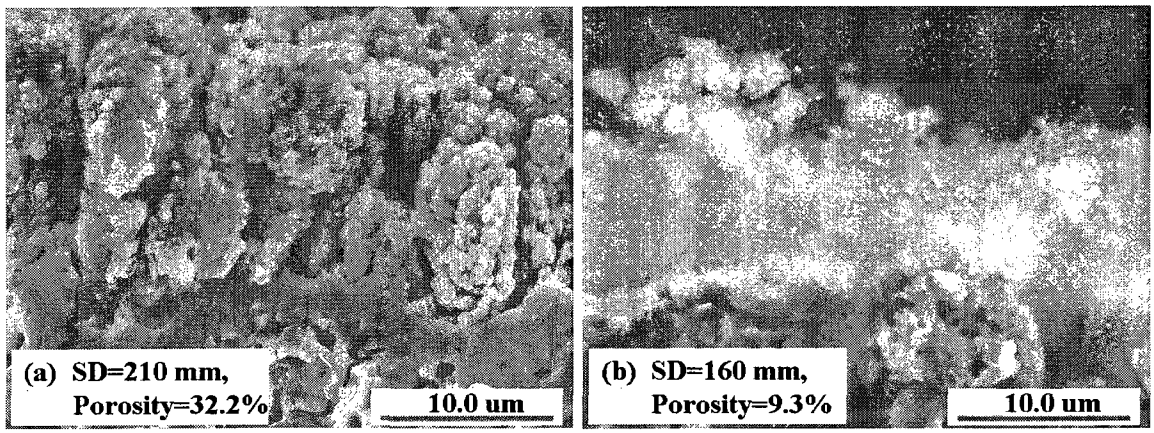

Fig. 5 FESEM micrographs of the fractured cross section of anode coating deposited at different spraying distance

Therefore, the variation of spraying distance along the cross-section of the NiO-GDC coating will lead to a remarkable variation in porosity and microstructure for the final NiO-GDC anode coating. Thus, in the following deposition experiments, the spraying distance was kept to reduce from 210 mm to 170 mm during the deposition process in order to to adjust the anode coating porosity and microstructure. It will be beneficial to fabricate the porosity and microstructure graded Ni-GDC anode with high performance.

Furthermore, in order to realise the NiO/GDC composition gradient distribution in the anode coating, the solution injection model was designed on the basis of repeated experiments. As mentioned above, the laboratory developed solution feeding system could separately inject two kinds of anode materials with different flow rates into plasma to form composite film. The nickel nitrate solution injection flow rate was decreased from 10 mL/minute to 2 mL/minute, and GDC solution injection flow rate was kept at 5 mL/minute in this deposition process. This injection model allows varying NiO/GDC mass ratio from 78.8/21.2 to 42.6/57.4 in the anode coating.

3.2 Functionally graded anode phase analysis

Fig.6 shows the X-ray diffraction patterns taken from the top surface of the NiO-GDC functional graded anodes deposited by solution plasma spraying process. Obviously, the NiO and $Gd_{0.2}Ce_{0.8}O_{1.9}$ phases were detected in the anode, and trace of Ni was also observable on the XRD patterns. The Ni signal must be collected from the peripheral surface of the substrate. The NiO and $Gd_{0.2}Ce_{0.8}O_{1.9}$ phases were formed during SolPS deposition through chemical vapour reaction. The concentration ratio of Ce and Gd in solution precursor was chosen such that the anode coating prepared with SolPS process containing $Gd_{0.2}Ce_{0.8}O_{1.9}$ was to be expected. This indicates the stoichiometric integration of Ce and Gd from the precursor into the coating during SolPS process. The crystallite size of GDC and NiO phases was calculated from XRD line-broadening analysis according to the Scherer equation is 23.1 and 98.0 nm with a 3 % relative error, respectively, which also confirms the formation of the nano-structured anode.

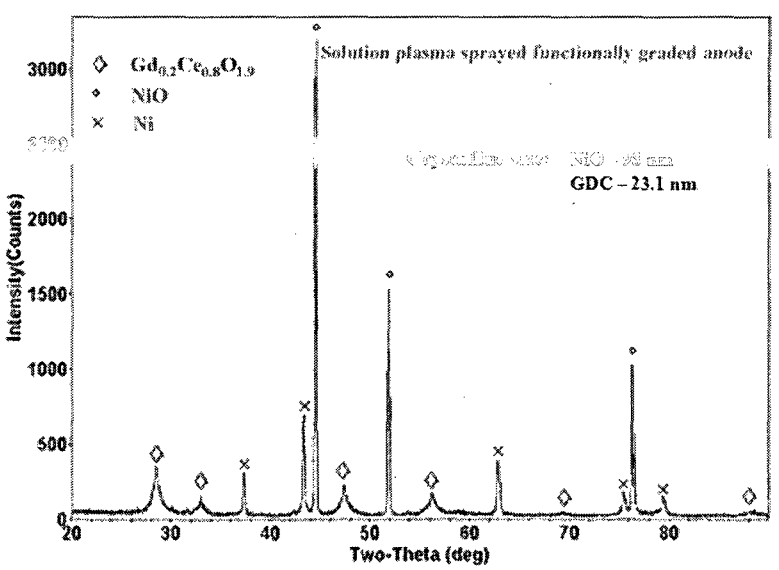

Fig. 6 X-ray diffraction pattern of NiO-GDC functionally graded anode fabricated by solution plasma spraying process

3.3 Anodes Compositional analysis

The polished cross section of the anode graded coating is examined in FESEM. The NiO-GDC network is well adhered to the substrate as shown in Fig.7a. It can be observed that almost all the available "branches" of the NiO-GDC network at the interfacial region are connected to the substrate. The coarse agglomerates (1-3 um diameter) are observed in the region close to the substrate (hydrogen side). The large interconnected pore channels within the coarse bottom layer facilitate hydrogen mass transport. The coating surface is actually nano-structured as shown in Fig.4b, offering extremely high surface area for hydrogen oxidation.

As mentioned above, the configuration of composition graded coating was obtained by programmed solution feeding. The EDS element mappings of Ni, Ce and Gd atoms confirm the gradient of the elements distribution in the coatings. As shown in Fig.7b the nickel content gradually decreased from the Ni/NiO-GDC interface to NiO-GDC airside, which the GDC distribution exhibited the opposite trend as shown in Fig 7c and d. The Ni rich area expects to have a high conductivity, and the GDC rich area will provide a fast electrochemical reaction rate. Unlike compositional layered structure fabricated by multiple functional layers, where the abrupt composition change was usually easily observed between adjacent layers, composition of the structures fabricated by SolPS changed gradually across the interface. As a result, the mismatch of the thermal expansion between the reformer, anode and electrolyte is released, which must decrease the possibility of the cracking.

It is well known that long TPB, large surface area, uniform pore size and Ni distribution, and sufficient nickel content in the anode are essential for achieving high performance [45]. For a NiO-GDC anode, the nickel grains are regarded as the active sites for H_2 oxidation, while the GDC grains serve as mechanical support for nickel, so the distribution uniformity between Ni and GDC particles are of great importance. It is obvious from Fig.7, SolPS deposited functionally graded anode coating has the distribution uniformity between Ni and GDC particles, and thus, should exhibit high electrochemical activity.

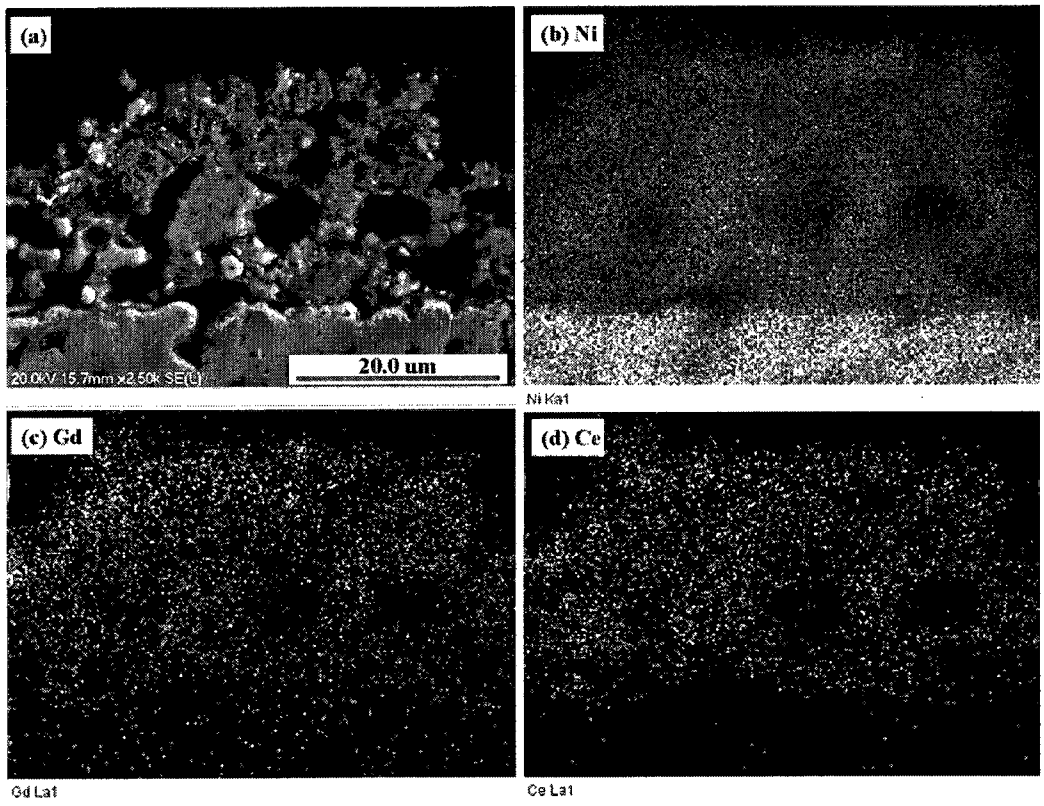

Fig. 7 (a) Polished Cross-sectional surface of the functionally graded anode produced using SolPS process, (b), (c) and (d) EDS dot mappings showing Ni, Gd and Ce distributions on the cross-section surface

3.4 · Anode coating porosity and pore diameter distribution

It also can be found from Fig.7a that the coating shows the loose and porous characteristics. In the direction across the coating thickness, there is an obvious variation in porosity and pore diameter. In the part of the coating close to the substrate, a high porosity appears with the pore diameters about 2 to 6 um. In contrast, in the part close to the coating surface, the porosity is low and the pore diameters are about 1 um. The variations in porosity and pore diameter mainly originate from the changes of spraying distance along the direction across the coating thickness.

The porosity of different regions along the direction across the coating thickness was measured. It can be found that a high porosity of up to 35% is obtained in the part of the coating close to the substrate. At the same time, a low porosity of 9% is obtained in the part close to the coating surface. This relatively high porosity on one side of the anode coating are effective in facilitating fast gas diffusion and decrease the concentration polarisation, while a low porosity on the other side is in favour of the following preparation of the dense electrolyte films. In the middle part between the coating surface and substrate, a continuous variation in porosity appears. The anode coating with a gradient in porosity expects to have better mechanical strength compared with the single lay anode coating, in which cracks often occur between the interface of substrate and electrolyte coating.

4. Conclusions

The NiO-GDC functionally graded anode with nanostructure was prepared by solution plasma spraying (SolPS) process via optimizing plasma process parameters and

laboratory developed solution feeding system. The gradient not only in chemical content but also in coating porosity was demonstrated in this anode coating. A columnar microstructure with a high porosity of up to 35% were obtained in the part of coating close to the substrate, while a globular microstructure with a low porosity of 9% were realised in the part close to the coating surface. This functionally graded anodes deposited by SolPS process is beneficial to minimize the thermal expansion mismatch and increase the length of triple phase boundary, which may lead to the improvement of the anodic performances.

Acknowledgement

Financial support from Natural Sciences and Engineering Research Council of Canada (NSERC) through strategic grant # SG30685 is gratefully acknowledged.

References:

[1] S. C. Singhal, "Advances in Solid Oxide Fuel Cell Technology," *Solid State Ionics*, 2000, **135**, 305-313.

[2] M. C. Williams, "Status of Solid Oxide Fuel Cell Development and Commercialization in the U. S.," *Proceeding- Electrochemical Society*, 1999, **99-19** (Solid Oxide Fuel Cells (SOFC VI)), 3-9.

[3] M. Mogensen, K. V. Jensen, M. J. Jorgensen, and S. Primdahl, "Progress in Understanding SOFC Electrodes," *Solid State Ionics*, 2002, **150**, 123-129.

[4] Ahmed A. E. Hassan, N. H. Menzler, G. Blass, M. E. Ali, and H. P. Buchkremer, "Development of an Optimized Anode Functional Layer for Solid Oxide Fuel Cell Applications," *Advanced Engineering Materials*, 2002, **4**(3), 125-129.

[5] P. Holtappels, C. Sorof, M. C. Verbraeken, S. Rambert, and U. Vogt, "Preparation of Porosity-Graded SOFC Anode Substrates," *Fuel Cells*, 2006, **2**, 113-116.

[6] Y. Z. Yang, H. O. Zhang, G. L. Wang, and W. S. Xia, "Fabrication of Functionally Graded SOFC by APS," *Journal of Thermal Spray Technology*, 2007, **16**(5-6), 768-775.

[7] K. Jono, S. Suda, and M. Hattori, "Effect of Graded Porous Structure on Ni-YSZ Anode Performance," *ECS Transactions*, 2007, **7**(1), 1541-1546.

[8] B. Meng, Y. Sun, X. D. He, and M. W. Li, "Graded Ni-YSZ Anode Coatings for Solid Oxide Fuel Cell Prepared by EB-PVD," *Materials Science and Technology*, 2008, **24**(8), 997-1001.

[9] J. R. Kong, K. N. Sun, D. R. Zhou, N. Q. Zhang, J. Mu, and J. S. Qiao, "Ni-YSZ Gradient anodes for Anode-Supported SOFCs," *Journal of Power Sources*, 2007, **166**, 337-342.

[10] B. Ferrari, and R. Moreno, "Ni-YSZ Graded Coatings Produced by Dipping," *Advanced Engineering Materials*, 2004, **6**(12), 969-971.

[11] J. G. Cheng, H. B. Li, X. Q. Liu, and G. Y. Meng, "Gradient Ni/SDC Anodes for Solid Oxide Fuel Cells by Tape Casting," *Materials Science Forum*, 2003, **423-425**, 449-452.

[12] L. C. R. Schneider, C. L. Martin, Y. Bultel, L. Dessemond, ad D. Bouvard, "Percolation Effects in Functionally Graded SOFC Electrodes," *Electrochimica Acta*, 2007, **52**, 3190-3198.

[13] M. Ni, M. K. H. Leung, and D. Y. C. Leung, "Micro-Scale Modeling of a Functionally Graded Ni-YSZ Anode," *Chemical Engineering & Technology*, 2007, **30**(5), 585-592.

[14] Y. Liu, S. W. Zha, M. L. Liu, "Nanocomposite Electrodes Fabricated by a Particle-Solution Spraying Process for Low-Temperature SOFCs, " *Chemical of Materials*, 2004, **16**, 3502-3506.

[15] C. S. Hwang, and C. H. Yu, "Formation of Nanostructured YSZ/Ni Anode with Pore Channels by Plasma Spraying," *Surface & Coatings Technology*, 2007, **201**, 5954-5959.

[16] U. P. Muecke, S. Graf, U. Rhyner, and L. J. Gauchler, "Microstructure and Electrical Conductivity of Nanocrystalline Nickel and Nickel Oxide/Gadolinia-doped Ceria Thin Films," *Acta Materialia*, 2008, **56**, 677-687.

[17] C. S. Ding, H. F. Lin, K. Sato, and T. Hashida, "Synthesis of NiO-$Ce_{0.9}Gd_{0.1}O_{1.95}$ Nanocomposite Powders for Low-Temperature Solid Oxide Fuel Cell Anodes by Co-precipitation" *Scripta Materialia*, 2009, **60**, 254-256.

[18] Y. Liu, C. Compson, M. L. Liu, "Nanostructured and Functionally Graded Cathodes for Intermediate Temperature Solid Oxide Fuel Cells," *Journal of Power Sources*, 2004, **138**, 194-198.

[19] C. R. Xia, M. L. Liu, "Microstructures Conductivities, and Electrochemical Properties of $Ce_{0.9}Gd_{0.1}O_2$ and GDC-Ni Anodes for Low-Temperature SOFCs," *Solid State Ionics*, 2002, **152-153**, 423-430.

[20] G.Y. Meng, H.Z. Song, Q. Dong, and D.K. Peng, "Application of Novel Aerosol-Assisted Chemical Vapor Deposition Techniques for SOFC Thin Films," *Solid State Ionics*, 2004, **175**, 29–34.

[21] L.R. Pederson, P. Singh, and X.-D. Zhou, "Application of Vacuum Deposition Methods to Solid Oxide Fuel Cells," *Vacuum*, 2006, **80**, 1066–1083.

[22] J.L. Young, and T.H. Etsell, "Polarized Electrochemical Vapor Deposition for Cermet Anodes in Solid Oxide Fuel Cells," *Solid State Ionics*, 2000, **135**, 457–462.

[23] M. Rieu, P.Lenormand, P.J.Panteix, and F.Ansart, "A New Route to Prepare Anodic Coatings on Dense and Porous Metallic Supports for SOFC Application," *Surface and Coatings Technology*, 2008, **203**(5-7), 893-896.

[24] D. Simwonis1, H. Thülen, F. J. Dias, A. Naoumidis, and D. Stöver, "Properties of Ni/YSZ Porous Cermets for SOFC Anode Substrates Prepared by Tape Casting and Coat-mix Process," *Journal of Materials Processing Technology*, 1999, **92-93**, 107-111.

[25] D. Rotureau, J.-P. Viricelle, C. Pijolat, N. Caillol, and M. Pijolat, "Development of a Planar SOFC Device Using Screen-Printing Technology," *Journal of the European Ceramic Society*, 2005, **25**, 2633–2636.

[26] G. Schiller, R. Henne, M. Lang, and M. Müller, "Development of Solid Oxide Fuel Cells (SOFC) for Stationary and Mobile Applications by Applying Plasma Deposition Processes," *Materials Science Forum*, 2003, **426-432** (3), 2539-2544.

[27] K. Okumura, Y. Aihara, S. Ito, and S. Kawasaki, "Development of Thermal Spraying-Sintering Technology for Solid Oxide Fuel Cells," *Journal of Thermal Spray Technology*, 2000, **9** (3), 354-359.

[28] H. Tsukuda, A. Notomi, and N. Histatome, "Application of Plasma Spraying to Tubular-Type Solid Oxide Fuel Cells Production," *Journal of Thermal Spray Technology*, 2000, **9** (3), 364-368.

[29] Hathiramani, D., Vaßen, R., Stöver, D., and Damani, R. J., "Comparison of Atmospheric Plasma Sprayed Anode Layers for SOFCs Using Different Feedstock," *Journal of Thermal Spray Technology*, 2006, **15**(4), 593-597.

[31] J. Oberste Berghaus, J.-G. Legoux, C. Moreau, R. Hui, and D. Ghosh, "Suspension Plasma Spraying of Intermediate Temperature SOFC Components Using an Axial Injection dc Torch," *Materials Science Forum*, 2007, **539-543** (2), 1332-1337.

[32] Fauchais, P., Etchart-Salas, R., Delbos, C., Tognonvi, M., Rat, V., Coudert, J. F., and Chartier, T., "Suspension and Solution Plasma Spraying of Finely Structured Layers: Potential Application to SOFCs," *Journal of Physics D (Applied Physics)*, 2007, **40**(8), 2394-2406.

[33] Ma, X. Q., Dai, J. X., Zhang, H., Roth, J., Xiao, T. D., and Reisner, D. E., "Solid Oxide Fuel Cell Development by Using Novel Plasma Spray Techniques," *Transactions of the ASME*, 2005, **2**, 190-196.

[34] Wang, Y., and Coyle, T. W., "Solution Precursor Plasma Spray of Nickel-Yittia Stabilized Zirconia Anodes for Solid Oxide Fuel Cell Application," *Journal of Thermal Spray Technology*, 2007, **16**(5-6), 898-904.

[35] Lang, M., Henne, R., Schaper, S., and Schiller, G., "Development and Characterization of Vacuum Plasma Sprayed Thin Film Solid Oxide Fuel Cells," *Journal of Thermal Spray Technology*, 2001, **10**(4), 618-625.

[36] Refke, A., Barbezat, G., Hawley, D., and Schmid, R. K., "Low Pressure Plasma Spraying (LPPS) as a Tool for the Deposition of Functional SOFC Components," *Proceedings of the International Thermal Spray Conference*, 2004, 61-65.

[37] P. J. Hou, H. G. Wang, B. L. Zha, X. J. Yuan, L. Jiang, in Thermal Spray 2007: Global Coating Solutions, (Eds: B. R. Marple), ASM International, 2007, 1001.

[38] O. Kesler, "Plasma Spray Processing of Solid Oxide Fuel Cells", *Materials Science Forum*, 2007, **539-543** (2), 1385-1390.

[39] W.S. Xia, H.O. Zhong, G.L. Wang, and Y.Z. Yang, "Functionally Graded Layers Prepared by Atmospheric Plasma Spraying for Solid Oxide Fuel Cells," *Advanced Engineering Materials*, 2009, **11** (1-2), 111-116.

[40] L. Jia, and F. Gitzhofer, "Preparation of Nanostructured Electrolyte Thin Film for Solid Oxide Fuel Cells by Radio Frequency Suspension Plasma Spraying," in press.

[41] L. Jia, C. Dossou-Yovo, C. Gahlert, and F. Gitzhofer, "Induction Plasma Spraying of Samaria Doped Ceria as Electrolyte for Solid Oxide Fuel Cells," *Thermal Spray 2004: Advances in Technology and Application, Proceedings of the Int. Thermal Spray Conference,* 2004, 85-89.

[42] F. Hudon, "Fabrication Par Plasma Inductif d'Anodes et d'Électrolytes de Piles à Combustible à Électrolyte Solide (SOFC) à Basse Température," *Master Thesis*, Université de Sherbrooke, 2006, 24-34.

[43] M. von Bradke, F. Gitzhofer, and R. Henne, "Porosity Determination of Ceramic Materials by Digital Image Analysis--A Critical Evaluation," *Scanning*, 2005, **27**(3), 132-135.

[44] X. Q. Ma, J. Roth, T. D. Xiao, L. D. Xie, M. Gell, E. H. Jordan, and N. P. Padture, "Solution Precursor Plasma Spray: a Promising New Technique for Forming Functional Nanostructured Films and Coating," *Ceramic Engineering and Science Proceedings*, 2004, **25**(4), 381-387.

[45] A. Atkinson, S. Barnett, R. J. Gorte, J. T. S. Irvine, A. J. Mcevoy, M. Mogensen, S. C. Singhal, and J. Vohs, "Advanced Anode for High-Temperature Fuel Cells," *Nature Materials*, 2004, **3**, 17-27.

5. CONCLUSION (Français)

La technologie des plasmas inductifs a été appliquée avec succès à la fabrication des composants nano-structurés de SOFCs en utilisant le procédé d'atomisation par plasma de solutions et de suspensions. Plus spécifiquement, la projection par plasma de suspension a permis de produire des électrolytes minces, étanches au gaz et nano-structurés. La projection de suspension par plasma combine une température élevée du plasma, des petits écrasements de particules (de l'ordre du micron), et la possibilité de grader la microstructure en même temps que d'obtenir une nanostructure du fait des épaisseurs nanométriques des écrasements. Le système d'alimentation de suspension développé permet une injection séparée de deux suspensions monophasées qui une fois combinées dans le plasma, permettent de former des revêtements composés d'électrolyte de GDC avec un dopage variable.

Parmi les critères retenus pour réaliser cette recherche, le fait de viser la synthèse d'électrolytes denses, minces (quelques microns d'épaisseur) et complètement étanches à l'hydrogène a nécessité le développement de conditions de projection spécifiques. Les meilleurs revêtements ont été obtenus avec un plasma inductif dans lequel des gouttelettes de 10 microns étaient produites ce qui permettait de complètement fondre les particules formées puis de les accélérer à vitesse élevée dans la plume du plasma grâce à une tuyère supersonique. Une fois ces gouttelettes fondues, elles s'aplatissent comme des crêpes au moment de leur impact sur le substrat. Grâce à cette technologie, en utilisant une distance courte de déposition (100 mm), des couches denses et étanches au gaz ont été obtenues même pour des couches aussi minces que 5 μm. Cependant, la réduction de la distance de

projection a causé l'augmentation des efforts thermiques qui causent les microfissures dans la couche déposée. Un système dynamique de masquage a été développé pour diminuer les effets thermiques liés aux hautes températures du plasma vues par le dépôt. On a démontré son efficacité pour les couches synthétisées d'électrolyte en prouvant que les couches produites sans masque sont plus poreuses et plus fissurées que celles obtenues avec le masque. Ainsi, des électrolytes nanostructurés et étanches ont été produits sur des anodes ou des reformeurs ultraporeux en utilisant la technologie de projection des suspensions avec une vitesse de déposition élevée

comparée aux électrolytes produits par SolPS, la couche de GDC produite par SPS est complètement dense et même les pores fermés sont pratiquement éliminés. Ces couches sont obtenues en déposant des écrasements qui ont une taille de 0.2-2.0 μm, soit dix à cent fois plus petites que la taille obtenue en projection par plasma conventionnelle de poudres. La finesse de la structure ainsi obtenue avec de si petits écrasements permet de remplir de façon tridimensionnelle les rugosités de l'anode et ce qui permet un accrochage bien meilleur entre l'électrolyte et l'anode, ce qui permet de créer par conséquent de plus grandes longueurs de phases triples. Ces résultats ont prouvé que la projection de SPS est une technologie simple et potentiellement commerciale pour préparer les électrolytes de SOFCs.

Pour synthétiser les anodes, c'est la technologie SolPS qui a été retenue. Des anodes nanostructurées avec une composition gradée en NiO et GDC ont été préparées par le procédé de SolPS. En optimisant les paramètres plasma (utilisation d'une buse subsonique, en réduisant la puissance du plasma, en augmentant la pression du réacteur, et

en augmentant la distance de déposition) et en utilisant le système d'alimentation de solution développé au laboratoire. La caractéristique principale des anodes gradées est que non seulement la composition chimique varie avec l'épaisseur, mais aussi la porosité. Ainsi, une microstructure colomnaire avec une porosité de 35 % a été obtenue dans la région proche du substrat, alors qu'une microstructure globulaire avec une faible porosité de 9 % était obtenue dans la région proche de la surface.

Ceci a fonctionnellement évalué des anodes déposées par SolPS que le processus est salutaire pour réduire au minimum la disparité de dilatation thermique et pour augmenter la longueur de la frontière triple de phase, qui mène à l'amélioration des exécutions anodiques.

Les résultats obtenus dans ce travail ont démontré la faisabilité de produire par atomisation de solution des anodes nanostructurées poreuses et des électrolytes nanostructurés denses en utilisant la projection par plasma inductif subsonique et supersonique respectivement. Ceci démontre le potentiel de cette technologie pour fabriquer des SOFCs nanostructurées entièrement intégrées en utilisant le procédé d'atomisation par plasma de solution et de suspension.

Les suites potentielles de ce travail concernent la caractérisation électrochimique des électrodes et la réalisation intégrée de cellules complètes en utilisant les diverses techniques développées lors de cette recherche et des recherches précédentes entre autres sur la cathode. La cellule complète sera étudiée en caractérisation microstructurale, électrique et électrochimique. Le potentiel de la technologie des plasmas inductifs a été démontré et doit être confirmé. Une chaîne de production pour la fabrication continue des

cellules par déposition plasma est de réaliser les dépôts consécutivement en utilisant les paramètres optimisés dans une chambre de déposition spécialement adaptée. Une analyse budgétaire permettra d'estimer le coût de fabrication des cellules dans une telle installation pour prouver la possibilité d'application industrielle.

5. CONCLUSION (English)

Induction plasma technology has been successfully applied to the fabrication of nano-structured SOFCs components using solution and suspension plasma spraying process in this work.

The potential of RF suspension plasma spraying as a novel method for the production of thin, gas-tight and nano-structural SOFC electrolytes is explored. The high plasma temperature, the small splat sizes, and the possible control of the coating microstructure make this technique a promising candidate. The developed suspension feeding system enabling a separate injection of two single phase suspensions to form composite GDC electrolyte coatings, which provides the opportunity to produce the functional and/or graded SOFC composite components.

For the electrolyte dense and completely gas-tight layers are required which should be as thin as possible. This is only achievable with RF plasma spraying with completely molten particles, which are accelerated to high velocity in the plasma flame and therefore flatten to dense lamellae on impact on the substrate. By taking advantage of Tekna plasma torch equipped with supersonic nozzle and short spray distance (10 cm), such dense and gas-tight GDC layer was obtained, even with a low thickness of 5 μm. However, the short spray distance will increase the thermal stresses which cause the micro-cracks in the deposited layer. The dynamic mask system has been developed to diminish the heating effects of a

high-temperature deposition process. It was demonstrated the electrolyte coatings deposit with mask exhibit lower porosity compares to electrolyte coatings deposit without mask.

Nano-structured thin-film electrolytes were deposited on porous anodes with a high deposition rate using SPS process. Compared to the electrolytes produced by SolPS, the GDC layer is completely dense and even the closed pores are almost eliminated. These layers are produced by layering splats and have a size of 0.2-2.0 μm, which are ten to twenty times of magnitude smaller than that obtained in conventional plasma spraying. 3-D dimensional penetration structure eliminated the rough surface of the anode and made a much better coherency between the electrolyte and anode, hence may creating longer TPB lines and so better electrochemical performance. These results have shown that SPS coating is a simple and potentially commercial technology for preparing the SOFCs electrolytes.

The NiO-GDC functionally graded anode with nanostructure was prepared by SolPS process via optimizing plasma process parameters (for example, using subsonic torch nozzle, reducing the plasma power, reducing the jet and particle velocity by raising the reactor pressure, and increasing the spray distance between torch and substrate.) and laboratory-developed solution feeding system. The gradient not only in chemical content but also in coating porosity was demonstrated in this anode coating. A columnar microstructure with a high porosity of up to 35% were obtained in the part of coating close to the substrate, while a globular microstructure with a low porosity of 9% were realised in the part close to the coating surface. This functionally graded anodes deposited by SolPS

process is beneficial to minimize the thermal expansion mismatch and increase the length of triple phase boundary, which leads to the improvement of the anodic performances.

The results obtained in this work have demonstrated the feasibility of induction plasma spraying process applied to produce the porous nano-structured electrodes as well as dense electrolyte coatings. This represents an opportunity to fabricate the fully integrated nano-structured SOFC using solution and suspension plasma spraying process.

In the future work, the electrochemical characterization of electrodes and electrolyte need to be first performed, and then the complete cell will be deposited in a consecutive RF plasma spray process. The single cell will be investigated by applied of microstructural, electrical and electrochemical characterization. The potential of RF plasma spray technology to be developed into a mass production process need to be valued. A production line for the continuous fabrication of cells by consecutive deposition of the different layer must consist of three torches-where each torch is applied for the deposition of the individual layer in a same reactor. Cost will be estimated for the manufacture of the cells in such a multi-torch installation, to prove the possibility of industrial application.

REFERENCE:

Adler, S. B., "Factors Governing Oxygen Reduction in Solid Oxide Fuel Cell Cathodes," *Chemical Review*, 2004, **104**(10), 4791-4843.

Anderson, H. U., "Review of p-Type Doped Perovskite Materials for SOFC and Other Applications," *Solid State Ionics*, 1992, **52**(1-3), 33-41.

Atkinson, A., Barnett, S., Gorte, R. J., Irvine, J. T. S., McEvoy, A. J., Mogensen, M., Singhal, S.C., and Vohs, J. M., "Advanced Anodes for High-Temperature Fuel Cells," *Nature Materials*, 2004, **3**(1), 17-27.

Badwal, S. P. S., Ciacchi, F. T., and Milosevic, D., "Scandia-Zirconia Electrolytes for Intermediate Temperature Solid Oxide Fuel Cell Operation," *Solid State Ionics*, 2000, **136-137**, 91-99.

Barthel, K., and Rambert, S., "Thermal Spraying and Performance of Graded Composite Cathodes as SOFC-Component," *W.A. Kaysser (Ed.)*, Proceedings of the 5th International Symposium on Functionally Graded Materials, Dresden, Germany, Trans Tech Publications Ltd., 1998, 800–805.

Barthel, K., Rambert, S., and Siegmann, St., "Microstructure and Polarization Resistance of Thermally Sprayed Composite Cathodes for Solid Oxide Fuel Cell Use," *Journal of Thermal Spray Technology*, 2000, **9**(3), 343-347.

Basu, R. N., Pratihar, S. K., Saha, M., and Maiti, H. S., "Preparation of Sr-Substituted $LaMnO_3$ Thick Films as Cathode for Solid Oxide Fuel Cell," *Materials Letters*, 1997, **32**(4), 217-222.

Baur, E., and Preis, H., *Z. Electrochemistry*, 1937, **43**, 727–732.

Benyoucef, A., Klein, D., Coddet, C., and Benyoucef, B., "Development and Characterization of (Ni, Cu, Co)-YSZ and Cu-Co-YSZ Cermets Anode Materials for SOFC Application," *Surface & Coatings Technology*, 2008, **202**(10), 2202-2207.

Berghaus, J. Oberste, Bouaricha, S., Legoux, J. G., Moreau, C., and Chraska, T., "Suspension Plasma Spraying of Nano-Ceramics Using an Axial Injection Torch," *Thermal Spray 2005: Thermal Spray Connects: Explore Its Surfacing Potential!,* May 2-4, 2005 (Basel, Switzerland), E. Lugscheider, Ed., DVS, 2005.

Berghaus, J. Oberste, Legoux, J. G., Moreau, C., Hui, R., and Ghosh, D., "Suspension Plasma Spraying of Intermediate Temperature SOFC Components Using an Axial Injection DC Torch," *Materials Science Forum*, 2007, **539-543**, 1332-1337.

Berghaus, J. Oberste, Legoux, J.-G., Moreau, C., Hui, R., Decès-Petit, C., Qu, W., Yick, S., Wang, Z., Maric, R., and Ghosh, D., "Suspension HVOF Spraying of Reduced Temperature Solid Oxide Fuel Cell Electrolytes," *Journal of Thermal Spray Technology*, 2008, **17**(5-6), 700-707.

Bonneau, M., Gitzhofer, F., and Boulos, M., "SOFC/CeO2 Doped Electrolyte Deposition Using Suspension Plasma Spraying," *Proceedings of the International Thermal Spray Conference*, 2000, 929-934.

Brandon, N., Skinner, S., and Steel, B. C. H., "Recent Advances in Materials for Fuel Cells," *Annual review of materials research*, 2003, **33**, 183-213.] [Fergus, J. W., "Electrolytes for Solid Oxide Fuel Cells," *Journal of Power Sources*, 2006, **162**(1), 30-40.

Cannarozzo, M., Grosso, S., Agnew, G., Del Borghi, A., and Costamagna, P., "Effects of mass transport on the performance of solid oxide fuel cells composite electrodes," *Journal of Fuel Cell Science and Technology*, 2007, **4**(1), 99-106.

Choudhary, C. B., Maiti, H. S., and Subbarao, E. C., "Solid Electrolytes and Their Applications," ed. E. C. Subbarao, Plenum Press, New York, 1980.

Dees, D. W., Claar, T. D., Easler, T. E., Fee, D. C., and Mrazek, F. C., "Conductivity of Porous Ni/ZrO_2-Y_2O_3 Cermets," *Journal Electrochemical Society*, 1987, **134**(9), 2141–2146.

Delbos, C., Fazilleau, J., Coudert, J. F., Fauchais, P., Bianchi, L., and Wittman-Teneze, K., "Plasma Spray Elaboration of Finely Structured YSZ Thin coating by Liquid Suspension Injection," *Thermal Spray 2003: Advancing the Science & Applying the Technology,* May 5-8, 2003 (Orlando, FL), C. Moreau, and B. Marple, Ed., ASM International, 2003, 661-669.

Draper, R., and DiGiuseppe, G., "High Power Density Solid Oxide Fuel Cells for Auxiliary Power Unit Applications," *Journal of Fuel Cell Science and Technology*, 2008, **5**(3), 1-9.

Fauchais, P. "Understanding Plasma Spraying," *Journal of Physics D: Applied Physics*, 2004, **37**(9), R86-108.

Fauchais, P., Rat, V., Delbos, C., Coudert, J. F., Chartier, T., and Bianchi, L., "Understanding of Suspension DC Plasma Spraying of Finely Structured Coatings for SOFC," *IEEE Transactions on Plasma Science*, 2005, **33**(2),920-930.

Fauchais, P., Etchart-Salas, R., Delbos, C., Tognonvi, M., Rat, V., Coudert, J. F., and Chartier, T., "Suspension and Solution Plasma Spraying of Finely Structured Layers: Potential Application to SOFCs," *Journal of Physics D (Applied Physics)*, 2007, **40**(8), 2394-2406.

Fauchais, P., Montavon, G., Denoirjean, A., Rat, V., Coudert, J.-F., Ageorges, H., Bacciochini, A., Brousse, E., Darut, G., Caron, N., and Wittmann-Teneze, K., "Present Knowledge in Suspension Plasma Spraying," *2008 IEEE 35th International Conference on Plasma Science*, 2008, **1**.

Fazilleau, J., Delbos, C., Rat, V., Coudert, J. F., Fauchais, P., and Pateyron, B., "Phenomena Involved in Suspension Plasma Spraying Part 1: Suspension Injection and Behavior," *Plasma Chemistry and Plasma Processing*, 2006, **26**, 371–391

Fergus, J. W., "Electrolytes for Solid Oxide Fuel Cells," *Journal of Power Sources*, 2006, **162**(1), 30-40.

Fergus, J. W., "Oxide Anode Materials for Solid Oxide Fuel Cells," *Solid State Ionics, Diffusion & Reactions*, 2006, **177**(17-18), 1529-1541.

Figueiredo, F. M., Labrincha, J. A., Frade, J. R., and Marques, F. M. B., "Reactions between a Zirconia-Based Electrolyte and $LaCoO_3$-Based Electrode Materials," *Solid State Ionics*, 1997, **101-103**(Part 1), 343-349.

Franco, T., HoshiarDin, Z., Szabo, P., Lang, M., and Schiller, G., "Sprayed Diffusion Barrier Layers Based on Doped Perovskite-Type $LaCrO_3$ at Substrate-Anode Interface in Solid Oxide Fuel Cells," *Journal of Fuel Cell Science and Technology*, 2007, **4**(4), 406–412.

Gadow, R., Killinger, A., Ruiz, A. Candel, Weckmann, H., Öllinger, A., and Patz, O., "Investigation on HVOF Technique for Fabrication of SOFCs (Solid Oxide Fuel Cells) Electrolyte Layers," *Proceedings of the 2007 International Thermal Spray Conference, Global Coatings Solutions*, May 14-16 2007 (Beijing, China), ASM International, 2007, 1053-1058.

Giannakopoulos, A. E., Suresh, S., Finot, M., and Olsson, M., "Elastoplastic Analysis of Thermal Cycling: Layered Materials with Compositional Gradients," *Acta Metallurgica et Materialia*, 1995, **43**(4), 1335-1354.

Gitzhofer, F., Boulos, M., Heberlein, J., Henne, R., Ishigaki, T., and Yoshida, T., "Integrated Fabrication Processes for Solid-Oxide Fuel Cells Using Thermal Plasma Spray Technology," *MRS Bulletin*, 2000, **25**(7), 38-42.

Gleiter, H., "Nanostructured Materials," *Advanced Materials*, 1992, **4**(7-8), 474-481.

Gruner, H., and Tannenberger, H., "Plasma Sprayed Coatings for Fuel Cell Techniques," *DVS-Bericht*, 1990, **130**, 194-196.

Guan, X. F., Zhou, H. P., Liu, Z. H., Wang, Y. N., and Zhang, "High Performance Gd^{3+} and Y^{3+} Co-doped Ceria-Based Electrolytes for Intermediate Temperature Solid Oxide Fuel Cells," *Materials Research Bulletin*, 2008, **43**(4), 1046-1054.

Haile, Sossina M., "Fuel Cell Materials and Components," *Acta Materialia*, 2003, **51**(19), 5981-6000.

Han, P., and Worrell, W. L., "Mixed (Oxygen Ion and p-Type) Conductivity in Yttria-Stabilized Zirconia Containing Terbia," *Journal of Electrochemical Society*, 1995, **142**(12), 4235-4246.

Han, M. F., Tang, X. L., Yin, H. Y., and Peng, Su. P., "Fabrication, Microstructure and Properties of an YSZ Electrolyte for SOFCs," *Journal of Power Sources*, 2007, **165**(2), 757-763.

Hart, N. T., Brandon, N. P., Day, M. J., and Shemilt, J. E., "Functionally Graded Cathodes for Solid Oxide Fuel Cells," *Journal of Materials Science*, 2001, **36**, 1077-1085.

Hathiramani, D., Vaßen, R., Stöver, D., and Damani, R. J., "Comparison of Atmospheric Plasma Sprayed Anode Layers for SOFCs Using Different Feedstock," *Journal of Thermal Spray Technology*, 2006, **15**(4), 593-597.

Hayashi, K. Hosokawa, M., Yoshida, T., Ohya, Y., Takahashi, Y., Yamamoto, O., and Minoura, H., "$La_{1-x}Sr_xMnO_3$-YSZ Composite Film Electrodes Prepared by Metal-Organic Decomposition for Solid Oxide Fuel Cells," *Materials Science & Engineering B (Solid-State Materials for Advanced Technology)*, 1997, **B49**(3), 239-242.

Heberlein, J., Chen, H. C., and Henne, R., "Integrated Fabrication Process for Solid Oxide Fuel Cells in a Triple Torch Plasma Reactor," *Journal of Thermal Spray Technology*, 2000, **3**, 348-353.

Hellmig, R. J., and Ferkel, H., "Using Nanoscaled Powder as an Additive in Coarse-Grained Powder," *Journal of American Ceramic Society*, 2001, **84**(2), 261–266.]

Henne, R., "Solid Oxide Fuel Cells: A Challenge for Plasma Deposition Processes," *Journal of Thermal Spray Technology*, 2007, **16**(3), 381-403.

Huang, K., Wan, J., Goodenough, J. B., "Oxide-ion Conducting Ceramics for Solid Oxide Fuel Cells," *Journal of Materials Science*, 2001, **36**(5), 1093-1098.

Hui, R., Wang, Z., Kesler, O., Rose, L., Jankovic, J., Yick, S., Maric R., and Ghosh, D., "Thermal Plasma Spraying for SOFCs: Applications, Potential Advantages, and Challenges" *Journal of Power Sources*, **170**(2), 2007, 308–323.

Hui, S., and Petric, A., "Electrical Properties of Yttrium-Doped Strontium Titanate under Reducing Conditions" *Journal of Electrochemical Society*, 2002, **149**(1), J1–J10.

Hwang, C.-S., Tsai, C.-H., Lo, C.-H., and Sun, C.-H., "Plasma Sprayed Metal Supported YSZ/Ni-LSGM-LSCF ITSOFC with Nanostructured Anode," *Journal of Power Sources*, 2008, **180**(1), 132-142.

Inaba, H., and Tagawa, H., "Ceria-Based Solid Electrolytes" *Solid State Ionics, Diffusion & Reactions*, 1996, **83**(1-2), 1-16.

Ivers-Tiffee, E., Weber, A., and Herbstritt, D., "Materials and Technologies for SOFC Components," *Journal of European Ceramic Society*, 2001, **21**(10-11), 1805-1811.

Jiang, S. P., and Chan, S. H., "A Review of Anode Materials Development in Solid Oxide Fuel Cells," *Journal of Materials Sciences*, 2004, **39**(14), 4405-4439.

Joo, J. H., and Choi, G., "Thick-Film Electrolyte (Thickness <20 μm)-Supported Solid Oxide Fuel Cells," *Journal of Power Sources*, 2008, **180** (1), 195-198.

Kang, H.-K., and Taylor, P. R., "Direct Production of Porous Cathode Material ($La_{1-x}Sr_xMnO_3$) Using a Reactive DC Thermal Plasma Spray System," *Journal of Thermal Spray Technlogy*, 2001, **10**(3), 526-531.

Karthikeyan, J., Berndt, C. C., Tikkanen, J., Reddy, S., Herman, H., "Plasma Spray Synthesis of Nanomaterial Powders and Deposits," *Materials Science & Engineering A (Structural Materials: Properties, Microstructure and Processing)*, 1997, **A238**(2), 275-286.

Kassner, H., Siegert, R., Hathiramani, D., Vassen, R., and Stöver, D., "Application of Suspension Plasma Spraying (SPS) for Manufacture of Ceramic Coatings Source," *Journal of Thermal Spray Technology*, 2008, **17**(1), 115-123.

Kesler, O., "Plasma Spray Processing of Solid Oxide Fuel Cells," *Materials Science Forum*, 2007, **539-543**(2), 1385-1390.

Khor, K. A., Yu, L.-G., Chan, S. H., and Chen, X. J., "Densification of Plasma Sprayed YSZ Electrolytes by Spark Plasma Sintering (SPS)," *Journal of European Ceramic Society*, 2003, **23**(11), 1855–1863.

Kim, J.-H., and Yoo, H.-I., "Partial Electronic Conductivity and Electrolytic Domain of $La_{0.9}Sr_{0.1}Ga_{0.8}Mg_{0.2}O_{3-\delta}$," *Solid State Ionics*, 2001, **140**(1-2), 105-113.

Lang, M., Henne, R., Schaper, S., and Schiller, G., "Development and Characterization of Vacuum Plasma Sprayed Thin Film Solid Oxide Fuel Cells," *Journal of Thermal Spray Technology*, 2001, **10**(4), 618-625.

Lau, M. L., Jiang, H. G., Perez, R. J., Juarez-Islas, J., and Lavernia, E. J., "Synthesis of Nanocrystalline M50 Steel Powders by Cryomilling," *Nanostructured Materials*, 1996, **7**(8), 847-856

Laughton, M. A., "Fuel Cells," *Engineering Science and Education Journal*, 2002, **11**(1), 7-16.

Lee, S.-I., Ahn, K., Vohs, J. M., and Gorte, R. J., "Cu-Co Bimetallic Anodes for Direct Utilization of Methane in SOFCs," *Electrochemical Solid-State Letters*, 2005, **8**, A48-51.

Li, P. W., and Chyu, M. K., "Electrochemical and Transport Phenomena in Solid Oxide Fuel Cells," *Transactions of the ASME. Journal of Heat Transfer*, 2005, **127**(12), 1344-1362.

Li, Z., Mallener, W., Fuerst, L., Stöver, D., and Scherberich, F. D., "Thermal Spray: Research, Design and Applications," Berndt, C. C., and Bernecki, T. F., Editors, *Processing of the 6th NTSC*, ASM Int, Materials Park (OH), USA, 1993, 343-349.

Liu, Y., Zha, S., and Liu, M., "Novel Nano-structured Electrodes for Solid Oxide Fuel Cells Fabricated by Combustion Chemical Vapor Deposition (CVD)," *Advanced Materials*, 2004, **16**(3), 256-260.

Ma, X. Q., Zhang, H., Dai, J., Roth, J., Hui, R., Xiao, T.D., and Reisner, D. E., "Intermediate Temperature Solid Oxide Fuel Cell Based on Fully Integrated Plasma-Sprayed Components"*Journal of Thermal Spray Technology*, 2005, **14**(1), 61-66.

Ma, X. Q., Hui, S., Zhang, H., Dai, J., Roth, J., Xiao, T. D., and Reisner, D. E., "Intermediate Temperature SOFC Based on Fully Integrated Plasma Sprayed Components," *Proceedings of the International Thermal Spray Conference*, 2003, **1**, 163-168.

Ma, X. Q., Roth, J., Xiao, T. D., and Gell, M., "Study of Unique Microstructure in SPS Ceramic Nanocoatings," *Thermal Spray 2003: Advancing the Science and Applying the Technology, Proceedings of the International Thermal Spray Conference*, Orlando, FL, United States, May 508, 2003 , **2**, 1471-1476.

Ma, X. Q., Roth, J., Xiao, T. D., Xie, L. D., Gell, M., Jordan, E. H., and Padture, N. P., "Solution Precursor Plasma Spray: a Promising New Technique for Forming Functional Nanostructured Films and Coating," *Ceramic Engineering and Science Proceedings*, 2004, **25**(4), 381-387.

Ma, X. Q., Dai, J. X., Zhang, H., Roth, J., Xiao, T. D., and Reisner, D. E., "Solid Oxide Fuel Cell Development by Using Novel Plasma Spray Techniques," *Transactions of the ASME*, 2005, **2**, 190-196.

Mailhot, K., Gitzhofer, F., and Boulos, M. I., "Supersonic Induction Plasma Spraying of Yttria Stabilised Zirconia Films," *Processing of 15th International Thermal Spray Conference*, May 1998 (Nice, France), 1419-1424.

Mallener, W., Wippermann, K., Jansen, H., Li, Z., and Stöver, D., "VPS Fabrication of Electroactive Solid Oxide Fuel Cell Membranes," Berndt, C. C., Editor, *Thermal Spray: International Advances in Coating Technology*, ASM International, Materials Park, OH, USA, 1992, 835-841.

Mark Ormerod, R., "Solid Oxide Fuel Cells," *Chemical Society Reviews*, 2003, **32**, 17-28.

Matsuzaki, Y., and Yasuda, I., "The Poisoning Effect of Sulfur-Containing Impurity Gas on a SOFC Anode: Part I. Dependence on Temperature, Time, and Impurity Concentration," *Solid State Ionics*, 2000, **132**(3-4), 261–269.

Mizusaki, J., Tagawa, H., Saito, T., Kamitani, K., Yamamura, T., Hirano, K., Ehara, S., Takagi, T., Hikita, T., Ippommatsu, M., and Nakagawa, S., "Reaction Kinetics at the

Nickel Pattern Electrode on YSZ and its Dependence on Temperature," *Proceedings of the Fourth International Symposium on Solid Oxide Fuel Cells (SOFC-IV)*, 1995, 741-749.

Mobius, H. H., "On the History of Solid Electrolyte Fuel Cells," *Journal of Solid State Electrochemistry*, 1997, **1**(1), 2-16.

Monterrubio-Badillo, C., Chartier, T., Ageorges, H., Coudert, J. F., and Fauchais, P., "Preparation of Stable Suspensions of Perovskites for Plasma Spraying," *Materials Science Forum*, 2003, **442**, 91-96.

Monterrubio-Badillo, C., Ageorges, H., Chartier, T., Coudert, J. F., and Fauchais, P., "Preparation of $LaMnO_3$ Perovskite Thin Films by Suspension Plasma Spraying for SOFC Cathodes," *Surface & Coatings Technology*, 2006, **200**(12-13), 3743-3756.

Mori, T., Kobayashi, T., and Wang, Y. R., "Synthesis and Characterization of Nano-Hetero-Structured by Doped CeO_2 Solid Electrolytes using a Combination of Spark Plasma Sintering and Conventional Sintering," *Journal of American Ceramic Society*, 2005, **88**(7), 1981-1984.

Moskovits, M., Ravi, B. G., and Chaim, R., "Sintering of Bimodal Y_2O_3-Stabilized Zirconia Powder Mixtures with a Nanocrystalline Component," *Nanostructured Materials*, 1999, **11**(2), 179–185.

Müller, M., Bouyer, E., Bradke, M. v., Branston, D.W., Heimann, R. B., Henne, R., Lins, G., and Schiller, G., "Thermal Induction Plasma Processes for the Synthesis of SOFC

Materials," *Beitrag für Materialwissenschaft und Werkstofftechnik*, Wiley VCH, 2002, **33**(3), 322-330.

Nernst, W., *Z. Electrochemistry*, 1899, **6**, 41-43.

Nozawa, K., Orui, H., Komatsu, T., Chiba, R., and Arai, H., "Development of Highly Efficient Planar Solid Oxide Fuel Cells," *NTT Technical Review*, 2008, **6**(2).

Ohrui, H., Matsushima, T., and Hirai, T., "Performance of a Solid Oxide Fuel Cell Fabricated by Co-firing" *Journal of Power Sources*, 1998, **71**(1-2), 185–189.

Ostergard, M. J. L., Clausen, C., Bagger, C., and Mogensen, M., "Manganite-Zirconia Composite Cathodes for SOFC: Influence of Structure and Composition," *Electrochimica Acta*, 1995, **40**(12), 1971-1981

Østergard, M. J. L., Clausen, C., Bagger, C., and Mogensen, M., "Manganite-Zirconia Composite Cathodes for SOFC: Influence of Structure and Composition" *Electrochimica Acta*, 1995, **40**(12), 1971-1981.

Princivalle, A., and Djurado, E., "Nanostructured LSM/YSZ Composite Cathodes for IT-SOFC: A Comprehensive Microstructural Study by Electrostatic Spray Deposition," *Solid State Ionics*, 2008, **179**(33-34), 1921-1928.

Quadakkers, W.J., Malkow, T., Piron-Abellan, J., Flesch, U., Shemet, V., and Singheiser, L., "Suitability of Ferritic Steels for Application as Construction Materials for SOFC Interconnects," *Fourth European Solid Oxide Fuel Cell Forum. Proceedings*, 2000, **2**, 827-836.

Rambert, S., McEvoy, A. J., and Barthel, K., "Composite Ceramic Fuel Cell Fabricated by Vacuum Plasma Spraying," *Journal of the European Ceramic Society*, 1999, **19**(6-7), 921-923.

Rampon, R., Toma, F.-L., Bertrand, G., and Coddet, C., "Liquid Plasma Sprayed Coatings of Yttria-Stabilized Zirconia for SOFC Electrolytes," *Journal of Thermal Spray Technology*, 2006, **15**(4), 682-688.

Rampon, R., Marchand, O., Filiatre, C., and Bertrand, G., "Influence of Suspension Characteristics on Coatings Microstructure Obtained by Suspension Plasma Spraying," *Surface & Coatings Technology*, 2008, **202**(18), 4337–4342.

Rauch, J., Stiegler, N., Killinger, A., and Gadow, R., "High Velocity Suspension Flame Spraying (HVSFS): Process Development and Industrial Applications," *Thermal Spray 2009, Proceeding of the International Thermal Spray Conference,* Marple, B. R., Hyland, M. M., Lau, Y. –C., Li, C. –J., Lima, R. S., and Montavon, G., editors, 150-155.

Refke, A., Barbezat, G., Hawley, D., and Schmid, R. K., "Low Pressure Plasma Spraying (LPPS) as a Tool for the Deposition of Functional SOFC Components," *Proceedings of the International Thermal Spray Conference*, 2004, 61-65.

Refke, A., Hoehle, H.-M., and Gindrat, M., "New High Efficient Thermal Spray Solutions for Perovskite Coatings and Dense Thin Electrolytes Using TriplexPro-200 APS and LPPS-Thin Film Technology," *ECS Transactions*, 2007, **7**(1, PART 1), 339-346.

Renouard-Vallet, G., Gitzhofer, F., Boulos, M., Fauchais, P., Vardelle, M., and Bianchi, L., "Optimization of Axial Injection Conditions in a Supersonic Induction Plasma Torch: Application to SOFCs," *Thermal Spray 2003: Advancing the Science & Applying the Technology*, C. Moreau and B. Marple, Eds., ASM International, Mat. Park, Ohio, USA, 2003, 195-202.

Renouard-Vallet, G., Bianchi, L., Sauvet, A. L., Fauchais, P., Vardelle, M., Boulos, M., and Gitzhofer, F., "Elaboration of SOFCs' Electrolytes by Air Plasma Spraying (APS) and Vacuum Plasma Spraying (VPS) - Comparison of Electrolytes' Properties," *Proceedings of the International Thermal Spray Conference*, 2004, 132-137.

Rose, L., Kesler, O., Tang, Z., and Burgess, A., "Application of Sol Gel Spin Coated Yttria-Stabilized Zirconia Layers for the Improvement of Solid Oxide Fuel Cell Electrolytes Produced by Atmospheric Plasma Spraying," *Journal of Power Sources*, 2007, **167**(2), 340–348.

Scagliotti, M., Parmigiani, F., Samoggia, G., Lanzi, G., and Richon, D., "Structural Properties of Plasma-Sprayed Zirconia-Based Electrolytes," *Journal of Materials Science*, 1988, **23**(10), 3764-3770.

Schiller, G., Müller, M., and Gitzhofer, F., "Preparation of Perovskite Powders and Coatings by Radio Frequency Suspension Plasma Spraying,"*Journal of Thermal Spray Technology*, 1999, **8**(3), 389-393.

Schiller, G., Muller, M., and Gitzhofer, F., "Preparation of Perovskite Powders and Coatings by RF-Suspension Plasma Spraying," *Proceedings of the International Thermal Spray Conference*, 1998, **2**, 1363-1367.

Schiller, G., Henne, R., Lang, M., Ruckdschel, R., and Schaper, S., "Development of Vacuum Plasma Sprayed Thin-Film SOFC for Reduced Operating Temperature," *Fuel Cells Bulletin*, 2000, **3**(21), 7-12.

Schiller, G., Müller, M., Bouyer, E., and Bradke, M. v., "RF Plasma Synthesis and Deposition of SOFC Materials," *16th International Symposium on Plasma Chemistry*, June 22-27, 2003, (Taormina, Italy).

Schoonman, J., "Nanostructured Materials in Solid State Ionics," *Solid State Ionics*, 2000, **135**(1-4), 5–19.

Singh, P., Pederson, L. R., Simner, S. P., Stevenson, J. W., and Viswanathan, V. V., "Solid Oxide Fuel Cell Power Generation Systems," *Proceedings of the Intersociety Energy Conversion Engineering Conference*, 2001, **2**, 953-958.

Singhal, S. C., "Advances in Solid Oxide Fuel Cell Technology," *Solid State Ionics, Diffusion & Reactions*, 2000, **135**(1-4), 305-313.

Singhal, S. C., "Science and Technology of Solid-Oxide Fuel Cells," *MRS Bulletin*, 2000, **25**(3), 16-21.

Singhal, S.C., and Kendall, L., "High Temperature Solid Oxide Fuel Cells: Fundamentals, Design and Applications, " Elsevier, NY, 2003, 197–228.

Singhal, S. C., "Solid Oxide Fuel Cells: Status, Challenges and Opportunities," *Industrial Ceramics*, 2008, **28**(1), 53-59.

Sodeoka, S., Suzuki, M., Ueno, K., Sakuramoto, H., Shibata, R., and Ando, M., "Thermal and Mechanical Properties of ZrO_2-CeO_2 Plasma-Sprayed Coatings," *Journal of Thermal Spray Technology*, 1997, **6**(3), 361-367.

Spacil, H. S., and Tedmo, C. S., "Electrochemical Disscociation of Water Vapor in Solid Oxide Electrolyte Cells," Journal of the Electrochemical Society, 1969, **116**, 1618-1633.

Stambouli, A. Boudghene, and Traversa, E., "Fuel Cells, an Alternative to Standard Sources of Energy," *Renewable and Sustainable Energy Reviews*, 2002, **6**(3), 295-304.

Steele, B. C. H. "Appraisal of $Ce_{1-y}Gd_yO_{2-y/2}$ Electrolytes for IT-SOFC Operation at 500°C," *Solid State Ionics, Diffusion & Reactions*, 2000, **129**(1-4), 95-110.

Steele, B. C. H., and Heinzel, A., "Materials for Fuel-Cell Technologies," *Nature*, 2001, **414**(6861), 345-352.

Stöver, D., Buchkremer, H. P., and Uhlenbruck, S., "Processing and Properties of the Ceramic Conductive Multilayer Device Solid Oxide Fuel Cell (SOFC)," *Ceramics International*, 2004, **30**(7), 1107-1113.

Stöver, D., Hathiramani, D., Vassen, R., and Damani, R. J., "Plasma-Sprayed Components for SOFC Applications," *Surface & Coatings Technology*, 2006, **201**(5), 2002-2005.

Sun, C. W., and Stimming, U., "Recent Anode Advances in Solid Oxide Fuel Cells," *Journal of Power Sources*, 2007, **171**(2), 247-260.

Takenoriri, S., Kadokawa, N., and Koseki, K., "Development of Metallic Substrate Supported Planar Solid Oxide Fuel Cells Fabricated by Atmospheric Plasma Spraying," *Journal of Thermal Spray Technology*, 2000, **9**(3), 360-368.

Tannenberger, H., and Schmitt, R., Swiss Patent No. 491 510, 31.

Thierfelder, W., Greiner, H., and Kock, W., "High-Temperature Corrosion Behaviour of Chromium Based Alloys for High Temperature SOFC," *Proceedings of the Fifth International Symposium on Solid Oxide Fuel Cells (SOFC-V)*, 1997, 1306-1315.

Tietz, F., Buchkremer, H.-P., Haanappel, V. A. C., Mai, A., Menzler, N. H., Mertens, J., Quadakkers, W. J., Rutenbeck, D., Uhlenbruck, S., Zahid, M., and Stöver, D., "Improved SOFC Cathodes and cathode Contact Layers," *Ceramic Engineering and Science Proceedings*, 2004, **25**(3), 269-274.

Tietz, F., Buchkremer, H.-P., and Stöver, D., "10 Years of Materials Research for Solid Oxide Fuel Cells at Forschungszentrum Julich," *Journal of Electroceramics*, 2006, **7**(2-4), 701-707.

Tietz, F., Buchkremer, H.-P., and Stöver, D., "Components Manufacturing for Solid Oxide Fuel Cells," *Solid State Ionics*, 2002, **152-153**, 373-381.

Tsai, T., and Barnett, S. A., "LSM-YSZ Cathodes for Medium-Temperature Solid Oxide Fuel Cells," *Proceedings of the Fifth International Symposium on Solid Oxide Fuel Cells (SOFC-V)*, 1997, 368-377.

Tsai, T., and Barnett, S. A., "Effect of LSM-YSZ Cathode on Thin-Electrolyte Solid Oxide Fuel Cell Performance" *Solid State Ionics*, 1997, **93**(3-4), 207-217.

Tsai, T., and Barnett, S. A., "Effect of Mixed-Conducting Interfacial Layers on Solid Oxide Fuel Cell Anode Performance," *Journal Electrochemical Society*, 1998, **145**(5), 1696-1701]

Tsipis, Ekaterina V., Kharton, Vladislav V., "Electrode Materials and Reaction Mechanisms in Solid Oxide Fuel Cells: A Brief Review: I Electrochemical Behavior vs. Materials Science Aspects," *Journal of Solid State Electrochemistry*, 2008, **12**(11), 1367-1391.

Vaßen, R., Hathiramani, D., Mertens, J., Haanappel, V. A. C., and Vinke, I. C., "Manufacturing of High Performance Solid Oxide Fuel Cells (SOFCs) with Atmospheric Plasma Spraying (APS)," *Surface & Coatings Technology*, 2007, **202**, 499-508.

Virkar, A. V. "Theoretical Analysis of Solid Oxide Fuel Cells with Two-Layer, Composite Electrolytes: Electrolyte Stability," *Journal of Electrochemical Society*, 1991, **138**(5), 1481-1487.

Virkar, A. V., Chen, J., Tanner, C. W., and Kim, J.-W., "The Role of Electrode Microstructure on Activation and Concentration Polarizations in Solid Oxide Fuel Cells," *Solid State Ionics, Diffusion & Reactions*, 2000, **131**(1-2), 189-198.

Virkar, A. V., and Wilson, L., "Low Temperature Anode Supported High Power Density Solid Oxide Fuel Cells with Nanostructured Electrodes," *Fuel Cell Annual Report*, 2003.

Wachsmann, E. D., Jayaweera, P., Jiang, N., Lowe, D. W., and Pound, B. G., "Stable High Conductivity Ceria/Bismuth Oxide Bilayered Electrolytes," *Journal of Electrochemical Society*, 1997, **144**(1), 233-236.

Wagman, D. D., Evans, W. H., Parker, V. B., Schumm, R. H., Halow, I., Bailey, S. M., Churney, K. L., and Nutall R. L., "Erratum: The NBS Tables of Chemical Thermodynamic Properties. Selected Values for Inorganic and C1 and C2 Organic Substances in SI Units," Journal of Physical and Chemical Reference Date, 1989, **18**(4), 1807-1812.

Wang, Y., and Coyle, T. W., "Solution Precursor Plasma Spray of Nickel-Yittia Stabilized Zirconia Anodes for Solid Oxide Fuel Cell Application," *Journal of Thermal Spray Technology*, 2007, **16**(5-6), 898-904.

Wang, Z. C., Weng, W. J., Chen, K., Shen, G., Du, P. Y., and Han, G. R., "Preparation and Performance of Nanostructured Porous Thin Cathode for Low-Temperature Solid Oxide Fuel Cells by Spin-Coating Method," *Journal of Power Sources*, 2008, **175**(1), 430-435.

Wang, Z. W., Berghaus, J. Oberste, Yick, S., Decès-Petit, C., Qu, W., Hui, R., Maric, R., and Ghosh, D., "Dynamic Evaluation of Low-Temperature Metal-Supported Solid Oxide

Fuel Cell Oriented to Auxiliary Power Units," *Journal of Power Sources*, 2008, **176**(1), 90-95.

Weckmann, H., Finkenwirth, O., Henne, R., and Refke, A., "Microstructure of Ni-graphite/YSZ Composite Coatings on Porous Metallic Substrates Obtained by Atmospheric Plasma Spraying (APS)," *Proceedings of the International Thermal Spray Conference (ITSC)*, 2005, (Basel, Switzerland).

White, B. D., Kesler, O., and Rose, L., "Air Plasma Spray Processing and Electrochemical Characterization of SOFC Composite Cathodes," *Journal of Power Sources*, 2008, **178**(1), 334-343.

Xia, W. S., Zhong, H. O., Wang, G. L., and Yang, Y. Z., "Functionally Graded Layers Prepared by Atmospheric Plasma Spraying for Solid Oxide Fuel Cells," *Advanced Engineering Materials*, 2009, **11**(1-2), 111-116.

Will J., Mitterdorfer A., Kleinlogel C., Perednis D., and Gauckler L.J., "Fabrication of Thin Electrolytes for Second-Generation Solid Oxide Fuel Cells," *Solid State Ionics,* 2000, **131** (1), 79-96.

Yahiro, H., Baba, Y., Eguchi, K., and Arai, H., "High Temperature Fuel Cell with Ceria-Yttria Solid Electrolyte," *Journal of Electrochemical Society*, 1988, **135**(8), 2077-2080.

Yahiro, H., Eguchi, K., and Arai, H., "Electrical Properties and Reducibilities of Ceria-Rare Earth Oxide Systems and Their Application to Solid Oxide Fuel Cell," *Solid State Ionics, Diffusion & Reactions*, 1989, **36**(1-2), 71-75.

Yakable, H., Baba, Y., Sakurai, T., and Yoshitaka, Y., "Evaluation of the Residual Stress for Anode-Supported SOFCs", *Journal of Power Sources*, 2004, **135**(1-2), 9-16.

Yamamoto, O., Takeda, Y., Kanno, R., and Noda, M., "Perovskite-Type Oxides as Oxygen Electrodes for High Temperature Oxide Fuel Cells" *Solid State Ionics*, 1987, **22**(2-3), 241-246.

Yoshida, T., Okada, Hamatani, T. H., and Kumaoka, H., "Integrated Fabrication Process for Solid Oxide Fuel Cells Using a Novel Plasma Spraying," *Plasma Sources Science Technology*, 1992, **1**, 195-201.

Zhu, B., "R & D for Intermediate Temperature Solid State Fuel Cells," *Ionics*, 1998, **4**(5-6), 435-443.

Zhu, B., Yang, X. T., Xu, J., Zhu, Z. G., Ji, S. J., Sun, M. T. and Zhu, Z. G., "Innovative Low Temperature SOFCs and Advanced Materials," *Journal of Power Sources*, 2003, **118**, 47-53.

Zhu, Q., and Fan, B., "Low Temperature Sintering of 8YSZ Electrolyte Film for Intermediate Temperature Solid Oxide Fuel Cells" *Solid State Ionics*, 2005, **176**, 889–894.